

Variational Mechanics and Stochastic Methods Applied to Structural Design

Rabindranath Andujar Moreno



Universitat Politecnica de Catalunya

Departament de Fisica Aplicada

Thesis directors:

Dr. Jaume Roset Calzada

Departament de Fisica Aplicada

Universitat Politecnica de Catalunya

Dr. Vojko Kilar

Department of Structural Engineering,

Faculty of Architecture

University of Ljubljana

Barcelona July 2014

Thesis presented to obtain the title of Doctor by the Universitat Politecnica de Catalunya

Acknowledgments

To my mentors, my family, Ljubljana and Slovenia. They all made this thesis possible. Lots of thanks.

This thesis is dedicated to my nephew Jon.

Index

Acknowledgments.....	3
Index.....	4
List of figures.....	7
List of Tables.....	12
Keywords.....	13
Abstract.....	14
1.-Introduction.....	15
1.1.-Motivation of the thesis.....	16
1.2.-Working hypotheses.....	18
1.2.1.-The deterministic approach to structural design.....	18
1.2.2.-Variational mechanics and physics simulations.....	19
1.2.3.-Hypotheses.....	20
1.3.-Expected scientific contributions.....	21
2.-State of the art: Overview of numerical methods for structural dynamics analysis.....	22
2.1.-Introduction.....	23
2.1.1.-Elements of Applied Physics	24
2.1.2.-Elements of Applied Mathematics.....	30
2.2.-Methods for numerical integration of the equations of structural dynamics.....	34
2.2.1.-Time Integration Methods: ODEs.....	35
2.2.2.-Kinematic Constraints Integration Methods: DAEs.....	38
2.2.3.-Matter Integration Methods: PDEs	40
2.2.4.-Evaluation of numerical methods.....	44
2.3.-Industry tendencies.....	47
2.4.-Discussion.....	49
3.-Comparison and study of numerical methods by means of variational mechanics.....	51
3.1.-Introduction.....	52
3.1.1.-Targets and interest of our research.....	52
3.1.2.-Variational mechanics.....	53
3.1.3.-Numerical methods for structural analysis.....	53
3.1.4.-Numerical experiments.....	54
3.2.-Variational mechanics.....	55
3.2.1.-Principle of least action.....	55
3.2.2.-Euler-Lagrange equation and energy balance.....	55
3.2.3.-Kinetic energy of a system, T	56
3.2.4.-Elastic potential energy, U	56

3.2.5.-Work done by dissipative forces.....	61
3.2.6.-Work done by external forces.....	62
3.2.7.-Total action of the system, energy balance and the Lagrange-d'Alembert principle.	62
3.3.-Numerical experiments.....	64
3.3.1.-Studied methods.....	64
3.3.2.-The studied specimens.....	67
3.3.3.-Transient input forces.....	70
3.3.4.-Parametric sensitivity study.....	71
3.3.5.-Methodology: Energy computation of a simulation.....	72
3.3.6.-Numerical results: Influence of time step.....	77
3.3.7.-Numerical results: Influence of the damping ratio.....	81
3.3.8.-Numerical results: Influence of the number of integration points for matter integration methods.....	85
3.4.-Discussion.....	87
4.-State of the art: non-deterministic methods for structural design.....	88
4.1.-Introduction.....	89
4.1.1.-The origins of deterministic structural design.....	89
4.1.2.-The iterative process of structural design.....	92
4.2.-The process of analysis in structural design.....	99
4.2.1.-Deterministic analysis: working stress approach.....	99
4.2.2.-Semi-probabilistic analysis: Load and resistance factor / Limit state approach.....	101
4.2.3.-Fully probabilistic analysis: Reliability assessment approach.....	103
4.2.4.-The limits of accuracy: uncertainty quantification in numerical simulation.....	104
4.3.-The process of optimization in structural design.....	107
4.3.1.-Mathematical programming techniques.....	107
4.3.2.-Optimality criteria techniques.....	108
4.3.3.-Techniques of stochastic optimization of structures.....	109
4.4.-Discussion.....	112
5.-A Statistical Mechanics framework for structural systems.....	113
5.1.-Introduction.....	114
5.1.1.-Assessing a structural system in terms of energy.....	114
5.2.-Statistical Mechanics of structural systems.....	117
5.2.1.-Internal energy, dU	117
5.2.2.-Internal work, dW	118
5.2.3.- Added Heat, dQ , Temperature, T and entropy change, dS	119
5.2.4.-The kinetic energy of a system, KE	123
5.2.5.-Rayleigh's quotient.....	125
5.2.6.-Simulated annealing of structural systems.....	125
5.3.-Numerical experiments and results.....	129
5.3.1.- The studied specimens.....	129
5.3.2.-Experiment 1: Modification of the applied force.....	130
5.3.3.-Experiment 2: Modification of the cross sectional properties.....	138
5.4.-Discussion.....	142
6.-Development of a computational environment for probabilistic structural design.....	144

6.1.-Introduction.....	145
6.1.1.-The .NET framework.....	146
6.1.2.-Integrating multiple software applications via .NET.....	147
6.2.-Visual programming implementation of routines for variational mechanics	149
6.2.1.-Simultaneous comparison of numerical methods.....	150
6.2.2.-Energy balance study of numerical methods for structural dynamics.....	157
6.3.-Visual programming implementation of routines for statistical mechanics	158
6.3.1.-Montecarlo.....	158
6.3.2.-Simulated Annealing.....	159
6.4.-Discussion.....	160
7.-Conclusions.....	161
7.1.-Discussion.....	162
7.2.-Revision of the working hypotheses.....	163
7.3.-Original scientific contributions.....	165
7.4.-Further research.....	166
8.-References.....	167

List of figures

- Figure 2.1: Original figure used by Euler in his derivation of the action functional. The abscissa interval A-Z represents a time lapse, while ordinates represent the variation of the difference between kinetic (K) and potential (U) energies. The area under the curve is the action functional (S).....24**
- Figure 2.2: Principle of Least Action. The sphere going from point A to point B could use any of the infinite paths. Its kinetic and potential energies would differ from one another. Euler and Lagrange’s variational mechanics, through the least action principle, establish that it would do it using only the one which minimizes the action integral. The chosen coordinates of the example are Cartesian, but any other would also be valid.....25**
- Figure 2.3: Kinematics and constraint formulation. Kinematics describe the movement by means of position with respect of a reference frame (in the picture, a cartesian one). Parameters such as distance or velocity are associated to the studied moving points (located in the center of the green spheres in the example). Cylinders represent longitudinal constraints, while spheres account for rotational ones.....26**
- Figure 2.4: Different parameters of the movement of rigid solids. The red ball has a momentum p of 20 kg m/s; the blue, 40 kg m/s and the box a null momentum due to its null velocity v . Their respective angular momentums L can be calculated through the vectorial product of their position r and momentum vectors p . After the collision, their particular linear and angular momentums will be modified, hence their impulses, but the system’s global momentum must remain invariant according to Newton’s Second Law.....27**
- Figure 2.5: Motion of a material body of surface A and volume V in a Cartesian reference. v is the velocity vector resulting of applying a force F on the differential volume dV . Another velocity results from applying a tension $T(n)$ on the differential surface dA28**
- Figure 2.6: Graphic representation of a parabolic ODE. The ODE above happens to be a parabolic curve. It is ordinary because only derivatives with respect one variable appear (dx), and first order because there are only first derivatives in the equation (dy/dx). Its exact solution (analytically obtained) is the integral below. For each one of the possible values of c there is one possible curve. The whole set of possible curves is the general solution of the ODE. A particular value of c would define an Initial or a Boundary Problem.....31**
- Figure 2.7: Graphic representation of partial derivation. The function above has two independent variables (x and y). By fixing one of them (in the picture, $x=8$), we get the curve $f(y)=64+8y+y^2$. This curve we can derivate, hence obtaining the partial derivative of $f(x,y)$ with respect to y31**
- Figure 2.8: Visual display to the relationships between knowledge disciplines and numerical integration methods of the different kind. The complexity of the topic is better understood by grouping the different methods/principles around the physical concepts they solve.....34**
- Figure 3.1: Stress-Strain diagram for a typical engineering material. The value of the area of the OAB triangle is the elastic potential energy stored in the material due to strain. The triangle MHN corresponds to a larger strain, passing through the plastic range. Its larger size is due to the “strain hardening” phenomenon.....56**
- Figure 3.2: Stress-strain components in a beam. The directions of the infinitesimal strains and stresses are arranged according to the length of the beam.59**
- Figure 3.3: Bending of a column. The energy needed to cause elastic deformation is a potential function of the constituent material properties (E), the shape of the section (I) and the exerted force (M).....60**
- Figure 3.4: Schematic of some numerical methods and their associated physical notions. In bold letters those implemented for the numerical experiments of this thesis. The arrow represents a possible sequence of methods for a dynamics simulation.....64**
- Figure 3.5: Constraint reduction. The global stiffness matrix is made non singular by symmetrically subtracting**

<i>the columns and rows corresponding to the constrained degrees of freedom.....</i>	<i>66</i>
<i>Figure 3.6: Lagrange multipliers scheme. The global stiffness matrix is made non singular by symmetrically adding columns and rows where ones are placed in the location of the constrained degrees of freedom.....</i>	<i>66</i>
<i>Figure 3.7: Penalty Method scheme. The singularity of the global stiffness matrix is treated by scaling the diagonal elements of the constrained degrees of freedom with a very large number.....</i>	<i>66</i>
<i>Figure 3.8: Geometry of the three studied models. Dimensions in cm. Three frames of increasing complexity consisting of beams, nodes and constraints.....</i>	<i>68</i>
<i>Figure 3.9: Frequency response functions for the three tested models. Values are in good agreement with those of the modal analysis. Model C has the highest sensitivity to low frequencies, while models A and B should behave similarly.....</i>	<i>69</i>
<i>Figure 3.10: Sine function, two cycles. $f=0,4$ Hz, $T=2,5$ s.....</i>	<i>70</i>
<i>Figure 3.11: Sine function, one cycle, then free vibration. $f=0,4$ Hz, $T=2,5$ s.....</i>	<i>70</i>
<i>Figure 3.12: Incremental triangular function. $f=1,2$ Hz, $T=0,83$ s.....</i>	<i>71</i>
<i>Figure 3.13: Ramp pulse. $F=0.625$ Hz, $T=1.6$ s.....</i>	<i>71</i>
<i>Figure 3.14: Model A. Time history analysis of the displacement of the tip. Chung-Hulbert method, generalized alpha value=-0.1, $dt=0.0025$, damping ratio=2%.....</i>	<i>73</i>
<i>Figure 3.15: Model A. Time history for the variation of different energy operators. Chung-Hulbert method, generalized alpha value=-0.1, $dt=0.0025$, damping ratio=1%.....</i>	<i>76</i>
<i>Figure 3.16: Energy error analysis. Model A. Influence of time step size. Damping ratio=2%.....</i>	<i>78</i>
<i>Figure 3.17: Energy error analysis. Model B Influence of time step size. Damping ratio=2%.....</i>	<i>79</i>
<i>Figure 3.18: Energy error analysis. Model C Influence of time step size. Damping ratio=2%.....</i>	<i>80</i>
<i>Figure 3.19: Rayleigh damping coefficients. The values are directly proportional to the value of the chosen damping ratio. For higher frequencies of the model, the value of the mass coefficient is higher, and vice-versa for the stiffness coefficient.....</i>	<i>81</i>
<i>Figure 3.20: Energy error analysis. Model A. Influence of damping ratio. Time step=0.01 s.....</i>	<i>82</i>
<i>Figure 3.21: Energy error analysis. Model B. Influence of damping ratio. Time step=0.01 s.....</i>	<i>83</i>
<i>Figure 3.22: Energy error analysis. Model C. Influence of damping ratio. Time step=0.01 s.....</i>	<i>84</i>
<i>Figure 3.23: Comparison of angular momentum computation for matter integration methods against number of integration points. Analytical (ANA) vs Finite Differences (FDM) vs Finite Element (FEM) vs Mass Spring System (MSS).....</i>	<i>85</i>
<i>Figure 4.1: Schematic of a clothespin and simplified modelization in a structural design application. The geometrical dimensions are shown in (a), with the design variables h, $L1$ and $L2$. The simplified model shown in (b) is based on beam elements. Symmetry is applied to halve the computational effort.....</i>	<i>94</i>
<i>Figure 4.2: Plot of the objective function and the inequality constraints. The feasible design is contained within the green area. The optimum, in the intersection of the blue line ($h2(x)<0$) and the red line (objective function). </i>	<i>97</i>

- Figure 4.3:** Stress-strain diagram for a generic material. Capacity is defined according to the limits established in this curve. Point 1 is the ultimate strength limit. Point 2 is the elastic limit. The green line is the design limit... 100
- Figure 4.4:** Analysis of raw data for wind speed in Washington. The extreme value theory gives the probabilities of occurrence of the maximum and minimum wind speeds. a) maximum annual wind speeds against time. b) histogram of relative frequencies for each recorded speed c) Gumbel-like probability density function..... 102
- Figure 4.5:** Bell curve, superimposed over a histogram of pavement concrete compressive strength data. The average value has the highest probability of occurrence..... 102
- Figure 4.6:** Graphical representation of a probability region for a given structural system. Both capacity and demand are treated in a fully probabilistic way by means of bounded histograms. The red color covers the failure region where the ratio Capacity / Demand is bigger than unity. 103
- Figure 4.7:** Variation of the uncertainty of the axial stiffness function with respect to the variation of its variables A, E and L. The total uncertainty of the function increases linearly at a rate almost three times its composing variables, given that it is three of them contributing equally. Sensitivity analysis allows for the characterization of the degree of influence of the variables in the final total uncertainty of a model..... 106
- Figure 5.1:** Total internal energy versus the stiffness of a system with a single element. This quantity is a quadratic function of the applied force and varies inversely proportional to the stiffness..... 118
- Figure 5.2:** Histogram for one of the studied models with the frequency of energy states of all the nodes after 1000 simulations The lowest group of values gets the most of occurrences..... 120
- Figure 5.3:** Probability mass function and Pareto probability density function of nodal energy states for one the studied models. The PMF is obtained by normalization of the frequency. The PDF is approximated as a long-tail Pareto law..... 121
- Figure 5.4:** Evolution of the values of entropy with the probability. Higher values of probability do not necessarily imply higher entropy. In fact, the highest entropy of the system would be achieved if the probabilities of all the nodes were in the vicinity of 37%..... 122
- Figure 5.5:** Quasi-static kinetic energy versus the mass of a structural system consisting of a single element. The kinetic energy defined here is a quadratic function of the applied force and varies inversely proportional to the mass. It is worth noting the equivalence to the plotted lines in Figure 1, as both dU and $Keqs$ are quadratic functions of the displacement..... 124
- Figure 5.6:** Schematic distribution of the nodes and beams which were the subject of the study. The behaviour of each model varies with the disposition of the braces as described in the seismic regulation Eurocode 8..... 130
- Figure 5.7:** Variation of internal elastic energy with respect to total applied energy. Robust configurations have a short span of values in the horizontal axis as they oppose to changes in total energy dU . Although shortened for graphical clarity, the line for Model A reaches values as high as 500 kNcm. Models B and C, however, have much shorter trails and, for the same range of forces, oscillate only between 0 and 8 kNcm..... 131
- Figure 5.8:** Variation of the internal elastic energy with respect to the force applied to the system. The ordinates presented by means of a \log_{10} scale. In the linear regime, the internal work varies quadratically with respect to the applied force..... 132
- Figure 5.9:** Variation of entropy with respect to the force applied to the system. A higher force results in a higher total energy dU . As dU increases, the individual nodal energies reach higher values, whose probabilities are lower according to the Pareto law. This leads to lower values of the entropy..... 133
- Figure 5.10:** Variation of heat with respect to the force applied to the system. The large values of dQ represent big differences between the internal work dW and the total energy, dU . When positive, they reflect dissipative behaviour; when negative, internal accumulation in the nodes..... 134

- Figure 5.11: Variation of quasi-static kinetic energy with respect to force applied on the system. The slope of the line is the inverse of Rayleigh's quotient. Steeper lines indicate higher flexibility, flatter lines, higher stiffness.** 134
- Figure 5.12: Temperature vs Kinetic energy. The quadratic relation between T and KE can be linearized to obtain the parameter τ when kinetic energies are low.**..... 135
- Figure 5.13: Variation of quasi-static kinetic energy with respect to force applied on the system. The relationship between kinetic energy and applied force is quadratic. Flexible structures present narrow paraboles.** 135
- Figure 5.14: The deformed shapes of the models under the applied load. Model A was magnified by a factor of 1000, whereas models B, C, and D were magnified by a factor of 10000. Models A and B have the same amount of connected nodes, although B presents a much lower kinetic energy. C and D have more connected nodes that explain their negative heat as they store energy internally instead of dissipating it.**..... 137
- Figure 5.15: Structure's mass vs standard deviation of the nodal strain energy density for a random population of 10000 specimens. The design space is a surface of $2,5 \times 10^9$ points. The optimal is a minimum in the boundary of this surface. Feasible and unfeasible designs are selected according to the maximum displacement serviceability limit state.**..... 139
- Figure 5.16: Structure's total energy vs standard deviation of the nodal strain energy density for a random population of 10000 specimens. The standard deviation of the nodal strain energy density is a more effective measure of the dispersion of the nodal energy than the entropy as it only requires one calculation per state.**..... 140
- Figure 5.17: Structure's mass vs temperature for a random population of 10000 specimens.. Larger masses imply lower capacity of movement hence lower values of temperature. By means of the Simulated Annealing algorithm, the value of our computed temperature intervenes as a control variable in the search.**..... 141
- Figure 5.18: Structure's mass vs standard deviation of the nodal strain energy density. 50 iterations in the Simulated Annealing algorithm. The design space is constrained to a much smaller line of exponential nature.** 141
- Figure 6.1: Grasshopper definition of the complete program. The visual programming interface makes it possible to have a global view of the whole process and the interconnection between elements at a glance.**..... 149
- Figure 6.2: Close-up of the group of input panel components used to define model characteristics. Each model is completely defined by four blocks of information: node positions, beam section characteristics, support boundary conditions and force magnitude.**..... 150
- Figure 6.3: View of the transient input force generation components. The control of the parameters is made by means of slider components and the results are easily visualized both numerically and graphically.**..... 151
- Figure 6.4: Direct stiffness matrix assembly. This module contains the code for generating the necessary stiffness, mass and damping matrices.**..... 152
- Figure 6.5: Integration of boundary conditions. It is possible to link either to Penalty Method or the Lagrange Multipliers method. In the picture, Lagrange Multiplier is deactivated for efficiency reasons.**..... 152
- Figure 6.6: Intermediate linking component and common control parameters for time integration. In order to be able to make several combinations of methods, a connection hub was devised where links from one boundary constrain method could be fixed while switching time integration methods.**..... 153
- Figure 6.7: Time integration methods. It can be seen how most of the input variables are common to every method. Just a few calibration parameters differentiate the methods from one another. The time history of a selected node's displacement is presented for debug reasons. The total computed action is clearly presented and comparable.**..... 154

- Figure 6.8: Intermediate linking component and common control parameters for time integration. In order to be able to make several combinations of methods, a connection hub was devised where links from one boundary constrain method could be fixed while switching time integration methods..... 155**
- Figure 6.9: Matter integration methods. Finite Element, Finite Differences and Mass Spring System were compared. Boxes in grey are deactivated for computational efficiency..... 155**
- Figure 6.10: Energy balance of numerical methods for structural dynamics. The methods of Newmark Beta, Wilson Theta, Hilbert-Hugh-Taylor and Chung-Hulbert available in the SAP2000 application were seamlessly compared with two ad-hoc components. Resulting data was processed using Excel also programmatically..... 156**
- Figure 6.11: Computation of the energy parameters defined in chapter 5 by means of Monte Carlo exploration. The components used in previous research were reused when possible. In this case, time history integration was replaced with random perturbation of the input force..... 158**
- Figure 6.12: Computation of the energy parameters defined in chapter 4 by means of Simulated Annealing and optimization analysis. The random variable in this case were the geometric properties of the section of the beams.. 159**

List of Tables

<i>Table 2.1: Summary of ODE / Time integration methods.....</i>	<i>46</i>
<i>Table 2.2: Summary of DAE / Constraint integration methods.....</i>	<i>46</i>
<i>Table 2.3: Summary of PDE / Matter integration methods.....</i>	<i>46</i>
<i>Table 2.4: Comparison of different disciplines, methods and implementations.....</i>	<i>47</i>
<i>Table 3.1: Displacement and force based formulae of elastic strain energy in a beam.....</i>	<i>59</i>
<i>Table 3.2: Properties of the beam elements composing the specimens.....</i>	<i>67</i>
<i>Table 3.3: Modal frequencies for damping characterization.....</i>	<i>69</i>
<i>Table 3.4: Time integration parameters.....</i>	<i>72</i>
<i>Table 4.1: Design parameters of a column and their associated uncertainty.....</i>	<i>106</i>
<i>Table 5.1: Pseudocode for the Simulated Annealing algorithm.....</i>	<i>127</i>
<i>Table 5.2: Properties of the beam elements composing the specimens.....</i>	<i>129</i>
<i>Table 5.3: Properties of the studied specimens.....</i>	<i>130</i>
<i>Table 5.4: Summary of the average values after 100 iterations.</i>	<i>138</i>
<i>Table 5.5: Available profile sections used in the Simulated Annealing optimization procedure.....</i>	<i>139</i>

Keywords

Numerical methods, Structural optimization, Lagrangian Mechanics, Energy balance, Statistical mechanics.

Abstract

This thesis explores a very well understood area of physics: computational structural dynamics. The aim is to stretch its boundaries by merging it with another very well established discipline such as structural design and optimization. In the recent past both of them have made significant advances, often unaware one of each other for different reasons. It is the aim of this thesis to serve as a bridging tool between the realms of physics and engineering.

The work is divided in three parts: variational mechanics, structural optimization and implementation.

The initial part deals with deterministic variational mechanics. Two chapters are dedicated to probe the applicability of energy functionals in the structural analysis. First, by mapping the state of the art regarding the vast field of numerical methods for structural dynamics; second, by using those functionals as a tool to compare the methods. It is shown how, once the methods are grouped according to the kind of differential equations they integrate, it is easy to establish a framework for benchmarking. Moreover, if this comparison is made using balance of energy the only parameter needed to observe is a relatively easy to obtain scalar value.

The second part, where structural optimization is treated, has also two chapters. In the first one the non-deterministic tools employed by structural designers are presented and examined. An important distinction between tools for optimization and tools for analysis is highlighted. In the following chapter, a framework for the objective characterization of structural systems is developed. This characterization is made on the basis of the thermodynamics and energetic characteristics of the system. Finally, it is successfully applied to drive a sample simulated annealing algorithm.

In the third part the resulting code employed in the numerical experiments is shown and explained. This code was developed by means of a visual programming environment and allows for the fast implementation of programs within a consolidated CAD application. It was used to interconnect simultaneously with other applications to seamlessly share simulation data and process it. Those applications were, respectively, a spreadsheet and a general purpose finite element.

1.- Introduction

1.1.- Motivation of the thesis

After a number of years undertaking projects in structural engineering for the building industry, the author of this thesis experienced a number of situations where the current state of the tools for structural design rendered to be insufficient or, in some cases, even counterproductive.

Despite the immense efforts of the scientific and academic community for developing faster and more reliable models, modern structural design and analysis is yet, to a great extent, exclusively based on statics and the superposition theorem, hence tied to linear approaches to achieve design solutions. Buckling, vibrational response, terrain-structure interfaces, creeping, fatigue and many others are very important phenomena for which such models, although extensively adopted and canonical, give a fairly blurred picture.

On one side, the degree of elaboration achieved in the formulation of the models of elastodynamics often makes it preferable to resource the analysis to empirical “simplified” models which are easier to understand by the practitioner.

On the other, it seems evident that the very process of design, in many cases automatic and repetitive, could be greatly improved by the modern techniques of optimization. In the complex course that goes from object inception in the mind of the “shape” designer to the desk of the structural analyst, tools that objectively provide “best” solutions can be of much help to improve the dialogue between both parts.

The main problem with traditional optimization techniques, based on deterministic optimal criteria is their apparent arbitrariness. They supply an exact solution in a reasonable lapse of time but this is very sensitive to the chosen judgement of which result is superior to another. Stochastic non-deterministic search algorithms are more attractive as they facilitate a whole range of “possibles”, sorted by order of fitness.

Methods of stochastic optimization (stochastic hill climbing and tunnelling, evolutionary algorithms, swarm algorithms and many others) have been successfully applied in science and technology since the 1950s. Lately, these very methods, combined with modern numerical tools (Finite Element Method, Applied Element Method, Discrete Element Method, among many others) are proving very helpful in automotive, aerospace and naval engineering to achieve sophisticated, reliable and precise designs.

To make them practical, though, the current analysis methods must be made more efficient. The variational principles of mechanics devised by Euler and Lagrange are currently implemented into many physics engines. This field of research is under constant development and new and more efficient algorithms emerge every year.

Variational mechanics are an extremely powerful tool because they replace the paradigm of the analysis

focused in displacement and force vectors with one looking at energy change scalars. Not only the resulting implementations benefit from this but also the degree of understanding of the studied phenomena.

As it will be shown in the thesis, countless efforts are being made in advancing and improving the aforementioned techniques. However, to the knowledge of the author, a comprehensive work addressing simultaneously variational mechanics, energy principles and stochastic techniques was yet to be made. There seems to be a strong need of bringing together science (variational mechanics) and technology (structural design), so that both fields of knowledge can benefit from each other.

1.2.- Working hypotheses

In the preliminaries of this thesis, a series of assumptions were made around the two main ideas of non-deterministic structural design and variational mechanics. These two articulated the discourse and can be seen reflected in the internal structure of the chapters as well as in the results of the thesis.

1.2.1.- *The deterministic approach to structural design*

Nowadays, structural engineering has a strong deterministic bias. However, one increasingly important aspect of structural analysis that deterministic design finds difficult to address is that of uncertainty in structural parameters and in loading and boundary conditions.

Deterministic single- point evaluation of the response may under many circumstances produce an over-designed and excessively conservative system if the presence of parameter scatter is not taken into account.

It is very illustrative of this situation how building codes, initially conceived as good practice handbooks within the trade, have now become such a heavy reference that they can affect the production of building materials in a whole country.

Nowadays Limit States is the compulsory method for evaluating any building's performance (Eurocodes, ASCE, ACI, CTE,...). They are provided to the designers and are obtained under probability methodologies but have to be necessarily included into a deterministic analysis in the form of safety factors.

The inclusion of these algorithms in their most sophisticated forms mean in concrete terms - referring exclusively to the field of structural analysis - that the issues may be raised in such terms that:

- The variables (loads, elastic modulus, yield stress, geometric properties, etc..) may be characterized by a probability distribution type (normal, lognormal, extreme value, etc..) with their corresponding statistical parameters for the cases of discrete variables.
- The variables may hold random spatial distributions. For example loads, geometrical and physical properties randomly distributed in the domain of definition of the elements.
- One or more features of "performance" may be formulated to establish criteria or limits to be satisfied by the system or by its components (resistance, rigidity, etc.)

This should allow the engineer to establish the feasibility of the design or the need for changes on a basis much more comprehensive and objective-based methods than using in the safety factor.

Although computationally far more expensive, stochastic design methods have two major advantages

over the deterministic ones: a deeper understanding of the designed product and a quantification of the level of uncertainty of the given answer.

This new approach is lately conforming a fairly strong corpus of research and many publications and applications can be found.

1.2.2.- Variational mechanics and physics simulations

Modern structural design and analysis is almost exclusively based on statics and the superposition theorem, hence tied to linear approaches to achieve design solutions.

Buckling, vibrational response, terrain-structure interfaces, creeping, fatigue and many others are very important phenomena for which such models, although extensively adopted and canonical, give a fairly blurred picture.

Non linear intensive particle-based Lagrangian methods, on the other hand, is a relatively recent field of research, where the phenomena previously mentioned simply arises as a consequence of the simultaneous interaction of the simulated bodies or particles.

By means of these methodologies, it seems feasible to tackle and to achieve a further understanding of such phenomena.

From the practical point of view, much research has been done in order to obtain numerically stable and accurate simulations. There is also a good amount of work into the problem of rigid body collisions, provided it consumes a good amount of computational resources.

A more recent trend is combining Finite Element Method with Lagrangian and Hamiltonian dynamics, in order to account also for the deformational properties of the simulated bodies. This combination extends the inherent limitation of FEM to the continua with the capability of modeling also discontinuous interactions.

This also opens new ways to structural designers for it means the possibility of modeling materials different from steel and concrete, so environmentally unfriendly. Too often these building systems are the only way to go for the codes are the only ones that support. With new (and traditional) systems being safely modeled, broader possibilities open to design alternatives.

With enough computational power, these environments can be extended with the modeling of flows, giving a physical meaning to loads (i.e. wind, terrain, water). These loads, of inherent stochastic and non-linear nature, currently mean a good amount of uncertainty for designers.

Moreover, thermodynamic properties can also be implemented, hence allowing for other non-structural related analysis.

From the engineering point of view, available frameworks where the non-static and non-linear behavior of structures can be observed definitely would provide a far deeper understanding that should derive in better, more efficient and environmentally aware designs.

1.2.3.- Hypotheses

The working hypotheses can then be summarized as follows:

- A The vast body of numerical integration algorithms for structural dynamics simulation can be encompassed within an intuitive scheme that simplifies its study.

- B Variational principles help to better understand the results of the simulations and their application gives a wider ability to analyse.

- C Energy principles already improve the performance of structural dynamics simulations, but could also be used in combination with non-deterministic design tools. In this manner, design objective functions could be devised that accounted for optimal uses of the energetic capacity of the materials.

- D Theoretical advances gain value when they translate into practical and concrete tools. The research must contemplate this possibility and exploit the experimental implementations so that they can eventually reach others.

1.3.- Expected scientific contributions

The main target of this thesis is to obtain a clear and comprehensive view on how variational mechanics, combined with stochastic numerical methods, can be applied to change the paradigm of deterministic structural design.

It is not meant to substitute current procedures, but to complement them with expanded perception of the behaviour of structural systems.

As a side effect of this it was intended to achieve a computer tool with the following features:

- Real-time based physics computation for structural frames.
- Behaviour-monitored structural elements and parameters.
- Different material models, and the possibility of creating new ones, considering physical and technological properties.
- Real-time design visualization and designer interaction.
- Stochastic methods applied to different structural systems and probability-based evaluation of their reliability.
- Stochastic models for non-deterministic non-linear loads (wind, earthquake, terrain, blast, snow, etc).

Further and practical applications of it would be:

- Building forensics of existing or failed buildings.
- Haptics for dynamic design of buildings.
- Interactive benchmarking of structural designs.
- Immersive virtual buildings.

2.- State of the art: Overview of numerical methods for structural dynamics analysis

2.1.- Introduction

In this chapter the current state-of-the-art of the computational techniques for the simulation of structural dynamics will be presented. A preliminary overview of concepts will be used to justify a general framework of classification according to the multidisciplinary character of the topic.

Previous surveys exist where a rigorous mathematical background is provided. However, these present a certain excess of specialization towards their natural trades, so [SHA1997] and [WAS2003] have a marked inclination towards Robotics and [NEA2005] and [ERL2002] are excellent reviews for the Computer Graphics community. This chapter aims to facilitate a comprehensive and more unified view on the subject of structural dynamics and the numerical methods employed to simulate them. For the sake of simplicity formulations have been considered unnecessary and only practical matters are discussed.

The analysis of structural dynamic behaviour is a topic of specialized research in many modern disciplines: Civil Engineering, Aeronautics, Automotive, Robotics, Medicine, Biomechanics, Molecular Dynamics and Graphics Animation are some of the industries currently developing with growing interest applications that allow to simulate the dynamics of structures and related literature about it.

Although, from a scientific point of view, this must be regarded as a great success and such diversity of points of view should be considered as positive, it also means that the intrinsic complexity of the subject increases somehow chaotically as each author contributes with a particular approach.

Furthermore, the already daunting list of numerical methods for the solution of problems of dynamics grows by means of mixed concepts making it very difficult to understand what they really do. It is common to encounter in the literature methods for the approximation of standard algebraic problems that are regarded as having “physical” properties or that some method to solve partial differential equations is enunciated as “explicit” referring to the ordinary differential equations also involved in the solution.

As a third source of confusion we have to consider the mathematical foundations of the numerical methods, by means of which these are conceived as general and abstract as possible. It means that for a particular method its applicability can go from economics to electric flux analysis. For this reason, it is often easy to get diverted and dazzled when trying to approximate this fascinating area of research.

The following section aims to be a general reference framework where researchers and developers from diverse disciplines can assess, according to its performance, the main methods currently used for structural simulation. There is a need to make all this knowledge accessible in a more intuitive manner [ROS2006].

For this reason, these methods will be grouped according to three physical concepts: time, matter and constraints, which not by chance correspond to very well defined mathematical areas: Ordinary Differential Equations (ODEs), Partial Differential Equations (PDEs) and Differential-Algebraic

Equations (DAEs).

The last section discusses these methods as they are utilized in the main industrial environments, and provides some explanation as to how and why they have evolved in that particular manner.

2.1.1.- Elements of Applied Physics

Physics is commonly categorized into five main branches (Classical Mechanics, Electromagnetism, Statistical Mechanics, Thermodynamics Quantum Mechanics and Relativity) which also have several ramifications.

The main branch of our interest here is that of Classical Mechanics, where we can find the three main subjects that cover most of the developments for our purposes: Classical Mechanics, Rigid Body Dynamics and Continuum Mechanics.

2.1.1.1.- Classical Mechanics

Classical mechanics is split in three main segments: Statics, Dynamics and Kinematics. This division accounts for the state of motion of the studied phenomena.

Another categorization can be made according to the mathematical formalism of the description: Newtonian Mechanics, Lagrangian Mechanics and Hamiltonian Mechanics.

Lagrangian Mechanics were introduced by Joseph-Louis Lagrange in 1788 in his “Mécanique analytique” [HAN2004, NEU2006]. It is a refined algebraic version of a graphical method developed by Euler in 1744 used to solve mechanical problems [EUL1744]. This revolutionary approach to the solution of problems of Mechanics uses kinetic energy and work function (scalar magnitudes) instead of force and momentum (vectorial magnitudes) to predict motion of bodies [LAN1952].

Euler and Lagrange introduced the calculus of variations as a tool for finding maxima and minima of

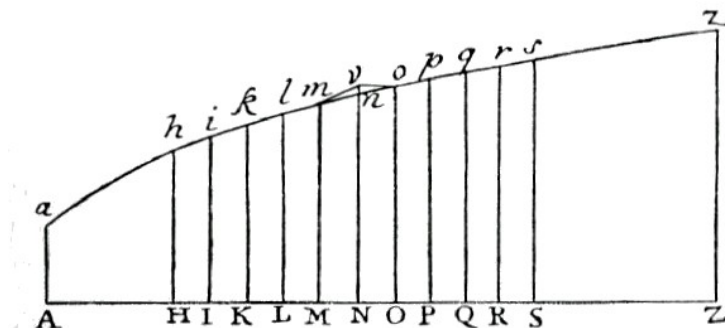


Figure 2.1: Original figure used by Euler in his derivation of the action functional. The abscissa interval A-Z represents a time lapse, while ordinates represent the variation of the difference between kinetic (K) and potential (U) energies. The area under the curve is the action functional (S).

functionals (functions whose arguments are not just variables but functions) such as the ones appearing in mechanical problems. When the studied functional is that of the difference between kinetic and potential energies of a system (which are themselves a function of time), we refer to it as the *action functional* (figures 2.1 and 2.2).

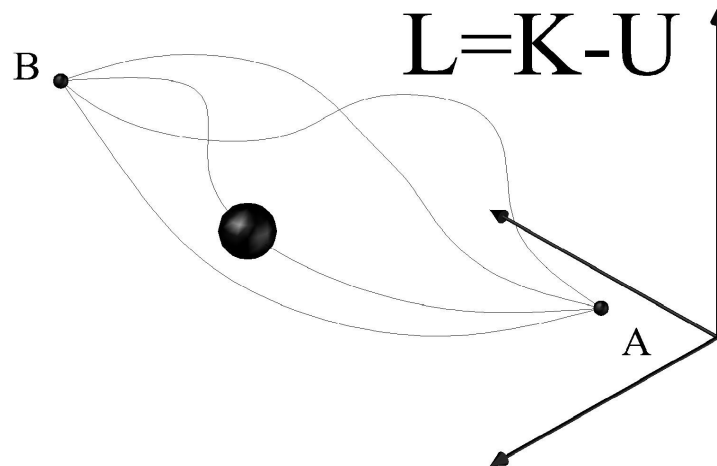


Figure 2.2: Principle of Least Action. The sphere going from point A to point B could use any of the infinite paths. Its kinetic and potential energies would differ from one another. Euler and Lagrange's variational mechanics, through the least action principle, establish that it would do it using only the one which minimizes the action integral. The chosen coordinates of the example are Cartesian, but any other would also be valid.

The equation of the action functional S involves the monitoring of the kinetic K , and the potential U energies for every time step between $t1$ and $t2$. Their difference is known as the Lagrangian, L .

These scalar magnitudes K and U can be obtained via many different formulations, depending on the coordinate system chosen by the analyst.

The above methodology of representing motion of a particle by means of the action functional provides the value of the action integral for one particular path. However, the set of possible paths followed by the particle between the points A and B is infinite. The Least Action Principle states that the path chosen by Nature is going to be no other but the one with a minimum value of the aforementioned integral. This is also called, in a more precise manner, the principle of stationary action. Thanks to it, the description of particle trajectories is simplified into a minimization problem [LAN1952].

The set of parameters which describe uniquely the kinematics (how things move) of a system is known as generalized coordinates. The minimum number of these coordinates necessary to completely describe a configuration is the degree of freedom of such system.

Understanding of the properties of these coordinates is necessary because when we hit on a certain type of

coordinates called "cyclic" or "ignorable", a partial integration of the basic differential equations is at once accomplished. If all our coordinates are ignorable, our problem is completely solved. Hence we can formulate the entire problem of solving the differential equations of motion as a problem of coordinate transformation. Many approaches to the solution of mechanical problems just do so: instead of trying to integrate the differential equations of motion directly by means of variational methods they try to produce more and more ignorable coordinates [LAN1952].

The Gaussian principle of least constraint is a minimum principle comparable with the principle of least action, but simpler in not requiring an integration with respect to the time. By means of Gauss's principle we use least squares to find action's minimal value, whereas the principle of least action would lead us to an extremum value of the integral [LAN1952]. Although mathematically equivalent, this formulation has several advantages in computational terms and allows for the consideration of frictional dissipative constraints [UDW1992].

2.1.1.2.- Rigid Body Dynamics

Rigid Body Dynamics studies the motion of bodies whose deformation is considered negligible with respect of their displacement or rotation. Unlike particles, where only three degrees of freedom are enough to describe the kinematics, rigid bodies need also three more parameters to describe their rotations with respect to their centre of gravity [MIR1996].

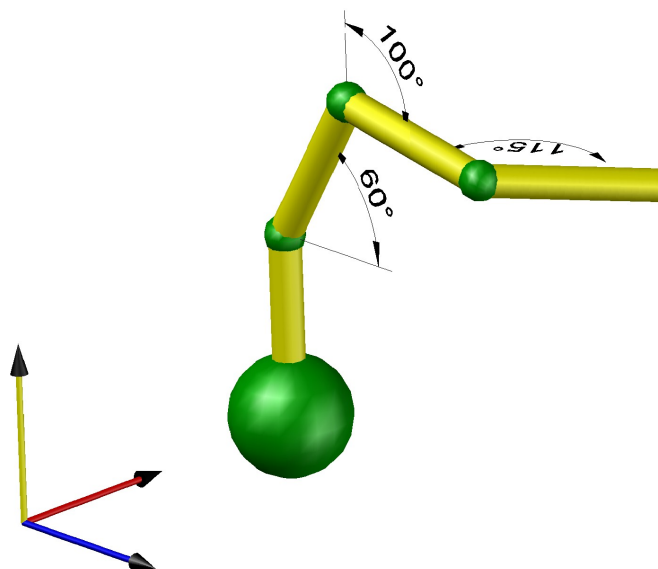


Figure 2.3: Kinematics and constraint formulation. Kinematics describe the movement by means of position with respect of a reference frame (in the picture, a cartesian one). Parameters such as distance or velocity are associated to the studied moving points (located in the center of the green spheres in the example). Cylinders represent longitudinal constraints, while spheres account for rotational ones.

Kinematics deals with the study of how things move independently of the causes of the movement. For such purpose it employs the concepts of reference frame and coordinate system, position, displacement and distance, velocity, speed and acceleration, which account for the spatial configuration of the studied bodies. In order to simulate body interactions and motions, it is needed to take into account the environmental constraints that affect to a system of rigid bodies. Constraint formulation implies the correct fixing in the values of any or all of the aforementioned variables (figure 2.3).

Linear momentum p is the product of the mass m and the velocity v of a body. It is therefore a vectorial magnitude. Newton's second law states that the rate of change of linear momentum of a body whose mass is constant equals the total of the forces exerted on the body.

Angular momentum L is the cross product of the linear momentum p and the position r vectors. It is an axial vector or pseudovector. It is not to be mistaken with the angular momentum associated to the rotational movement of a body, where the inertia momentum of the body and its angular velocity are involved (figure 2.4).

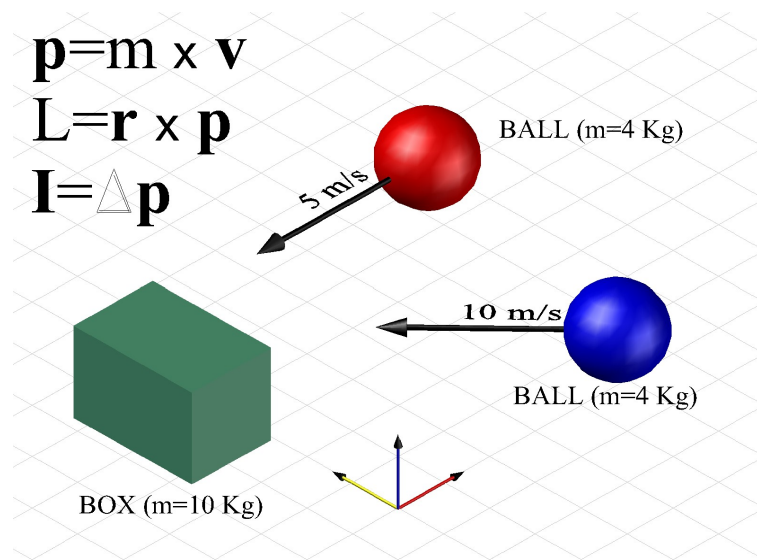


Figure 2.4: Different parameters of the movement of rigid solids. The red ball has a momentum p of 20 kg m/s; the blue, 40 kg m/s and the box a null momentum due to its null velocity v . Their respective angular momentums L can be calculated through the vectorial product of their position r and momentum vectors p . After the collision, their particular linear and angular momentums will be modified, hence their impulses, but the system's global momentum must remain invariant according to Newton's Second Law.

Impulse, I accounts for the rate of change of linear momentum by means of Newton's Second Law. In classical mechanics literature, also, impulse is just the integral in time of a force applied to a body, but it is commonly used to refer to a fast-acting force. This type of impulse is often idealized so that the change in momentum produced by the force happens with no change in time. This sort of change is a step change,

and is not physically possible. However, this is a useful model for computing the effects of ideal collisions and is widely used in many physics simulators [MIR1996, BEN2007].

Figure 2.4 illustrates the different parameters involved in the movement of a set of rigid bodies.

2.1.1.3.- Continuum Mechanics

Continuum Mechanics studies the behaviour of deformable bodies, as opposed to rigid bodies. It is traditionally subdivided into Solid and Fluid Mechanics, mostly depending on the deformational behaviour of the body. There are two main ways of kinematically describing the changes in configuration of the body: lagrangian and eulerian.

By means of the lagrangian description, continuum is represented as an atomic model where particles “float” in a vacuum and relate to each other in energetic terms. The eulerian approach makes a cellular division of this continuum and maps the changes that happen in constant locations, hence representing the flow implicitly, in the form of a field with its variations [SHA2008].

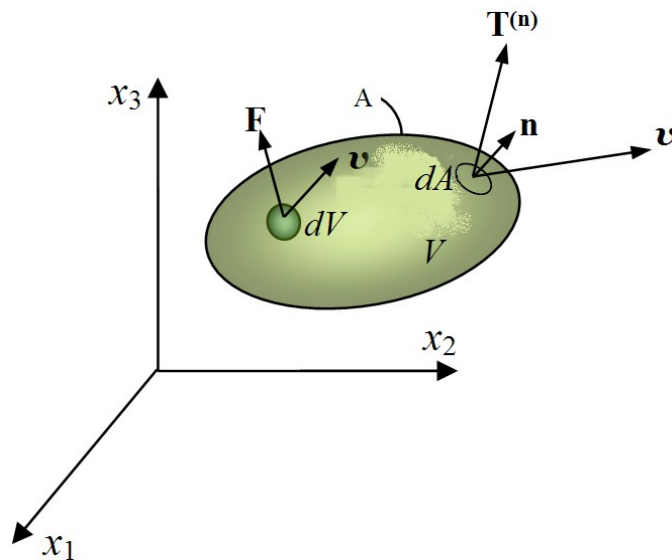


Figure 2.5: Motion of a material body of surface A and volume V in a Cartesian reference. v is the velocity vector resulting of applying a force F on the differential volume dV . Another velocity results from applying a tension $T(n)$ on the differential surface dA .

In the theory of continuum mechanics, stresses are used as measures of the forces and pressures. As in the case of strains, different definitions can be used for the stresses. Some of these definitions are associated with a reference configuration, whereas others are associated with the current deformed configuration. The effect of the forces on the body dynamics can only be taken into consideration by using both stresses and strains. These stress and strain components must be defined in the same coordinate system in order to have a consistent formulation. Two basic types of forces are easily distinguished from one another: those acting on all volume elements, and distributed throughout the body, and those forces which act upon and

are distributed in some fashion over a surface element of the body [MAS1999]. The concept is illustrated in figure 2.5, as a basis for the different reference frames.

2.1.1.4.- Deformation and motion

A change in the configuration of a continuum body results in a displacement. The displacement of a body has two components: a rigid-body displacement and a deformation. A rigid-body displacement consists of a simultaneous translation and rotation of the body without changing its shape or size. Deformation implies the change in shape and/or size of the body from an initial or undeformed configuration to a current or deformed configuration [SHA2008].

The displacement field is the set of vectors that describe the change of a body from one configuration to another. It serves to represent changes in the position of the different points in a region or the whole body. Unfortunately, the mathematical notation associated to displacement fields makes them less intuitive than what they really are: a function involving many vectors and points at the same time. [MAS1999]

The equations from which the behaviour of material points is described, and that need to be satisfied, are classified according to their nature:

- Conservation of matter
- Conservation of linear and angular momentum
- Conservation of energy
- Constitutive equations
- Strain-displacement equations

The possible manners of expressing these equations with different purposes gives place to the innumerable available formulations in literature, either optimizing the numerical methods associated or in the search for more general descriptions of the behaviour of materials. Almost invariably they are formulated in the form of differential equations [SHA2008].

The balance laws express the idea that the rate of change of a quantity (mass, momentum, energy) in a volume must arise from three causes [MAS1999]:

- The physical quantity itself flows through the surface that bounds the volume.
- There is a source of the physical quantity on the surface of the volume.
- There is a source of the physical quantity inside the volume.

2.1.2.- Elements of Applied Mathematics

All the above physical concepts are idealizations of reality derived from pure observation. Eventually, these observations become relations between variables and parameters which are managed by means of mathematical tools. Such tools are mainly located in the fields of differential equations and linear algebra. Differential equations are involved in the representation of the continuum, while linear algebra is utilized to solve the energy minimization variational principles of Euler and Lagrange.

2.1.2.1.- Differential Equations

A differential equation is any equation containing derivatives in it. The derivation can be ordinary (the function has only one independent variable on which we can derivate) or partial (more than one independent variable is present so we derivate just on one variable at a time and leave the rest as constants). Also, according to the number of derivations of the equation with respect of the variable, the equation can be first, second or higher order. In figure 2.6, an ordinary, second order equation is plotted.

Although time, matter and constraints are modelled and idealized as a continuum, they need to be discretized into a finite integer number of sub-elements for the computer to process them. This is important when numerical methods are considered for the solution of Differential Equations, as many analytical procedures give exact solutions which are impossible to achieve computationally. Likewise, there are problems that are not solvable analytically, hence the recurrence to numerical computational methods.

- Ordinary Differential Equations (ODEs): are those in which only the derivative with respect of one independent variable is present. The derivative can be the first, the second, etc. of the function but only for one independent variable in the relation. For the solution of ODEs there is a whole set of analytical methods that account for the form in which the coefficients and the variables are displayed in the equation. This leads to a series of classifications and definitions from which further association can be made. The more complex forms of ODEs out of these catalogues sometimes are not solvable, but often it is possible to manipulate their formulation in order to fit them into any known solvable scheme. It is important to distinguish between these analytical methods and the numerical ones further detailed in this chapter.
- Differential-Algebraic Equations (DAEs): these combine the terms differential and algebraic, so as to express that these are algebraic systems containing differential equations. Provided that engineering normally requires conservation laws to be studied altogether with constitutive equations and design constraints, it is much more efficient to do it by keeping these relations separate. This commonly leads to a set of differential and algebraic equations.

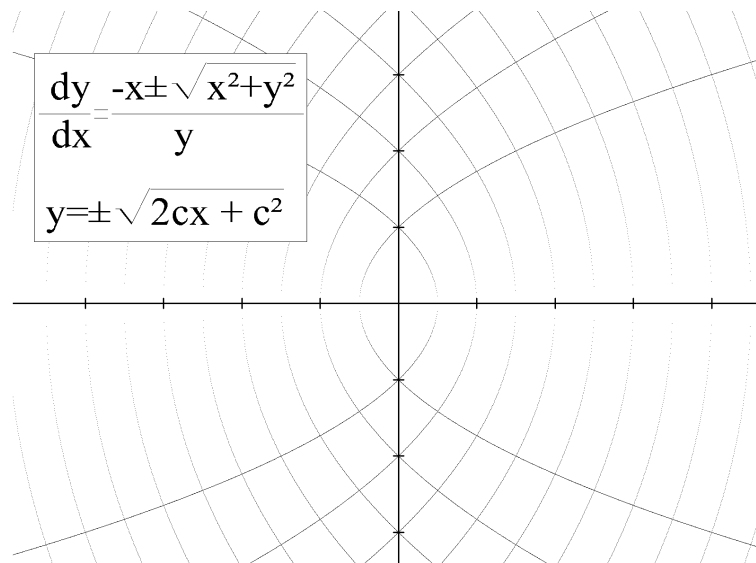


Figure 2.6: Graphic representation of a parabolic ODE. The ODE above happens to be a parabolic curve. It is ordinary because only derivatives with respect one variable appear (dx), and first order because there are only first derivatives in the equation (dy/dx). Its exact solution (analytically obtained) is the integral below. For each one of the possible values of c there is one possible curve. The whole set of possible curves is the general solution of the ODE. A particular value of c would define an Initial or a Boundary Problem.

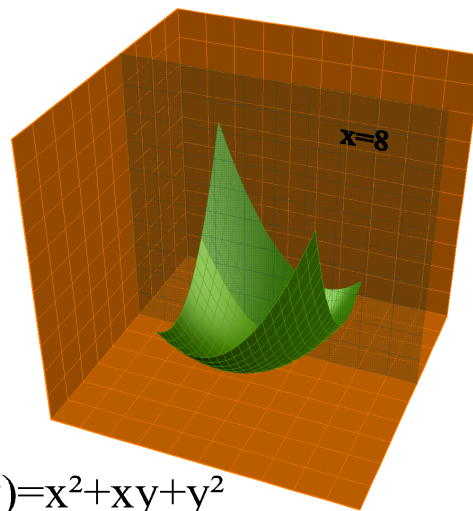


Figure 2.7: Graphic representation of partial derivation. The function above has two independent variables (x and y). By fixing one of them (in the picture, $x=8$), we get the curve $f(y)=64+8y+y^2$. This curve we can derivate, hence obtaining the partial derivative of $f(x,y)$ with respect to y .

- Partial Differential Equations (PDEs): A PDE is a relation u of several independent variables x,y,z,t,\dots and the partial derivatives of the relation with respect of these variables. A partial derivative of a function is its derivative with respect to one of its variables, with the others held constant. As an illustrative example, the graph of a function of more than one variable defines a surface when represented into Euclidean space (figure 2.7). In the literature, second order PDEs

are commonly classified as one of three types, with terminology borrowed from the conic sections, given the resemblances of their formulas with that of the conics: Elliptic, Hyperbolic and Parabolic.

2.1.2.2.- Linear Algebra

Linear algebra studies vectors. Its main structures are linear maps (functions that input vectors and output others) and vector spaces. For their representation matrices are typically used.

- **Linear equations:** Linear equations are algebraic relations in which each term is either a constant or the product of a constant and a single variable. If the power of the single variable is higher than one, then the equation is not considered linear any more, becoming quadratic (second power), cubic (third power), quartic (fourth power), etc. Linear equations can have one or more variables. When this happens they commonly group in a collection of equations that is easily representable in a matrix form. These matrix representations of the systems allows for algorithms such as Gauss or Gauss-Jordan leading to their solution.
- **Matrix algebra:** these allow for a clean and straightforward manner of representing linear equations and transformations. Thanks to the modern computational tools, the tedious work of operating with them (addition, multiplication, inversion, etc,) is greatly facilitated to the engineer and the researcher. Nevertheless, for the study of structural dynamics it is necessary to be proficient in more advanced notions such as matrix pseudo-inverse and null space or kernel (utilized for the solution of linear equations), determinant (useful to characterize invertible square matrices), eigenvectors (those vectors whose direction is not affected by being multiplied with a square matrix), and eigenvalues (the magnitudes by which eigenvectors are scaled). These concepts are extensively used throughout the literature and generally non-trivial.
- **Matrix Decomposition:** A matrix can be decomposed into a product of matrices of special types, for an application in which that form is convenient (i.e. getting a system solved). This can be achieved either via direct or iterative methods. Standard direct methods use some matrix decomposition and comprise:
 - Gaussian elimination
 - LU decomposition
 - Cholesky decomposition for symmetric and positive-definite matrix
 - QR decomposition for non-square matrices.

Iterative methods try to find the root of the system of equations by successive approximations

starting from an initial guess. These are generally the only choice for nonlinear equations. The most utilized are:

- Jacobi
 - Gauss–Seidel's
 - Newton-Raphson
 - Successive over-relaxation
 - Conjugate gradient
 - Monte Carlo iterations
-
- Computations: Once associated to a matrix, there are other types of operations that can be made out of sets of linear equations, generally as sub-steps to the final purpose of solving them. When the set of equations is larger than the set of unknowns (i.e. the system is overdetermined), the method of the Least Squares can be used, either in its linear or non-linear form, to approximate the solution of the system. It is also possible to perform a Gram-Schmidt process over the system in order to orthonormalize its matrix, leading to a further QR decomposition and its eventual solution. The process of solving special kinds of systems by means of Monte Carlo iterations also requires some pre-processing in order to render a matrix into an equivalent, solvable one.

2.2.- Methods for numerical integration of the equations of structural dynamics

In the previous chapter the conceptual elements required for understanding the dynamic behaviour of structural systems were briefly introduced. Here, an overview of the most relevant particular methods will be provided.

For the simulation of structural dynamics three different physical concepts need to be integrated: time, kinematic constraints and matter. Each one of these notions involves the simultaneous solution of Ordinary Differential Equations (ODEs), Differential-Algebraic Equations (DAEs) and Partial Differential Equations (PDEs), respectively. Their relationship to the areas of knowledge introduced in the previous chapter is illustrated in figure 2.8.

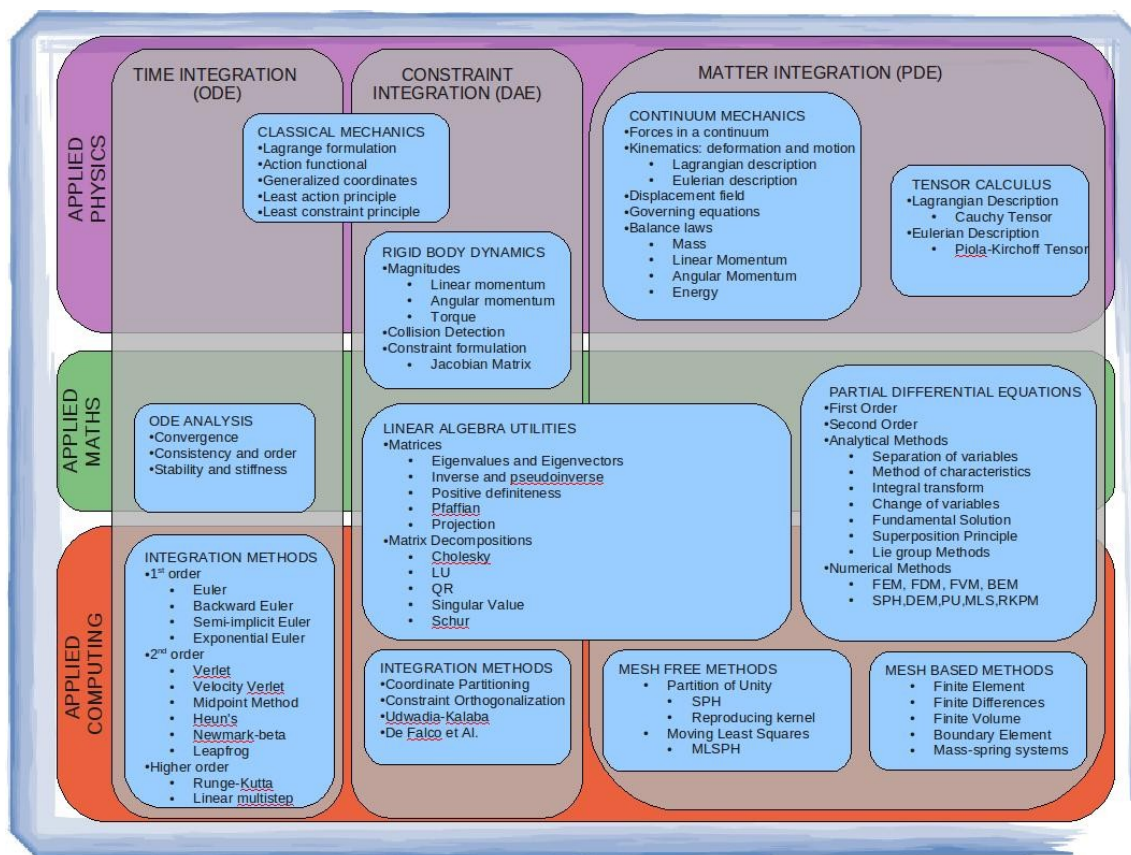


Figure 2.8: Visual display to the relationships between knowledge disciplines and numerical integration methods of the different kind. The complexity of the topic is better understood by grouping the different methods/principles around the physical concepts they solve.

The three main parameters that concern the engineer performing numerical simulations are the accuracy of the solution, the stability of the simulation and the efficiency of the calculation. The first problem derives from the fact that computational precision is finite, whereas the physical/mathematical models are

continuous hence only approximations to the behaviour can be obtained. By stable is meant that small errors due either to arithmetic inaccuracies or to the approximate nature of the derivative expressions will not accumulate and grow as one proceeds. Efficiency involves the speed of calculation and the occupied memory, which are also very sensitive to the design of the algorithms.

Generally, an early analytical approach is preferred to skip numerical issues along with the achievement of higher levels of precision. Nevertheless, the general problem of obtaining only approximations are inherent to the very description of any model and to any method.

For a dynamics simulation to occur at least time and continuum (ODEs + PDEs) or time and constraints (ODEs + DAEs) have to be integrated.

2.2.1.- Time Integration Methods: ODEs

Standard introductory differential equation courses focus on symbolic solutions, in which the functional form for the unknown function is to be guessed. In contrast, we will be concerned exclusively with numerical solutions, in which we take discrete time steps starting with the initial value of the position.

The first possible classification for ODEs solvers distinguishes between explicit, implicit and hybrid methods. Explicit methods are the most immediate to formulate, but present the problem of the so called numerical stiffness. Stiff ODEs require that the size of the adopted time step be so small that the time to convergence never arrives, or otherwise adopt time steps so large that the simulation becomes unstable. The stiffness can be produced by the physical characteristics of the multi-body system (components with large differences in their masses, stiffness and/or damping). However in many other instances, stiffness is numerically induced due to either the discretization process, the large number of components and equations of motion, or sudden or accumulated violations in the constraint conditions. The advantage of implicit methods is that they are usually more stable for solving a stiff equation, meaning that a larger step size can be used. However, extra computations need to be done internally and it requires extra time. Hybrid methods will not be covered in this thesis.

Another division is made according to the order of the derivative of the equation of motion employed. So a method is characterized as first, second, third or higher orders accordingly. The higher the order the more accurate the result would be, though it limits the span of possible time steps due to instabilities.

The third possibility is that of the method being Single or Multi-Step. Single-step methods refer to only one previous point and its derivative to determine the current value. Multi-step methods attempt to gain efficiency by keeping and using the information from previous steps rather than discarding it. Consequently, multi-step methods refer to several previous points and derivative values. In the case of linear multi-step methods, a linear combination of the previous points and derivative values is used.

The following does not intended to be a fully comprehensive list of methods but an illustration of the main issues that arise in the numerical computation of Ordinary Differential Equations applied to the specific field of Dynamics. A more detailed overview can be found in [PRE1992].

In the following chapter, variational integrators will be introduced as an alternative formulated from Hamilton's principle of least action rather than integrating an ODE or a PDE. Variational integrators are a class of integration methods for Lagrangian systems that result in good energy behaviour and conservation of momentum. These conservative properties makes them very attractive for they allow more accurate simulations at larger time steps [WES2004].

2.2.1.1.- Explicit Methods

Explicit methods use the the differential equation at time t to predict a solution at time $t+dt$. In structural dynamics, where stiff equations often arise, the required time step is very small to avoid unstabilities. Explicit methods are hence conditionally stable with respect to the time step size.

E Forward/Explicit EulerMethod (**EE**): In practical terms this method is never utilized as it presents problems of stability and accuracy, but has been included here for its pedagogical value. It is devised considering that from any point on a curve, it is possible to find an approximation of a nearby point on the curve by moving a short distance along a line tangent to the curve [MAR2009].

F Explicit Runge-Kutta Methods (**ERKn**): The basic idea of this family of methods is to eliminate the error terms by evaluating the function in points located half way and including them in the current step. Higher order Runge-Kutta methods exist, being the 4th order Runge-Kutta the most commonly used. An n order Runge-Kutta implementation requires n evaluations of the function per step, so for most problems four is a good compromise between computational cost and accuracy. A mnemonic device known as Butcher's Tableau is used to arrange the data necessary to describe the different methods. The original formulation is that of a single step solver. In general this is adequate for non stiff problems and provides an acceptable level of accuracy. Lower order formulations provide lower accuracy [FIT2006]. Explicit Euler's method (**EE**) can be also considered a 1st order Runge-Kutta. Dormand-Prince method (**RKDP**), Fehlberg method (**RKF**) and Cash-Karp method (**RKCK**) are slight variations on this method.

G Adams - Bashfort – Moulton Method (**ABM**): This methodology employs multiple previously recorded steps to achieve a solution, hence being more efficient. Initial values need to be provided and are usually obtained from a Runge-Kutta scheme. It also presents an acceptable level of accuracy depending on the chosen step size and is meant to solve non stiff systems. Shampine-Gordon method

(**SG**) is based on this methodology [BUT2008].

H Chung-Hulbert method (**CH**): This algorithm is devised for structural dynamics calculations where high frequency dissipation is needed. It uses a set of parameters to enable treating physical damping explicitly without reducing the accuracy [CHU1993].

I Leapfrog / Velocity Verlet Method (**LF**): Leapfrog integration is a simple method for integrating differential equations, particularly in the case of a dynamical system. The method is known by different names in different disciplines. In particular, it is similar to the Velocity Verlet method, which is a variant of Verlet integration. Leapfrog integration is equivalent to calculating positions and velocities at interleaved time points, interleaved in such a way that they 'leapfrog' over each other. For example, the position is known at integer time steps and the velocity is known at integer plus half time steps [BUT2008].

2.2.1.2.- Implicit Methods

For implicit methods the strategy consists on satisfying the differential equation at time t once the solution at time $t-dt$ is available. This requires the solution of a set of linear equations at each time step, but allows for larger time steps and gives further stability or even unconditionally stable schemes [WIL1996].

A Backward/Implicit Euler Method (**IE**): While forward Euler takes a step along the derivative at the current time and position the backward Euler method uses almost the same time stepping equation, but with an extra step. Backward Euler chooses the step, k , so that the derivative at the new time and position is consistent with k . Doing this requires solving this equation for k , which amounts to a root finding problem if $f(x)$ is nonlinear. The forward Euler step is a common place to start the root finding iteration [MAR2009].

B Implicit Runge-Kutta methods (**IRK n**): Implicit Runge-Kutta methods are usually more stable than any explicit method of the same family. The simplest example of an implicit Runge-Kutta method is the backward Euler method enumerated above. Crank-Nicholson method (**CN**), also known as the trapezoid method is another example of implicit Runge-Kutta methods [CRA1947].

C Gear's / Backward Differentiation Formula Method (**BDF**): BDFs are formulas that give an approximation to a derivative of a variable in terms of its function values and earlier times (hence the "backward" in the name). They are derived by forming the k -th degree interpolating polynomial approximating the function using the values up to the k -th value, differentiating it, and evaluating it.

Despite of being multi step, this is a generally less efficient method than RK4 of ABM. It is also often utilized for the solution of stiff problems and of Differential Algebraic Equations (DAEs) [GEA1984].

D Newmark-Beta Method (**NB**): The Newmark-Beta method is a particular one of several time-step methods originally proposed by Newmark in 1959. It is commonly used for the solution of linear and non-linear equations and uses a numerical parameter designated as Beta. It is devised specifically for structural analysis. The general method additionally contains a second parameter Gamma. Particular values of these parameters leads to well known methods for the solution of the differential equation of motion. Newmark's algorithms are unconditionally stable for linear problems, but only conditionally stable for non linear problems [BRA1998]. The Hilbert-Hughes-Taylor method (**HHT**) is a generalization of the Newmark-Beta method.

2.2.2.- Kinematic Constraints Integration Methods: DAEs

When bodies are subject to kinematic constraints, further equations besides to the purely time-related ones have to be satisfied. These constraints come in the taste of contacts between different bodies or as joints in particular chain configurations (planar constraints, cylindrical, spherical, rectangular, revoluted or screw joints, etc). These chains can be opened or close, hence facilitating the use of optimized types of algorithms for the solution of the DAEs.

In order to numerically tackle these conditions the equations of motion are rearranged to obtain different schema from which construct stable, accurate and faster formulations. The possibilities encountered in the literature are to do it either in the acceleration level, the velocity level or the position level.

2.2.2.1.- Acceleration level schema

This is the most common, “classic” approach utilized to solve the constraint equations. The methods using this approach are considered Constraint Based. By means of this, at the beginning of each time step the internal forces (elastic, viscous or pressure) and the external ones (gravity, collisions, etc) are computed and accumulated. Then, by means of Newton's second law, they are transformed into accelerations and then velocities and positions are updated for each integration time step. Given the tendency to numerical drift shown by these approaches, stabilization techniques are generally accessories to them, being Baumgarte's the most popular one [BAU1972].

A Penalty method (**PM**): This method adds a force to a multi-body system, if a constraint is not satisfied. The magnitude and direction of this force depends on the constraint violation. This numerical integration algorithm has the advantage of being much simpler than those shown below corresponding to other methods. However, it may not be the most efficient. In addition, as the numerical integration

proceeds using this algorithm, the constraint conditions are progressively violated leading to unacceptable results in all but very short simulations. [JAL1994]

B Lagrange Multipliers(LM): The Lagrange multipliers are numerical artifacts (additional algebraic variables) that enforce constraint conditions between the elements. Rather than eliminating the multipliers and obtaining coupled system coordinates, the values of the Lagrange multipliers are solved in time as part of the numerical technique. The constraint equations are included into the acceleration term by derivation of them twice with respect to time. It allows for the solution of the dynamic problem at the expense of solving for an augmented set of $(n+m)$ unknowns [JAL1994, BLE1981].

C Reduced Coordinates Method (RC): A reduced-coordinate formulation provides a more accurate simulation. Holonomic (redundant) constraints reduce the degrees of freedom of a multi-body system permanently. This property is used by reduced-coordinate methods. For a multi-body system a parameterization is required to reduce the number of coordinates that describe the system's state to a minimum. For each degree of freedom one coordinate is needed [BEN2007].

D Udwadia-Kalaba formulation (UK): This method represents a more compact and general form of solving the DAEs by means of the Moore-Penrose generalized inverse matrix. It is based on Gauss' Principle of Minimum Constraint, which establishes that the explicit equations of motion be expressed as the solution of a quadratic minimization problem subjected to constraints, but at the acceleration level [UDW1992].

2.2.2.2.- Velocity level schema

Originated by the necessity of efficiently handle the collision constraints, these methods utilize the notion of impulse as a fast acting force, hence they are more commonly known as Impulse Based methods. In this approach, forces are systematically replaced by impulses so that no complex differential equations need to be solved. It is achieved thanks to the fact that the integration of a force over a time interval results in a change of impulse, hence the name.

A Impulse Based Method (IB): Generally applied for the simulation of rigid solids and their collisions, its advantages include simplicity, robustness, parallelizability, and an ability to efficiently simulate classes of systems that are difficult to simulate using constraint based methods. The accuracy of impulse based simulation has been experimentally tested and is sufficient for many applications [MIR1996, BEN2007]. Currently under very active development, results particularly popular among

the Computer Graphics community given their remarkable speed.

B Tethered Particle System (TPS): For the simulation of deformable biological structures, tethered particle systems capture the gradual process of deformation by means of instantaneous impulses occurring in response to particle collisions. Unlike many other methods described above, requiring solutions to systems of equations or inequalities, all the calculations in a TPS simulation are analytic [GOL2011].

2.2.2.3.- Position level schema

This paradigm integrates the equations of motion directly from the position terms. This permits avoiding the appearance of DAEs as geometric constraints get inserted in a straightforward manner as projections without further need of derivation. This skips many drifting problems caused by the numerical integration of differential terms. It offers a certain amount of generality, as a wide variability of geometric constraints can be added without considering conservation laws, etc [KEL2010, MUL2006]. This is also a very recent line of research still subject to a good deal of discussion among Computer Graphics developers.

2.2.3.- Matter Integration Methods: PDEs

To describe the dynamics of matter we have an infinite number of degrees of freedom because the particles that conform them can have arbitrary displacements with respect to each other. Such systems are described using partial differential equations where time and spatial coordinates are related. These general partial differential equations, which are applicable to any solid or fluid material, were outlined in the first section of this chapter. For their solution, two different approaches can be taken in order to control the number of degrees of freedom (i.e. discretize): creating a mesh where these displacements are limited (mesh based methods) or establishing the equations in the form of potential functions so the particles regulate each other (mesh free methods) [LIU2003a].

2.2.3.1.- Rigid Body Models (RBM)

Rigid Body Models (RBM) are idealizations of solids of finite size in which deformation is neglected. This is the simplest approach to modelling the continuum and implies that no PDEs are integrated. Rigid bodies, in contrast to particles, occupy space and have geometrical properties (centre of mass, moments of inertia, etc.). These properties characterize motion in six degrees of freedom (translation in three directions plus rotation in three directions). When rotational motion is important, but material deformation does not have a significant effect on the motion of the system it is broadly utilized for modelling physical systems and machinery. The generated geometric models are commonly built taking into account the later ease of computation of collisions between bodies.

2.2.3.2.- Mesh based Methods

As mentioned earlier the governing equations of continuum mechanics present two main possibilities: Lagrangian description and Eulerian description.

In the Lagrangian description, the material quantities mass, energy and momentum move along with the mesh cells. Because the mass within each cell remains fixed, no mass flux crosses the mesh cell boundaries. When the material deforms, the mesh deforms accordingly [LIU2003b]. This description results efficient for computational solid mechanics problems, where small deformations occur, but is very difficult to apply when the mesh is heavily distorted. Also, the level of accuracy depends on the smallest element size, not on the chosen time step, leading to then less efficient solutions such as re meshing. It is typically represented by the Finite Element Method (FEM).

In the Eulerian scheme, the grid is fixed in space and the changes in material flow across. The shape and volume of a mesh cell remain unchanged along the whole simulation. However, the dependence on a regular grid is a source of trouble when dealing with irregular or complex geometry aiming for the precise location of inhomogeneities, free surfaces, deformable boundaries and moving interfaces. The main exponent of the Eulerian description is the Finite Difference Method (FDM).

There is still a third possibility aimed to strengthen the advantages of both while avoiding their drawbacks. These are the Arbitrary Lagrange Eulerian and the Coupled Eulerian Lagrange, but given their complexity will not be covered here.

A **Finite Element Method (FEM)**: There are over 11,000,000 references to the FE method in the world wide web. Naturally, a section dedicated to the method can only cover some highlights of it and introduce some of the more basic concepts and approaches. FEM's mathematical abstraction of a structure is that of a continuum body being formed by a set of points called nodes with certain mechanical properties. For FEM analysis the body is divided into elements. Assuming that these elements are small one can use low-order polynomials to describe the set of vectors that describe the change of the element from one configuration to another (its displacement field). Once the polynomials are introduced the entire body equations of motion can be obtained by assembling those of its elements using the connectivity conditions at the finite element boundaries. In the literature there are many finite element formulations that are developed for the deformation analysis of mechanical, aerospace, structural, and biological systems. Some of these formulations are devised for small-deformation and small-rotation linear problems (dominating in structural analysis), some for large-deformation and large-rotation nonlinear analysis, and others for large-rotation and small-deformation nonlinear problems. This provides a very rich set of powerful tools that, however, presents some well known limitations [LIU2003b, BEL1996, VID2004]:

- The dependence on nicely formed meshes consumes a substantial quantity of manpower.
- In stress calculations, the stresses obtained using FEM packages are less accurate.
- When handling large deformations, considerable accuracy is lost because of element distortions.
- Crack growth with arbitrary and complex paths has to be coincident with nodal lines, which is never known a priori.
- As FEM is based on continuum mechanics, fragmentation is very difficult to represent, hence many discontinuous materials can not be accurately modeled.
- The interfaces between bodies of different material properties and their coupled behavior is not completely accurate.

The answer to these limitations seems to be in the adaptive re-meshing approaches, that however only serves well on 2D meshes and also consumes a very high amount of computational power.

B Finite Differences Methods (FDM): Finite Difference methods apply a grid over the region and solve the Partial Differential Equation by approximating the derivatives via the Taylor series expansion and using differences as an approximation. For this method it is important that a uniform grid is applied over the region in order to reduce errors by the differencing method. FDM are thus less robust for irregular shaped bodies than finite element methods which divide the region into separate elements to fit the region and use a variational approach to solving the PDE. The benefits of FDM is that it is easy to understand, easy to explain, easy to program, meshing is simple, and the error is known in terms of the remainder from the Taylor series expansion of the derivatives. It used to be commonly used in fluid dynamic methods mainly because of its stability [NEA2005].

C Finite Volume Method (FVM)

The finite volume method is a discretization method which is well suited for the numerical simulation of various types of conservation laws (elliptic, parabolic or hyperbolic, for instance). It has been extensively used in several engineering fields, such as fluid mechanics, heat and mass transfer or petroleum engineering. Some of the important features of the finite volume method are similar to those of the finite element method: it may be used on arbitrary geometries, using structured or unstructured meshes, and it leads to robust schemes [EYM1997]. The implementations of FVM methods for Computational Solid Mechanics can be classified into two categories: the cell centered approach and the cell-vertex one. In the cell-vertex approach, the displacement and stress variables are stored at the vertexes of the mesh which are themselves enclosed by control volumes formed by the median duals of the mesh; whereas in the cell-centered method the variables are stored at the centroids of cells which are also used as control volumes

themselves. Thus the cell-vertex approach needs considerably less computational effort and memory for a given mesh.

D Mass-spring systems (**MSS**)

Mass-spring systems have been widely used in computer graphics because they provide a simple means of generating physically realistic motion for a wide range of situations of interest. Even though the actual mass of a real physical body is distributed through a volume, it is often possible to simulate the motion of the body by lumping the mass into a collection of points. While the exact coupling between the motion of different points on a body may be extremely complex, it can frequently be approximated by a set of springs. As a result, mass-spring systems provide a very versatile simulation technique. In most particle systems, the forces derived from internal strain energy are equivalent to spring forces. Hence, we can view the model as a network of particles connected by springs. Since particle systems already represent a discretization in space, only a system of ordinary differential equations has to be solved. The trajectory of each particle with mass m at position x is computed by Newton's equation of motion.

2.2.3.3.- *Mesh free Methods*

The key idea of the mesh-free methods is to provide accurate and stable numerical solutions for integral equations or PDEs with all kinds of possible boundary conditions from a set of arbitrarily distributed nodes (or particles) leaving aside any mesh that provides the connectivity of these nodes or particles. One important goal of the initial research is to modify the internal structure of the grid-based FDM and FEM to become more adaptive, versatile and robust. Much effort is concentrated on problems to which the conventional FDM and FEM are difficult to apply, such as problems with free surface, deformable boundary, moving interface (for FDM), large deformation (for FEM), complex mesh generation, mesh adaptivity, and multi-scale resolution (for both FDM and FEM). Recently, a number of mesh-free methods have been proposed for analysing solids and structures as well as fluid flows. These mesh-free methods share some common features, but are different in the means of function approximation and the implementation process.

The following is not a fully comprehensive list but just a short enumeration of the most important mesh-less methods available according to literature [VID2004, EYM1997, LIU2003b].

A Smoothed Particle Hydrodynamics (**SPH**)

In the SPH method, the state of a system is represented by a set of particles which possess individual material properties and change according to the governing conservation equations. SPH was developed for hydrodynamics problems in the form of PDEs of field variables such as velocity,

density, energy, etc. To achieve the numerical solution of the mentioned PDEs one needs to discretize the problem domain where they are defined. Next, a method for obtaining the approximated values and time derivatives at any point is need. The function approximation is then applied to the PDEs to obtain a set of ODEs in a discretized form with respect only to time. This set is then solvable by using one of the standard time integration methods described in previous chapters.

B Diffuse Element Method (**DEM**)

An alternative but related approach to developing a meshless approximation is to use a moving least square approximation. Moving least squares is a method of reconstructing continuous functions from a set of unorganized point samples via the calculation of a weighted least squares measure biased towards the region around the point at which the reconstructed value is requested. In computer graphics, the moving least squares method is useful for reconstructing a surface from a set of points. Often it is used to create a 3D surface from a point cloud through either downsampling or upsampling. This was employed by Nayroles and Touzot in 1992 to interpolate the material properties among nodes of a structre without need of predefining a mesh [NAY1992].

C Element Free Galerkin Method (**EFG**)

This method is an extension of the previous one in terms of mathematical rigour and accuracy. However, it still requires the definition of a series of background cells for the definition of quadrature point. This eliminates its mesh-less characteristics and results in a computationally more expensive procedure. Besides, this method can yield non-positive definite systems of equations, reducing even further the efficiency.

2.2.4.- Evaluation of numerical methods

Tables 2.1 to 2.3 present in a condensed manner the methods enunciated above (abbreviations can be found in bold letters in the previous section). These tables intend to facilitate an approximated evaluation and comparison over the four most relevant aspects regarding numerical methods: accuracy, stability, efficiency and ease of implementation.

The values range between one and three points (one for low and three for high) for the sake of generality and correspond solely to the informed opinion of the author of this thesis. It is important to keep in mind that there is not an easy manner to objectively compare numerical methods. This explains why most references in literature focus on particular applications for particular methods. Conclusions obtained from these works are commonly too specific for our purposes. Chapter 2 of this thesis will try to address this situation by applying energetic principles to the comparison of some of the methods presented here.

In terms of accuracy and stability ODE solvers depend directly on the time-step parameter and the order of the derivative. Paradoxically however, the higher the degree of accuracy of the simulation the smaller becomes its stability field.

For DAE methods, accuracy is directly affected by the previous choice of ODE parameters (time-step primarily). Besides, as they operate in the formulation level, for each of them exists a particular set of parameters. For instance the Penalty Method gains accuracy the more its penalty parameter approaches infinity. This value is obviously limited by the computer capabilities. Impulse Based methods require an extra iterative sub-process whose convergence is limited as to the type of problem to be solved.

Regarding the accuracy of PDE solvers, the main defining factor is the density of the mesh for mesh based methods, and the density of interpolation points in the mesh-free schema. But also the form of the characterizing functions and polynomials should be finely tuned according to different problems. Adjustment of these parameters depends highly on the choice of the analyst at the time of modelling, not so much in the method itself.

In terms of efficiency, in ODE methodologies there are obvious advantages for explicit schemes as they do not require extra computations. Implicit solvers, however, keep a higher degree of stability for larger time steps, which makes them eventually more attractive in simulations where low resolution is sufficient.

DAE methods generally involve extra algebraic sub steps, which are determinant in their computational cost, but they are not always applicable to every type of problem. For example, the Lagrange Multipliers method results in an expansion of the underlying system of linear equations that, depending on the number of constraints, can be computationally more expensive. However, this expansion reduces the potential numerical instability arising sometimes in the Reduced Coordinates method.

PDE methods have their most simplistic approach in the form of rigid bodies, where no differentiation nor operation is made, being the mesh free methods the least efficient as state computations have to be made over the whole population of approximating points on each time step.

Ease of implementation for each method is not only reflected in the number of sub algorithms contained but also in the conceptual background, intuitiveness of their inherent principles and availability of information on how they work.

In general ODE methods are broadly available, extended and well documented, but given their generality it can result difficult to discriminate when to apply them for particular problems.

DAE methods are often entangled within the very formulation of ODE methods in some applications, and their mathematical approach and explanation results often awkward and counter intuitive.

PDE methods range from the easiest Finite Difference to the very complex formulations of Finite

Elements and Smoothed Particle Hydrodynamics. In general, these are the most mathematically involved.

Table 2.1: Summary of ODE / Time integration methods

Scheme	Method	Accuracy	Stability	Efficiency	Ease of implementation
Explicit	EE	*	**	***	***
	ERKn	**	**	**	***
	RKDP	**	***	***	**
	RKF	**	***	***	**
	RKCK	**	**	***	**
	ABM	**	**	***	**
	SG	**	**	***	*
	LF	**	**	***	***
Implicit	IE	**	**	**	**
	IRKn	**	**	**	*
	CN	***	***	**	*
	BDF	***	***	**	*
	CH	***	***	***	*
	NB	**	**	**	**
	HHT	**	**	**	*

Table 2.2: Summary of DAE / Constraint integration methods

Scheme	Method	Accuracy	Stability	Efficiency	Ease of implementation
Acceleration	PM	*	*	***	***
	LM	**	**	*	***
	RC	**	**	**	**
	UK	***	***	**	*
Velocity	IB	**	***	**	***
	TPS	**	**	**	*
Position	PBD	**	**	**	***

Table 2.3: Summary of PDE / Matter integration methods

Scheme	Method	Accuracy	Stability	Efficiency	Ease of implementation
Rigid Body	RB	*	***	***	***
Mesh based	FEM	***	***	**	**
	FDM	**	***	**	**
	FBM	**	***	**	**
	MSS	***	***	**	**
Mesh free	SPH	***	***	*	**
	DEM	***	***	*	*
	EFG	**	***	*	*

2.3.- Industry tendencies

Table 2.4 enumerates some different scientific and engineering fields. By means of a sample of selected representative packages (either commercial or open source), and exposing the numerical methods in them implemented, it is shown how these industries are related to the integration concepts described in the previous section.

Table 2.4: Comparison of different disciplines, methods and implementations.

Field of Original Application / Industrial Background	ODE	DAE	PDE	Implementation Name
Mechatronics/Robotics	SG / ERK3 / ERK4 / ERK5	GC	FEM	SPACAR
	ERKF2 / ERKF3 / ERKF4 / ERKF5 / RKDP / ABM / BDF	GC / LM	RBM	Sim Mechanics
Aerospatial	CN / IE / BDF	LM	FVM	MBDyn
Automotive	ERK2	LM	RBM	SimCreator
	BDF / ABM / ERK4	IB / LM	FEM	Universal Mechanism
Games / Graphics / Animation	EE	IB	RBM	ODE
	ERK4	IB / LM	RBM	IBDS
	EE	IB	RBM / MSS	Havok Physics
Multiphysics	ERK5 / IRK4	LM	FVM / FEM	OpenFOAM
	BDF / ERK4 / ERK5 / IE	LM	FEM	COMSOL
Medical / Biomechanics	EE / ERK2 / ERK4 / IE	PM / IB	MSS / FEM / RBM / SPH	SOFA (Simulation Open Framework Architecture)
Structural Engineering	NB / HHT / IRK / CH	GC	FEM	SAP2000
	NB / IE / HHT / IRK2	PM	FEM	DIANA
	Explicit unspecified	LM / PM	FEM / FVM / SPH	EUROPLEXUS
	ERK4 / ERK5 / CN / NB	LM / PM	FEM / FVM / SPH	ANSYS
	NB / HHT	GC / PM / LM	FEM	ABAQUS FEA

The selection of implementations was made purely with illustrative purposes, so many other important and well established names may have been omitted. A complete survey on the matter of computer software for structural dynamics would be the topic for a much longer thesis and is left open by the author.

It can be appreciated how mechatronics, robotics and aerospace oriented packages, where a high level of accuracy and stability is compulsory, facilitate analysts a wide range of time solvers, whether implicit and

explicit, and rely on the more “classical” acceleration based methods for enforcing the constraints. The integration of continuum mechanics ranges from the simplistic Rigid Body Models, utilized in robotics, to the Finite Volume Method that allows for easier implementation of flow-solid interactions.

Automotive simulators and game engines, where real time experience and computer efficiency are the main concerns, make a wider use of explicit time integrators (lower accuracies), impulse-based methods (higher speed) to compute the constraints and show a dominating presence of the simpler Rigid Body Models. Also in the automotive field safety simulations and prototyping need top be carried away, hence the use of implementations with more sophisticated methods such as FEM.

Multiphysics packages, by means of which highly complex interactions are analysed (thermal, dynamic, electrical, etc.) utilize mostly FEM given its versatility in the solution of PDEs. General purpose time integrators either implicit and explicit are present, given the broad scope of these applications.

When it comes to health environments, where the level of detail is focused on complex tissue-like materials, the span of choices regarding matter integrators grows considerably. Given the need for real time interactivity in surgical simulations, the span of ODE integrators is fairly broad, along with the faster impulse based constraint solvers. Human limbs are approximated by means of Rigid Bodies for the study of the behaviour of articulations.

For the Structural Engineering field it is shown the dominance of FEM and the application of very specialized time integrators. It is remarkable how computational cost is not regarded so much as accuracy and numerical stability, as the choice of these integrators along with the more canonical constraint enforcing methods can prove. Also the tendency towards analyzing fluid-structure interactions appears in the form of FVM and SPH methods.

2.4.- Discussion

From the above chapters the interested reader might have achieved some perspective over the entangled subject of structural dynamics. This is an important contribution of this thesis as a comprehensive, clear and accessible introduction to the topic seems to be unavailable at the moment. This happens despite the existence of numerous specialized courses on non-linear structural analysis and also the huge amount of literature produced. It was not found by the author any organized scheme in terms of tangible concepts such as time, matter and constraints.

It is the opinion of the author that unfortunately the tendency appears to be that of over-specialization. It most likely discourages not only the newcomer but also those who try to look up into other branches of the same tree. Another perceived phenomenon is that of the over dominant position of the Finite Element approach, that relegates sometimes unfairly other equally effective methods.

It is suggested here that a better understanding of numerical methods utilized with simulation purposes can provide satisfactory and safe answers to structural engineering needs, as opposed to simplified methods and models. Such simplified methods, often encouraged from regulations and common practice, may have an apparent immediate advantage. However, they tend to obfuscate the global perspective given their tendency to prolificacy.

Table 2.4 enumerates some different scientific and engineering fields. By means of a sample of currently popular packages (either commercial or open source), and exposing the numerical methods in them implemented, it is shown how these industries are related to the integration concepts described in section 2.2.

The table displays how mechatronics, robotics and aerospace oriented packages, where a high level of accuracy and stability is compulsory, provide the user with a wide range of time solvers, either implicit and explicit, and rely on the more canonical acceleration based methods for enforcing the constraints. The integration of continuum mechanics ranges from the simplistic Rigid Body Models, utilized in robotics, to the Finite Volume Method that allows for easier implementation of flow-solid interactions.

Automotive simulators and game engines, where real time experience and computer efficiency are the main concerns, make a wider use of explicit time integrators (lower accuracies), the faster impulse-based methods to compute the constraints and show a dominating presence of the simpler Rigid Body Models. Also in the automotive field safety simulations and prototyping are made, hence the use of implementations with more sophisticated methods.

When it comes to health environments, where the attention is focused on complex tissue-like materials, the span of choices regarding matter integrators grows considerably. However, provided the need of also

efficient time and constraint simulations, more advanced techniques are made available.

Simulations of molecular dynamics mainly happen in academic and research environments (chemistry, biophysics, etc.), and in general do not imply constraints among bodies as the simulated elements are just particles. Explicit time integration is utilized as the common duration in this case is usually no longer than few seconds, hence short time steps can be taken to avoid numerical stiffness problems.

Regarding structural engineering it is shown the dominance of FEM and the application of very specialized time integrators. As computational cost is not regarded so much as accuracy and numerical stability, the choice of these integrators along with the more canonical constraint enforcing ones makes perfect sense within this field.

It permits also to clarify how FEM is a name too much generic for a very broad field of simulation tools. The fact that an implementation contains a continuum mechanics PDE solver by means of the FEM doesn't make this engine into a FEM. It is a common case to find in literature mentions to implicit FEM when describing numerical methods using an implicit ODE integrator where FEM is the method of choice for approximating material behaviour (PDE), regardless how misleading and confusing that might be.

Finally, a benchmarking scheme in the conceptual side of the state-of-the-art methods has been shown for evaluation and comparison. It should serve to locate the level of complexity and accuracy of the implementations used in structural dynamics. Insofar the trend within this discipline seems to be that of sacrificing computational efficiency in benefit of canonical schemes of higher accuracy.

3.- Comparison and study of numerical methods by means of variational mechanics

3.1.- Introduction

In this chapter it will be shown how focusing the structural analysis in energy changes instead of strains and stresses actually gives a better understanding of the studied phenomena. It is not meant to revise the existing variational integration methodologies, as this has already been done somewhere else ([MAR1999], [WES2004], [LEW2003]), but to give them a practical application to a common problem in engineering: the assessment of numerical methods.

As it was shown in the previous chapter, there is a preference in the practice of Structural Analysis to use forces and accelerations rather than energy concepts. Unfortunately this approach often restricts a global understanding of the phenomena, as for example, in the case of earthquakes, damage is a function of the square of the velocity, and not so much of the acceleration [HOU1956].

A consequence of this preference is that the magnitudes of energy and momentum, and the variational principles of mechanics, end up confined to the formulation of the different methods. For their robustness, energy principles are employed in the formulation of PDE methods like Galerkin's and FEM, but they quickly are put aside and in practice only strain and stress relationships are examined.

Variational mechanics date back as far as the Eighteenth Century, when Leibniz, Euler, Maupertuis and Lagrange devised the calculus of variations and the principles of least action. This methodology of treating physical phenomena is based on the notion that everything in Nature tends to a state of minimal energy [LAN1952].

The original formulation, that eventually led to the Hamiltonian theories and the Principle of Stationary Action [HAM1835], was enunciated in a general continuum hypothesis. Recently however, discretized versions of the principle of least action are giving place to a promising modern class of time integration algorithms named variational integrators, or, as they are also known, symplectic or geometric.

By means of the variational approach to the problems of discrete mechanics much of the previous existing literature is now being reviewed under a new perspective. Some of the important topics that come out naturally from this method are symplectic-energy-momentum methods, error analysis, Newmark algorithms, constraints and forcing [MAR1999].

3.1.1.- Targets and interest of our research

In the beginning, a framework based on variational principles will be presented for the assessment of the quality of the numerical methods outlined in the previous chapter. This is meant to reach an audience less familiar with those principles by linking the abstract ideas involved with actual implementation elements.

It will also be proposed a systematic treatment of the numerical methods for structural dynamics in a

comprehensive manner based on the classifications made in the previous chapter. These methods have proliferated since the 1950s with the ever-increasing power of computers and have given place to a cumbersome mix of mathematics, physics and computer science that is often difficult to grasp. In this thesis, it is proposed a categorization according to the physical qualities which they represent instead of according to their mathematical properties.

Eventually, a series of combinations of methods will be compared and assessed under the scope of their energy-conservation properties in a set of non-trivial examples.

3.1.2.- Variational mechanics

According to the principles of variational mechanics [WUN2002], the difference between kinetic energy and strain energy in a structural system equals the applied work due to external forces. In this way, by computing the energy scalars and carefully accounting for this difference at each time step, one should be able to infer the degree of accuracy of a simulation [BUG1991].

The correct values should not in any case diverge much from zero, and deviations from this value would give us an idea about how accurate and stable a method is.

3.1.3.- Numerical methods for structural analysis

In the previous chapter, it was shown how the vast amount of existing numerical methods can be grouped into three main sets according to the kind of physical phenomena they represent and the type of differential equations they discretize: matter integration techniques (Partial Differential Equations), constraint integration techniques (Algebraic Differential Equations) and time integration techniques (Ordinary Differential Equations).

Based on this concept, we have chosen the following matter integration implementations: Finite Element (FEM), Finite Differences (FDM), and Mass Spring Systems (MSS). For the constraint integration we will limit ourselves to the Constraint Reduction (CR) technique, whereas in the case of time integration we will study the Newmark Beta (NB), Hilber-Hughes-Taylor (HHT), Chung-Hulbert's generalized-alpha (CH) and Wilson Theta (WTH) methods.

All these time integration methods are available in a general-purpose commercial package, so we were able to establish a comparative reference for our own implementations. In the case of matter integration, we implemented our own algorithms from the literature, and adapted them to our own purposes, also making a previous benchmark of their results with respect to those obtained by the aforementioned software.

3.1.4.- Numerical experiments

Three simple structural models under four dynamic loadings will be tested. The influence of the parameters time step, damping ratio and the number of integration points will be studied.

The work done by the load patterns, along with the internal elastic, kinetic and dissipative energies, will be computed at each time step and combined together to verify the Hamiltonian energy balance. Its integral through time will provide different values of the total Lagrangian action of the structure-loads system. The deviation from a proposed analytical value, whose computation is straightforward, would account for the level of accuracy of the implementations.

It will be shown how, whether used on single elements or complex systems with more elements, this methodology could be employed as a reference since the value of the action is a simple scalar which is easy to monitor.

3.2.- Variational mechanics

3.2.1.- Principle of least action

In variational mechanics, the Lagrangian functional L , describing the dynamics of a system, is given by:

$$L = T - U \quad (3.1)$$

where T and U are the kinetic and potential energies of the system, respectively.

According to Hamilton's definition, action S is the integral through the studied time lapse of the Lagrangian,

$$S = \int_{t^1}^{t^2} (T - U) dt \quad (3.2)$$

The correct path for a dynamic system is the one for which the value of the action integral is stationary. This leads to a minimization problem which is rooted in the variational principles of Lagrange and Euler.

3.2.2.- Euler-Lagrange equation and energy balance

For a single particle-spring system subjected to an external force, the Lagrangian can be written as:

$$L(x, \dot{x}) = \frac{1}{2} m \cdot \dot{x}^2 - \frac{1}{2} k \cdot x^2 \quad (3.3)$$

where m is the mass of the particle, k is the stiffness of the spring, x is the instantaneous position and the superscript dot indicates derivation with respect to time.

From Hamilton's principle of stationary action, and after some variational calculus, the evolution of a physical system is described by the solutions of the *forced Euler-Lagrange equation* for the action of the system:

$$\frac{d}{dt} \frac{\partial L(x, \dot{x})}{\partial \dot{x}} - \frac{\partial L(x, \dot{x})}{\partial x} = Q_{ext}(x, \dot{x}) \quad (3.4)$$

where:

$$\frac{\partial L(x, \dot{x})}{\partial x} = \frac{dU(x)}{dx} = \frac{d}{dx} \left(\frac{1}{2} k \cdot x^2 \right) \quad (3.5)$$

$$\frac{\partial L(x, \dot{x})}{\partial \dot{x}} = \frac{dT(\dot{x})}{d\dot{x}} = \frac{d}{d\dot{x}} \left(\frac{1}{2} m \cdot \dot{x}^2 \right) \quad (3.6)$$

$$Q_{ext}(x, \dot{x}) = -c \cdot \dot{x} + f_{ext}(t) \quad (3.7)$$

Substituting (3.4), (3.5) and (3.6) into (3.3), and derivating (3.4) with respect to time, we get the Newtonian classical formulation:

$$\frac{d}{dt} \frac{\partial L}{\partial \dot{x}} - \frac{\partial L}{\partial x} = m \cdot \ddot{x} + c \cdot \dot{x} + k \cdot x - f_{ext}(t) = 0 \quad (3.8)$$

where the externally applied force f_{ext} is generally known and the velocity dependent damping term is a non-conservative force defined in terms of d'Alembert's virtual work [WAN2012].

3.2.3.- Kinetic energy of a system, T

For a structural system under dynamic forces, the above equations are used in a vector-matrix fashion, where each of the points of the structure and its degrees of freedom are represented as terms of a vector and the mass and stiffness of the whole system characterized by a matrix. This leads to the following expression for the computation of the kinetic term:

$$T = \frac{1}{2} \cdot \{\dot{x}\}^T \cdot [M] \cdot \{\dot{x}\} \quad (3.9)$$

In the present work, the construction of the mass matrix consists in the simple addition of the elements particular masses in their concurrent nodes (lumped mass matrix).

3.2.4.- Elastic potential energy, U

When a body of some material is subject to external forces, its internal structure is deformed. The displacement of these forces in the space are the source of a work.

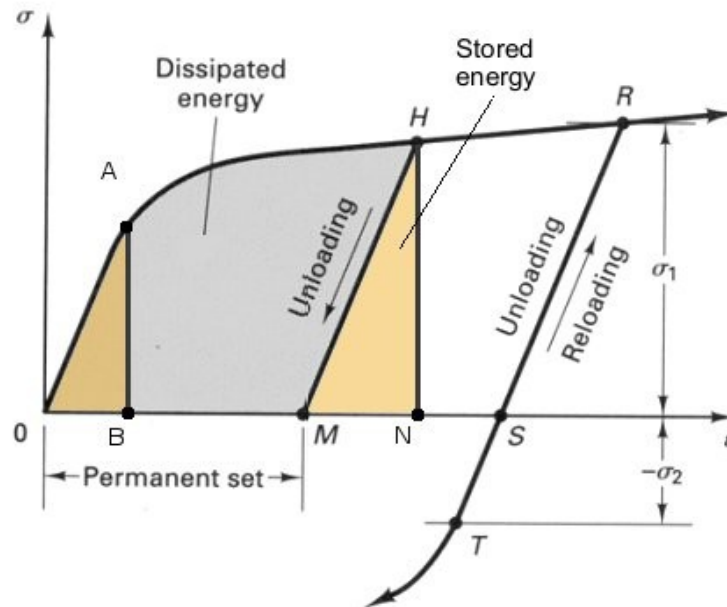


Figure 3.1: Stress-Strain diagram for a typical engineering material. The value of the area of the OAB triangle is the elastic potential energy stored in the material due to strain. The triangle MHN corresponds to a larger strain, passing through the plastic range. Its larger size is due to the “strain hardening” phenomenon.

The scalar value of such work, in order to preserve balance of energy, must be equal to that of the internal forces in the body (stresses) times the internal displacements within the material (strains).

In general, and for any engineering material, this internal energy can be characterized by means of a stress-strain curve like the one depicted above.

Typically these curves present two significant parts, one “elastic” (from point O to point A), with a straight line whose slope corresponds to the material's Young modulus, E, and the remainder being the “plastic” part until final rupture. The area contained within this curve and the abscissas can be accounted for as the total work needed to cause the deformation of the body.

Given the fact that deformation within the elastic range is fully recoverable, we can assume that the same will apply for the energy, so it is considered a potential energy that remains “stored” within the material's volume. Its scalar value totals to the geometric area of the triangle defined by the points OAB in the figure 3.1.

The energy that is not recoverable is commonly dissipated in the form of heat. However, for the sake of simplicity the scope of this article will remain within the elastic range.

3.2.4.1.- Linearisation of the continuum in beams

In engineering practice, the material conforming a beam is modelled under certain simplifications that make possible the linearisation of the continuum's differential governing equations. This is made possible by including in the formulae the geometric properties of the cross section and mass distribution along the beam element.

These differential equations, when linearised into a beam of rectangular section, can be formulated in matrix form as follows [WUN2002]:

Kinematic equations:

$$\begin{bmatrix} \varepsilon_{xx} \\ \gamma_{xy} \\ \kappa_{xy} \\ \gamma_{\phi} \end{bmatrix} = \begin{bmatrix} d_x & 0 & 0 & 0 \\ 0 & d_x & 1 & 0 \\ 0 & 0 & d_x & 0 \\ 0 & 0 & 0 & d_x \end{bmatrix} \begin{bmatrix} u_{xx} \\ w_{xy} \\ \theta_{xy} \\ \phi_x \end{bmatrix} \quad (3.10)$$

Material law:

$$\begin{bmatrix} N_x \\ Q_y \\ M_z \\ T_x \end{bmatrix} = \begin{bmatrix} EA & 0 & 0 & 0 \\ 0 & k_s GA & 0 & 0 \\ 0 & 0 & EI & 0 \\ 0 & 0 & 0 & G \end{bmatrix} \begin{bmatrix} \varepsilon_{xx} \\ \gamma_{xy} \\ \kappa_{xy} \\ \gamma_{\phi} \end{bmatrix} \quad (3.11)$$

Equilibrium equations:

$$-\begin{bmatrix} p_x \\ p_y \\ m_x \\ m_y \end{bmatrix} = \begin{bmatrix} d_x & 0 & 0 & 0 \\ 0 & d_x & 0 & 0 \\ 0 & -1 & d_x & 0 \\ 0 & 0 & 0 & d_x \end{bmatrix} \cdot \begin{bmatrix} N_x \\ Q_y \\ M_z \\ T_x \end{bmatrix} \quad (3.12)$$

where:

ε_{xx} is the axial strain
 γ_{xy} is the shear angle
 κ_{xy} is the moment curvature of the beam
 γ_ϕ is the torsional angle of the beam
 d_x is the d/dx operator
 u_{xx} is the axial displacement towards x
 w_{xy} is the axial displacement towards y
 θ_{xy} is the rotation of the section
 ϕ_x is the torsional rotation of the section
 N_x is the axial stress component
 Q_y is the shear stress component
 M_z is the moment stress component
 T_x is the torsional stress component
 EA is the axial rigidity
 k_s is a section's shape shear constant
 GA is the shear rigidity
 EI is the flexural rigidity
 GJ is the torsional rigidity
 p_x is the external force density towards x
 p_y is the external force density towards y
 m_x is the flexural moment density
 m_y is the torsional moment density

3.2.4.2.- Elastic strain energy in beams

In elastic materials, the stored potential strain energy can be accounted for as half of the integral over the volume of the internal strains times the internal stresses, whose formula [ARG1960]:

$$U_{el} = \frac{1}{2} \int_V \{\sigma\}^T \{\varepsilon\} dV \quad (3.13)$$

where:

$$\{\sigma\}^T = \{\sigma_{xx} \sigma_{yy} \sigma_{zz} \tau_{xy} \tau_{xz} \tau_{yz}\} \quad (3.14)$$

$$\{\varepsilon\}^T = \{\varepsilon_{xx} \varepsilon_{yy} \varepsilon_{zz} \gamma_{xy} \gamma_{xz} \gamma_{yz}\} \quad (3.15)$$

In the case of the linearised beam described above, we can then define four kinds of strain energies according to the four main stress components: axial (N), shear (Q), bending moment (M) and torsional moment (T).

From them, we can develop the analytical formulae for the elastic strain energies within a beam subjected to external loads, referred either to the internal forces or the deformations.

In table 3.1 the final formulae for each one of these strain energy components are enunciated. The given expressions can be either a function of the displacements along the beam or of the input forces.

Table 3.1: Displacement and force based formulae of elastic strain energy in a beam.

	<i>Displacement</i>	<i>Force</i>
<i>Axial</i>	$U_A = \frac{1}{2} \int_0^l EA \left(\frac{du}{dx} \right)^2 dx$	$U_A = \frac{1}{2} \int_0^l \frac{F^2}{EA} dx$
<i>Bending</i>	$U_M = \frac{1}{2} \int_0^l EI \left(\frac{d^2u}{dx^2} \right)^2 dx$	$U_M = \frac{1}{2} \int_0^l \frac{M^2}{EI} dx$
<i>Shear</i>	$U_S = \frac{1}{2} \int_0^l AG \left(\frac{du}{dx} \right)^2 dx$	$U_S = \frac{1}{2} \int_0^l \frac{F^2}{AG} dx$
<i>Torsion</i>	$U_T = \frac{1}{2} \int_0^l GJ \left(\frac{d\theta}{dx} \right)^2 dx$	$U_T = \frac{1}{2} \int_0^l \frac{T^2}{GJ} dx$

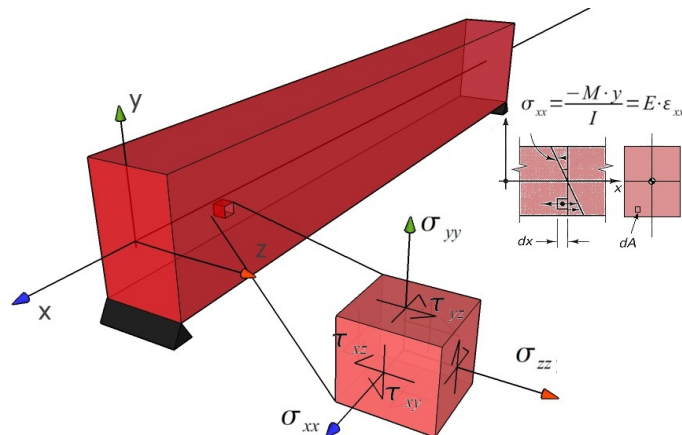


Figure 3.2: Stress-strain components in a beam. The directions of the infinitesimal strains and stresses are arranged according to the length of the beam.

For illustrative purposes, the development of the bending strain formula is provided next. One of the appeals of the energy approach to structural mechanics is the consistency with which problems can be enunciated, being equally applied for 2D or 3D cases.

3.2.4.3.- Bending elastic strain energy

From the small strain beam theory of Bernoulli-Euler, it is obtained that the strain and stress components are respectively, when deformations occur in the XY plane:

$$\epsilon_{xx} = -w_{xy}''(x) \cdot y = -\kappa_{xy} \cdot y = \frac{\sigma_{xx}}{E} \quad (3.16)$$

$$\sigma_{xx} = \frac{-M \cdot y}{I} = E \cdot \epsilon_{xx} \quad (3.17)$$

That substituted into the incremental form of (3.13) lead to the relations (force and displacement based, respectively):

$$dU_B = \frac{1}{2 \cdot E} \sigma_{xx}^2 dV = \frac{1}{2} \frac{M^2 \cdot y^2}{E \cdot I^2} dAdl \quad (3.18)$$

$$dU_B = \frac{E}{2} \epsilon_{xx}^2 dV = \frac{E}{2} (w''(x) \cdot y)^2 dAdl \quad (3.19)$$

that integrated under the assumption that the origin of the coordinate system lies on the neutral axis of the beam and the bending moment of inertia is $I = \iint_A y^2 dA$ results in:

$$U_B = \frac{1}{2} \int_l \frac{M^2}{E \cdot I} dl \quad (3.20)$$

$$U_B = \frac{1}{2} \int_l EI (w''(x))^2 dl \quad (3.21)$$

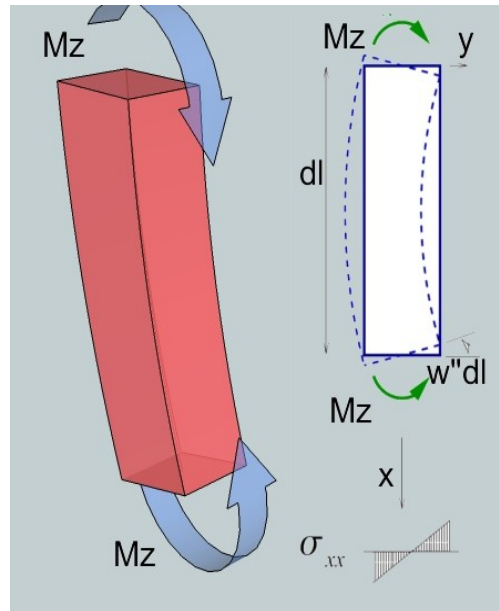


Figure 3.3: Bending of a column. The energy needed to cause elastic deformation is a potential function of the constituent material properties (E), the shape of the section (I) and the exerted force (M).

The remaining formulae from table 3.1 are obtained in a similar fashion, directly from the constitutive equations [ARG1960].

This allows for a coherent manner of treating the different numerical methods of the following chapter, whose formulations are so diverse and in general not possible to benchmark or compare under objective parameters.

For a structural system, where several elements are combined and attached in n nodes, the equations that establish the behaviour of each node with respect to others are defined in the stiffness matrix $[K]$, whose size is n times the number of degrees of freedom. This number can be as large as six, when rotations and displacements are evaluated in all three directions, or just two, when only 2D displacements need to be known.

The coefficients that conform this matrix are obtained through the different matter integration methods (FEM, FDM, MSS, BEM, etc.) by solving the above equations in combination for all three kind of stresses in all three planes. When a model is 2D instead of 3D one simply limits the number of terms in equations (3.14) and (3.15), hence reducing the range of $[K]$.

Eventually, in order to compute the total elastic energy U of the system, we use the following expression:

$$U = \frac{1}{2} \{x\}^T \cdot [K] \cdot \{x\} \quad (3.22)$$

being $\{x\}$ the vector of displacements obtained.

3.2.5.- Work done by dissipative forces

In every real structure the existence of damping is a known phenomenon whose nature is still not fully understood due to its inherent complexity. In order to incorporate it in a simulation, numerical artefacts are created that account for the energetic dissipation that it involves.

In general, a damping matrix $[C]$ is defined that accounts for the dissipative properties of the structural elements. This matrix affects the velocity in the Newton equation as a force acting opposite to the external force.

The work done by this force can be accounted for by means of the following relation:

$$R = \frac{1}{2} \{x\}^T \cdot [C] \cdot \dot{\{x\}} \quad (3.23)$$

The simplest model for dissipation in structural dynamics is due to Lord Rayleigh and is known as 'linear damping', 'Rayleigh damping' or 'classical damping'. In this idealization, the damping matrix is assumed to be a linear combination of the stiffness and the mass matrices. Despite the numerous criticisms this

model receives it is still widely used for its convenience when combined with the modal analysis procedure [ADH2000]. Once the stiffness matrix $[K]$ and the mass matrix $[M]$ are conformed, the damping matrix $[C]$ can be defined as follows:

$$[C] = \alpha \cdot [M] + \beta \cdot [K] \quad (3.24)$$

The value of the coefficients being determined by the solution of the eigenvalues of the $[K]$ matrix [ADH2000].

3.2.6.- Work done by external forces

The total work exerted over the structure by the external applied forces can also be represented in a vectorial fashion as:

$$W_{ext} = \frac{1}{2} \{F_{ext}\} \cdot \{x\} \quad (3.25)$$

Where the vector F_{ext} represents the forces in a global coordinate system.

3.2.7.- Total action of the system, energy balance and the Lagrange-d'Alembert principle

In order to account for the correctness of a simulation, we can utilize the Lagrange-d'Alembert principle⁽¹¹⁾, that establishes the following relation:

$$\delta \int_{t1}^{t2} L dt + \int_{t1}^{t2} F_{ext} \delta x dt = 0 \quad (3.26)$$

If we withdraw the variation operator and rearrange terms this leads to:

$$\int_{t1}^{t2} L dt = - \int_{t1}^{t2} F_{ext} x dt \quad (3.27)$$

Which, in discrete form leads to:

$$\sum_{t1}^{t2} L dt = - \sum_{t1}^{t2} F_{ext} x dt \quad (3.28)$$

Having defined previously each one of the terms, we can now write the elementary formula from which we can estimate the degree of exactness of a simulation:

$$\sum_{t1}^{t2} (T - U) dt = - \sum_{t1}^{t2} (W_{ext}) dt \quad (3.29)$$

This is basically the computation of an energy balance where the Hamiltonian action is treated, in its discrete form, as an average over time of each instantaneous Lagrangian. In order to account for the external forces involved, we also integrate over time their work. According to d'Alembert's principle, these two measures should be equal when internal dissipative forces (hysteretic damping) are not present.

Any divergence from this equality gives a measure on how inaccurate a numerical method is by means of a single value, without the need of finding simplified analytical models whose assumptions rarely fit the real problems of the engineering practice.

3.3.- Numerical experiments

In this section we provide the results of our numerical experiments, where several combinations of methods were used in diverse simulations. Three different specimens of increasing complexity were tested, and some engineering relevant parameters affecting each numerical method were systematically studied (time step, damping ratio and number of integration points).

In order to avoid excessive complexity, the specimens were treated as 2D models and kept within the elastic range, considering the shear effects in deformation to be negligible.

3.3.1.- Studied methods

As explained earlier in chapter 1, for the simulation of structural dynamics three different physical notions need to be integrated: time, matter and kinematic constrains. A series of methods was selected from the enumerated list and the necessary code was written in a custom-made application. These implementations are further described in chapter 5 of this this. In order to assess the correctness of these implementations, a third party general purpose commercial software was also used to make the simulations in parallel with good agreement in the results.

Figure 3.4 is a diagram of a possible sequence of combined methods as they were coded for this thesis and in general in any available application.

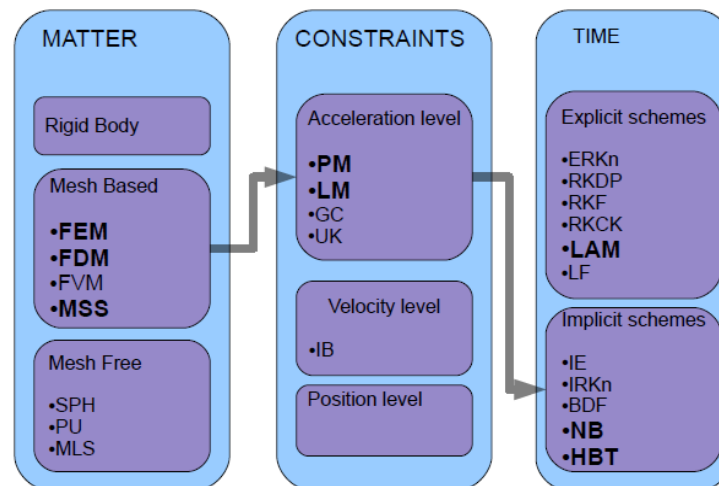


Figure 3.4: Schematic of some numerical methods and their associated physical notions. In bold letters those implemented for the numerical experiments of this thesis. The arrow represents a possible sequence of methods for a dynamics simulation.

The following is an overview of the main characteristics of our implementation.

3.3.1.1.- Matter integration methods

To describe the dynamics of matter we have an infinite number of degrees of freedom because the particles that conform it can have arbitrary displacements with respect to each other. Such systems are described using partial differential equations (PDEs) where time and spatial coordinates are related. These general partial differential equations, which are applicable to any solid or fluid material, are derived from the constitutive laws of the material.

For their solution, two different approaches can be taken in order to control the number of degrees of freedom (i.e. discretize): creating a mesh where the material displacements are limited (mesh based methods) or establishing the equations in the form of potential functions so that they compose a system of particles that regulate each other (mesh free methods) [LIU2003a].

We have particularized our study in three mesh based methods with different discretization schemes: Finite Element Method (FEM), Finite Differences Method (FDM) and a Mass Spring System (MSS).

For the general computation of nodal displacements and rotations, a framework employing the Direct Stiffness Method (DSM) was prepared [AGU2005]. In our case, where beam elements were used, the analytical solution of Bernoulli-Euler is lumped into local element matrices that are ultimately assembled in a global stiffness matrix [PRZ1968].

For the FEM implementation, the description of the elastic deformation of the beam is based on a Hermite interpolation polynomial, obtained from reference [WUN2002].

FDM establishes the relations between stations along the beam as a sequence of equations that form a linear system easily invertible [AGU2005] [STI1978] .

MSS is a bit more complex as it requires a previous discretization of the beam into a set of connected tetrahedra, but from the point of view of Physics it results clearer as the assumptions are that the nodes are simply connected by bars with a characteristic Young's modulus and area [MUL2008]. Some adjustments had to be made to the position of the masses in the cross section so the inertia of the section would match the value assigned in the polynomial-based methods.

The global nodal displacements and rotations computed by means of the DSM were transformed ultimately into local coordinates and served as input variables for each of the three methods above.

3.3.1.2.- Kinematic constraints integration

When bodies are subject to kinematic constraints, the set of differential algebraic equations (DAEs) defining the matter have to be satisfied besides from the purely time-related ones. In order to numerically tackle these conditions the equations of motion are rearranged to obtain different schema from which construct stable, accurate and faster formulations. The possibilities are to do it either in the acceleration

level, the velocity level or in the position level of the equation (3.8).

In the more common acceleration level schemes, the predominant ones are Constraint Reduction (CR), Lagrange Multipliers (LM) and Penalty Method (PM).

$$Kg = \begin{bmatrix} \cdot & \notin & \cdot & \cdot & \cdot & \cdot \\ \notin & \notin & \notin & \notin & \notin & \notin \\ \cdot & \notin & \cdot & \cdot & \cdot & \cdot \\ \cdot & \notin & \cdot & \cdot & \cdot & \cdot \\ \cdot & \notin & \cdot & \cdot & \cdot & \cdot \end{bmatrix} \Rightarrow Kg_{redd} = \begin{bmatrix} \cdot & \cdot & \cdot & \cdot & \cdot \\ \cdot & \cdot & \cdot & \cdot & \cdot \\ \cdot & \cdot & \cdot & \cdot & \cdot \\ \cdot & \cdot & \cdot & \cdot & \cdot \\ \cdot & \cdot & \cdot & \cdot & \cdot \end{bmatrix}$$

Figure 3.5: Constraint reduction. The global stiffness matrix is made non singular by symmetrically subtracting the columns and rows corresponding to the constrained degrees of freedom.

$$Kg = \begin{bmatrix} \cdot & \cdot & \cdot & \cdot & \cdot & \cdot \\ \cdot & \cdot & \cdot & \cdot & \cdot & \cdot \\ \cdot & \cdot & \cdot & \cdot & \cdot & \cdot \\ \cdot & \cdot & \cdot & \cdot & \cdot & \cdot \\ \cdot & \cdot & \cdot & \cdot & \cdot & \cdot \end{bmatrix} \Rightarrow Kg_{ext} = \begin{bmatrix} \cdot & \cdot & \cdot & \cdot & \cdot & \cdot \\ \cdot & \cdot & \cdot & \cdot & \cdot & \cdot \\ \cdot & \cdot & \cdot & \cdot & \cdot & \cdot \\ \cdot & \cdot & \cdot & \cdot & \cdot & \cdot \\ \cdot & \cdot & \cdot & \cdot & \cdot & \cdot \\ \cdot & \cdot & \cdot & \cdot & \cdot & \cdot \end{bmatrix} \begin{bmatrix} 1 & \cdot \\ \cdot & 1 \\ \cdot & \cdot \\ \cdot & \cdot \\ \cdot & \cdot \\ \cdot & \cdot \end{bmatrix}$$

Figure 3.6: Lagrange multipliers scheme. The global stiffness matrix is made non singular by symmetrically adding columns and rows where ones are placed in the location of the constrained degrees of freedom.

$$Kg = \begin{bmatrix} \cdot & \cdot & \cdot & \cdot & \cdot & \cdot \\ \cdot & \cdot & \cdot & \cdot & \cdot & \cdot \\ \cdot & \cdot & \cdot & \cdot & \cdot & \cdot \\ \cdot & \cdot & \cdot & \cdot & \cdot & \cdot \\ \cdot & \cdot & \cdot & \cdot & \cdot & \cdot \\ \cdot & \cdot & \cdot & \cdot & \cdot & \cdot \end{bmatrix} \Rightarrow Kg_{sc} = \begin{bmatrix} \infty & \cdot & \cdot & \cdot & \cdot & \cdot \\ \cdot & \infty & \cdot & \cdot & \cdot & \cdot \\ \cdot & \cdot & \cdot & \cdot & \cdot & \cdot \\ \cdot & \cdot & \cdot & \cdot & \cdot & \cdot \\ \cdot & \cdot & \cdot & \cdot & \cdot & \cdot \\ \cdot & \cdot & \cdot & \cdot & \cdot & \infty \end{bmatrix}$$

Figure 3.7: Penalty Method scheme. The singularity of the global stiffness matrix is treated by scaling the diagonal elements of the constrained degrees of freedom with a very large number.

In this case, the strategy is to alter the stiffness and mass matrices in such a way that they become invertible (after assembly, the stiffness matrix is symmetrical and singular).

This is achieved by either reducing the matrices (CR), or by expanding them, adding or removing those

rows and columns where the degrees of freedom are to be constrained (LM) or by modifying the corresponding values in the diagonal so their inversion gives a number as close to zero as possible (PM).

Figures 3.5 to 3.7 provide a visualization of these methodologies as they are commonly implemented.

3.3.1.3.- Time integration

Integration of time in a structural dynamics simulation reduces to the solution for each time step of an Ordinary Differential Equation (ODE). The first possible classification for ODEs solvers distinguishes between explicit, implicit and hybrid methods. From the available different schemes we have used for our comparison those provided by the SAP2000® (v15.0.0) commercial package: Newmark Beta (NB), Wilson Theta (WTH), Hilbert Hughes Taylor (HHT), Chung and Hulbert (CH), all of them implicit. We implemented our algorithms from references ^{(19), (22), (23),(24)} and ⁽²⁵⁾. Results were in very good agreement with those of the commercial package.

3.3.2.- The studied specimens

As mentioned above, and for the sake of simplicity, we omitted material and geometrical non-linearities from our analyses. The material and geometric properties shown in table 3.2 are common in engineering practice, with values similar to those of a 200x200x2 mm hollow extruded steel bar.

The geometric configuration of each model is displayed in Fig 3.8, in order of increasing complexity.

Table 3.2: Properties of the beam elements composing the specimens

Parameter	Value
Area, A	144 cm ²
Modulus of inertia, I	7872 cm ⁴
Modulus of elasticity, E	21000 kN/cm ²
Shear modulus, G	8076,92 kN/cm ²
Density, d	7.892E-8 kN/cm ³

Notwithstanding the obvious resemblance to a typical building engineering application, this work has a broad generality and is applicable to any structural dynamics problem. It has potential use in the simulation of any mechanical object regardless of size or shape.

Model A:

The simplest model of choice for our research was a 387,5 cm long cantilever column under a lateral loading acting in its tip. The cantilever model is extensively utilized for the validation of numerical

methods in the literature. It is composed of two elements, each half the length of the column.

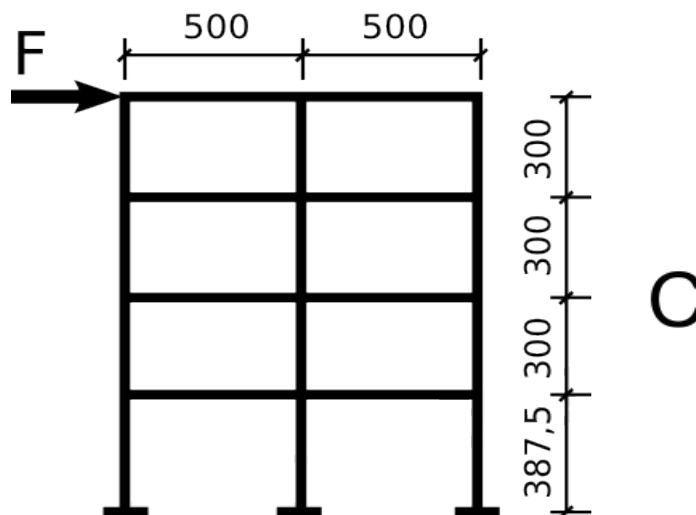
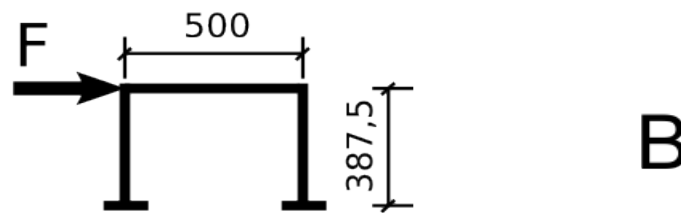


Figure 3.8: Geometry of the three studied models. Dimensions in cm. Three frames of increasing complexity consisting of beams, nodes and constraints.

Model B:

A natural extension to this model from the structural engineering point of view is a simple moment frame, with identical geometrical and mechanical properties for each beam element as in the previous case. The load F is applied to the upper left corner.

Model C:

The more complex three bay – four storey frame is also shown in figure 3.8. Its properties are displayed

in table 3.2, and load F is also applied to the upper left corner.

In order to represent the structural dissipative behaviour, Rayleigh damping was implemented according to reference [ADH2000]. It is based on modal analysis and uses the first two natural frequencies of the structure under study. The ones applicable to our models are listed in table 3.3

Table 3.3: Modal frequencies for damping characterization

Model	Mode	Frequency (Hz)
A	1st	12.79
	2nd	64.44
B	1st	11.37
	2nd	33.52
C	1st	2.71
	2nd	8.69

For comparison purposes, a frequency response function was computed for all three models. Its values are in agreement with those of the modal analysis of table 3.3 as can be seen in figure 3.9. It can be inferred from this figure that the more complex model C has the highest sensitivity to low frequencies, whereas models A and B should behave similarly as they have their strongest response to similar frequency values.

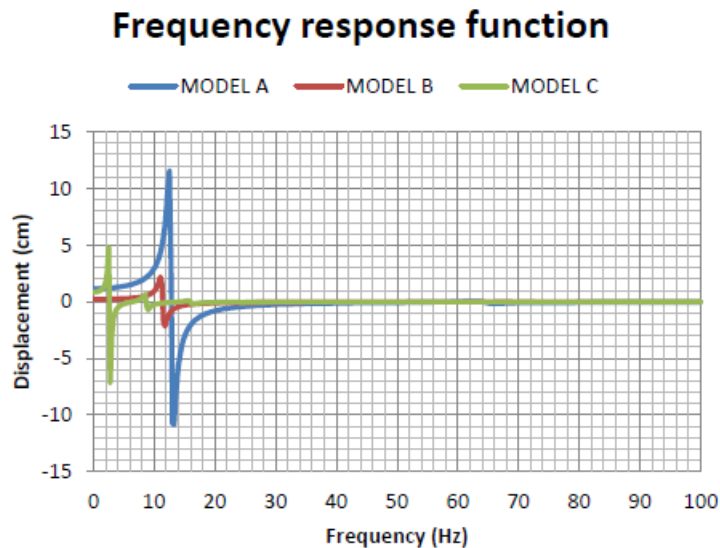


Figure 3.9: Frequency response functions for the three tested models. Values are in good agreement with those of the modal analysis. Model C has the highest sensitivity to low frequencies, while models A and B should behave similarly.

3.3.3.- Transient input forces

A load F of 10 kN applied to the tip of each specimen was scaled at each time step with an input signal of variable amplitude.

As presented in figures 3.10 to 3.12, four input signals were devised in order to stimulate the loading of our system: a simple sine function, a simple sine function suddenly interrupted, an incremental triangular function and a ramp pulse, all of them spanning through five seconds.

A sine function with such a low frequency is seldom encountered in engineering practice, but allows for the calibration and tuning of the combined methods given its smoothness and clarity.

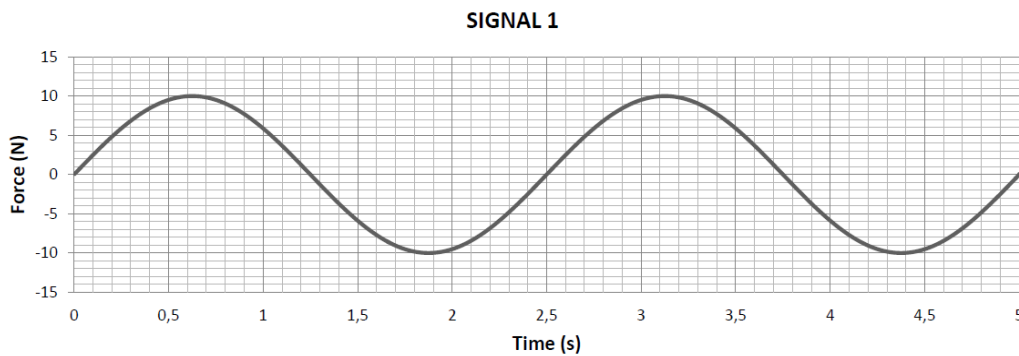


Figure 3.10: Sine function, two cycles. $f=0,4$ Hz, $T=2,5$ s

For the second signal, after completion of the first period it is interrupted abruptly in order to allow for free vibration of the system. The point of interruption, in zero amplitude, allows for observation of the effect of kinetic energy on the simulation.

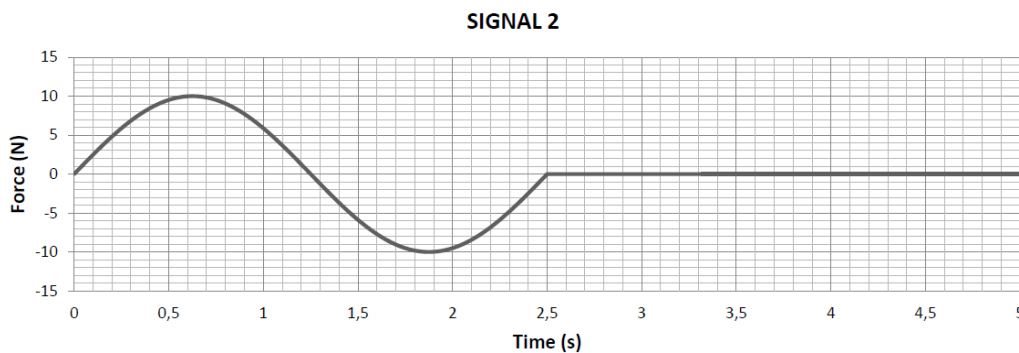


Figure 3.11: Sine function, one cycle, then free vibration. $f=0,4$ Hz, $T=2,5$ s

The incremental triangular function was constructed in order to account for earthquake engineering regulations, where sudden changes and peaks are to be simulated.

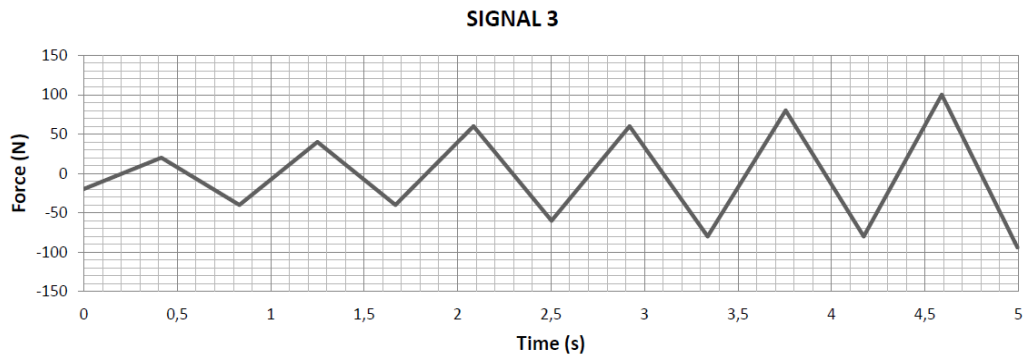


Figure 3.12: Incremental triangular function. $f=1,2$ Hz, $T=0,83$ s

Regarding the last pulse, it enables the comparison in performance of the numerical methods simulating free vibration and the effect of resonance.

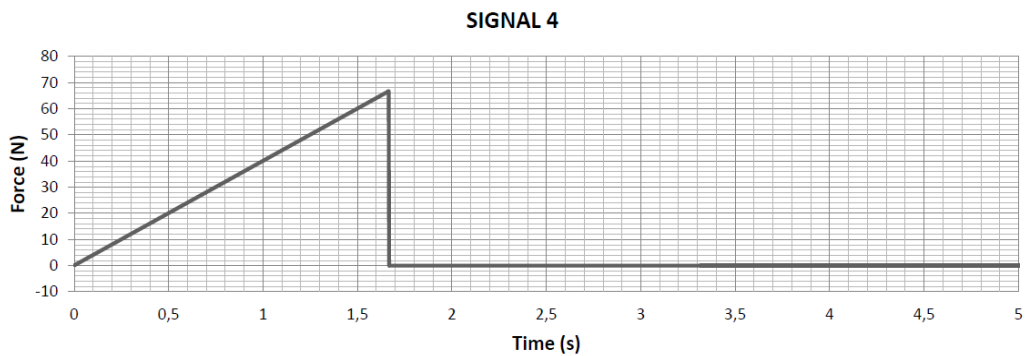


Figure 3.13: Ramp pulse. $F=0.625$ Hz, $T=1.6$ s

3.3.4.- Parametric sensitivity study

The significant parameters involved in the numerical computations have been iteratively modified in order to assess their influence in the simulations. For each type of integration the following parameters were studied:

- Time integration:
 - Time step influence.
 - Damping ratio influence.
- Matter integration:
 - Number of integration points along the beam element.

- Constraint integration:
 - No comparison was available, as only the Constraint Reduction technique is implemented in the reference software.

Table 3.4 shows the values used for the characteristic parameters of each numerical method in all the simulations.

Table 3.4: Time integration parameters

Method	alpha	beta	gamma	alpha-m	theta
NB	-	1/4	1/2	-	-
WTH	-	-	-	-	1.4
HHT	-1/3	0.444	0.8333	-	-
CH	-1/3	1/4	1/2	-1/10	-

These values were not the subject of our study, and were fixed according to recommended values from the literature [BAT1995], [NEW1959], [HIL1977], [CHU1993]. It is important to note that Chung-Hulbert's method (also known as Generalized-Alpha) under certain combinations of parameters includes previous ones, whose performances are, according to [CHU1993], less accurate when low frequency excitation is present.

3.3.5.- Methodology: Energy computation of a simulation

The evaluation of instantaneous energetic magnitudes provides a very holistic hindsight into the behaviour of a simulation, which is qualitatively superior to that of the displacement domain to which time history analysis is traditionally limited.

Besides, in the case of the single cantilever beam choosing the tip as the observed target is generally straightforward, but for more complex arrangements like, for example, models B and C, this is not so trivial. The common choice of a “representative point” (the centre of mass of each storey, conversion to SDOF, etc.) has a definition which is always difficult and elaborate.

Simple observation of the displacement behaviour of the tip of Model A would mislead the analyst to the conclusion that the results for signal 4 in figure 3.14 are better approximations than those for signal 3, as the displacement values seem to be closer to the analytical ones given the fact that the graph is more neat and has less spikes.

Nevertheless, this can be proven to be less accurate than expected. figure 3.15 shows the same simulation in the energy domain, computing some operators of the different terms from chapter II.

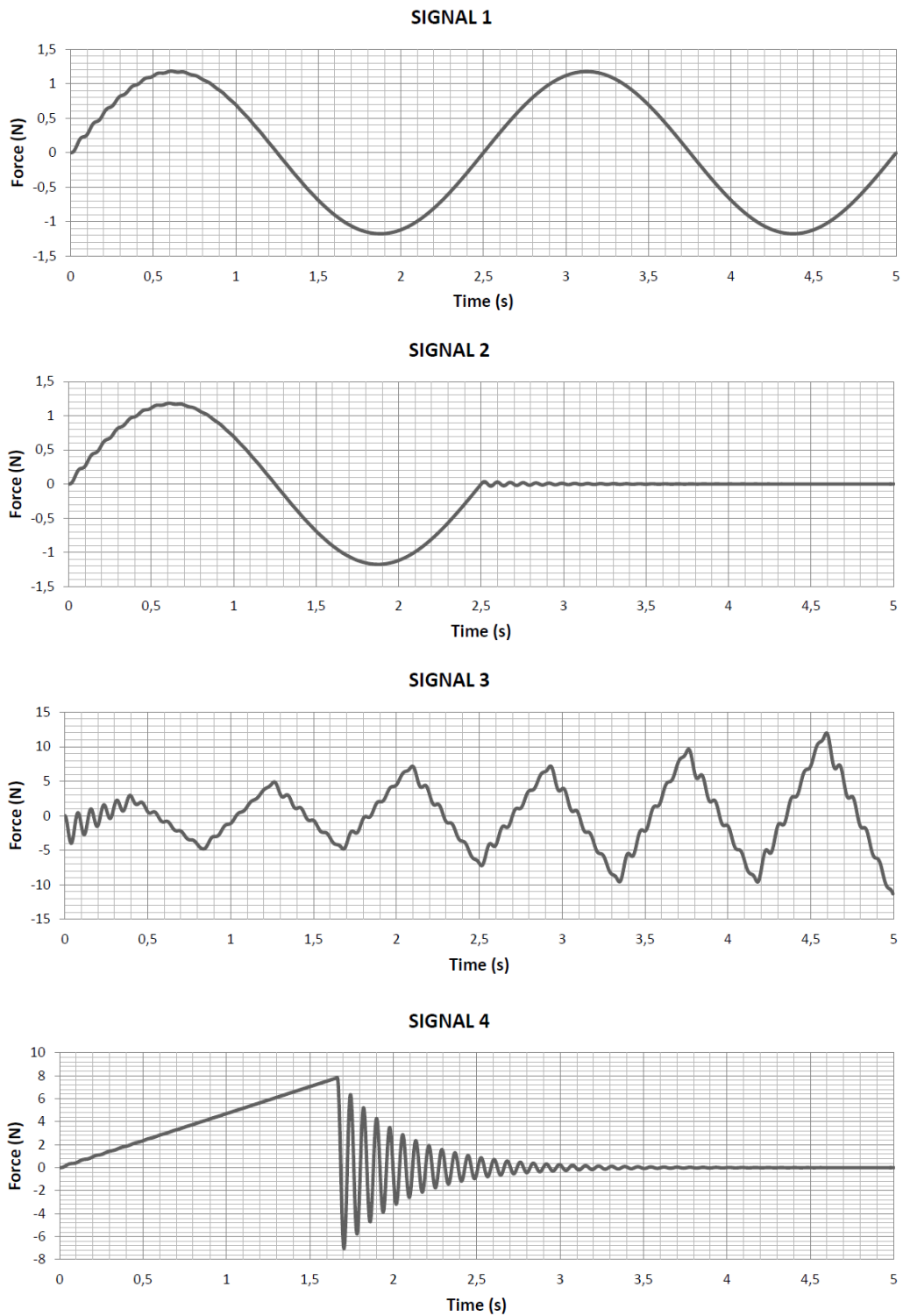


Figure 3.14: Model A. Time history analysis of the displacement of the tip. Chung-Hulbert method, generalized alpha value=-0.1, dt=0.0025, damping ratio=2%.

The application of equation (3.29) appears in figure 3.15 as W+T-U-R. From this operator one can obtain that, on average, under signal 4 the simulation "creates" +0.69 N-cm of spurious energy on each time step, whereas the same model, under signal 3 -visibly more flurry in the displacement domain-, "absorbs" -1.12 N-cm from nowhere. In terms of absolute value, the first is closer to zero, apparently still showing a better approximation for signal 4. However, a rigorous computation should also take into account that the total amount of work applied by signal 3 is, on average, three times larger than that of signal 4. It is not equivalent a large average deviation from zero with large values as it is with smaller ones. The formulation of an independent normalization parameter will be provided.

To define our measure of error we use equations (3.9), (3.22), (3.23) and (3.25) at each time step to compute the respective instantaneous values of Kinetic Energy (T), Strain Energy (U), Dissipative Energy (R) and External Work (W).

Our methodology, based on equation (3.29), uses the Hamiltonian action integral minus the average over time of the work due to the externally applied forces, thus measuring the difference to zero.

Moving the Hamiltonian action term to the right hand side we have:

$$\epsilon(t) = W_{ext}(t) + T(t) - U(t) \quad (3.30)$$

whose discrete integral in time gives:

$$\sum_{t1}^{t2} \epsilon(t) dt = \sum_{t1}^{t2} [W_{ext}(t) + (T(t) - U(t))] dt \quad (3.31)$$

As this value by itself is not very representative because different simulations often show still acceptable behaviour under different external signals despite high values of the total added epsilon, a reference parameter was devised.

It is based on the total work done by the external forces, but computed independently from the displacements, and based on equations (3.22) and (3.25). It is obtained by isolating the displacement vectors on the external and internal work equations:

$$\{x\}^2 = 2U \cdot [K]^{-1} \quad (3.32)$$

$$\{x\} = 2W_{ext} \cdot \{F_{ext}\}^{-1} \quad (3.33)$$

which leads to the definition of the reference parameter:

$$W_{ref} = 2 \frac{W_{ext}^2}{U} = \{F_{ext}\}^T [K]^{-1} \cdot \{F_{ext}\} \quad (3.34)$$

This parameter is completely self-contained and does not rely on the numerical method used to do the simulation, as the vector of external forces and the stiffness matrix are given data, hence becoming an

excellent reference for our benchmarking purposes.

In the following parametric studies, the total value of the computed epsilon is represented as a percentage of this reference parameter, hence giving an idea of the reliability of the different studied numerical methods.

The applied formula for each of our simulations is as follows:

$$Error = \frac{100 \cdot \sum_{t_0}^{t_1} \epsilon dt}{\sum_{t_0}^{t_1} W_{ref} dt} \quad (3.35)$$

In figure 3.15 the difference between the calculated work due to external forces and the reference input work ($W_{ext} - W_{ref}$) is presented together with the aforementioned energy indicators as it allows to trace discontinuities in the behaviour of the different methods through time.

Other options for the value of epsilon are also available. Similarly, one could compute the equation (3.29) using the Hamiltonian (T+U+R), and subtracting it from the applied work. Its time history is shown in figure 3.15 as $W - (T+U+R)$. This operator provides a lower bound for the evolution of the Lagrangian (most clearly visible for signal 4), as it balances the kinetic energy of the system against the potential and the dissipative energies. Its evolution in time gives information about whether the absolute value of the kinetic term is overestimated at each step. Given that the mass is kept constant this operator permits to verify that instantaneous velocities are computed correctly.

Yet another possibility is to calculate the instantaneous increment of the Hamiltonian, $d(T+U+R)$. In systems where the energy is constant, this value should be zero, but it is rarely the case in practical applications. Its main interest resides in the detection of segments in the simulation where the smooth transition from one time step to the next is lost.

One could also define the epsilon on each time step as the difference between the time-dependent calculated work and our presented analytical reference work ($W_{ref} - W$). In a way, this computation appears the most precise, as the involved terms are of the same kind and the reference work is derived from a numerically neutral relationship. Apart from the possible error in the inversion of the stiffness matrix, the term W_{ref} is immune to the fluctuations caused by the time integrators. Still, this operator is not fully satisfactory. As the possible errors in the instantaneous work only depend on the computed displacement, its time history only provides information about irregularities in this matter.

The choice, then, of the Lagrangian (minus the damping energy when applicable) to balance the external work seems the most appropriate.

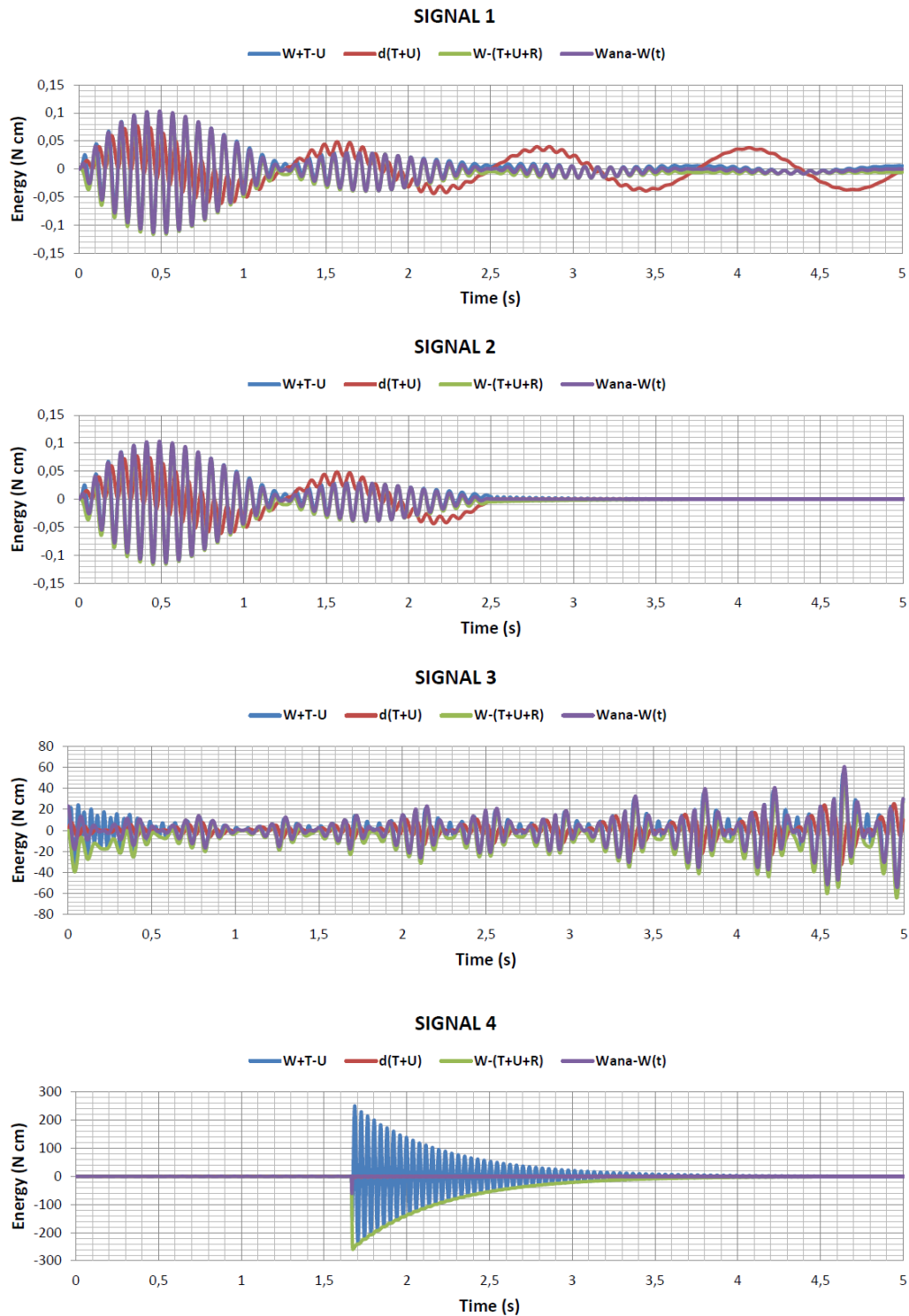


Figure 3.15: Model A. Time history for the variation of different energy operators. Chung-Hulbert method, generalized alpha value=-0.1, dt=0.0025, damping ratio=1%.

Not only its time history is a valuable source of information for the analysis of irregularities in a simulation but also its integral in time provides a single scalar whose value should be zero. Given that the energetic terms are all positive, a positive value of this integral can only be caused by an average

overestimation of the kinetic term (i.e. the velocities) against the displacements. Similarly, a negative value tells us to what degree displacements are unbalanced against velocities, as the internal potential energy is direct function of them.

3.3.6.- Numerical results: Influence of time step.

According to the methodology exposed above, a thorough parametric study was carried using the three models of choice. figures 3.16 to 3.18 present the values obtained from iteratively modifying the time step between values of 0,00125 s and 0,15 s, for each numerical method, with a constant damping ratio value of 2%.

As opposed to the analyst's intuition, in spite of dealing with linear models we obtained curves that vary significantly from one method to another. Nevertheless, and as expected, this divergence is more pronounced with larger time steps and also increases with the complexity of the model.

The character positive or negative of the value of the error also provides a valuable source of information, as it tells us when the internal strain energy is larger or smaller than the sum of the kinetic energy plus the external work. As this term is dependent on velocity, it shows when the kinetic term is overestimated or underestimated. In other words, the higher the decoupling between velocity and displacement, the further the simulation is from correctness.

When the time step is larger, it affects the velocity, which loses or gains in phase with the normal modes of the structure and with the input signal. In these cases the simulation might either dissipate or absorb energy artificially. This explains the ripple around the abscissa presented by all the methods in all the simulations.

In terms of evaluation of the particular methods, it is commonly accepted that CH has better performance than the others, as it gives the analyst control over the numerical damping for high frequencies without loss of accuracy. As the sensitivity to those parameters was not within the scope of this study, we cannot give a view about such effect, but we can point out how, in general, in this configuration they all show fairly similar results, only diverging significantly for larger and impractical time steps. Although all of them are of the implicit type, meaning unconditional stability regardless of the time step size, our results show how this set of methods in general tend to sacrifice energy conservation. In most linear structural dynamics problems it is still not an issue, but for the analysis of non-linear situations we strongly recommend the use of more modern integrators of the symplectic type, as those described in [KUH1999].

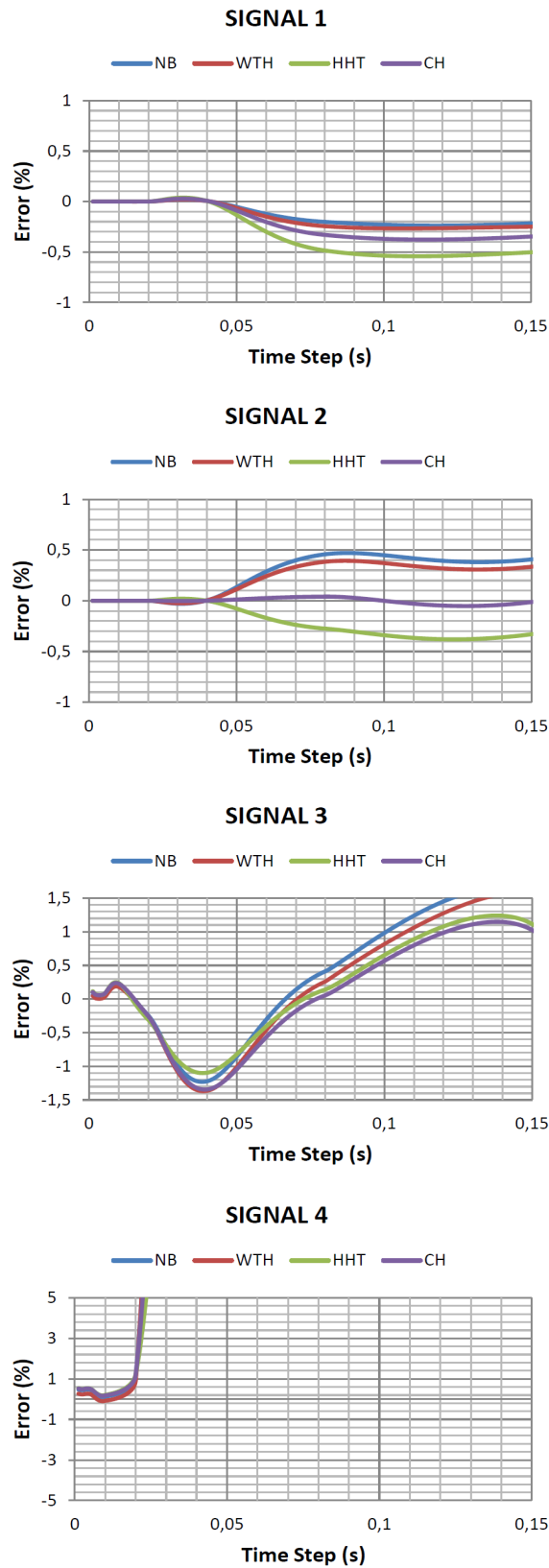


Figure 3.16: Energy error analysis. Model A. Influence of time step size. Damping ratio=2%.

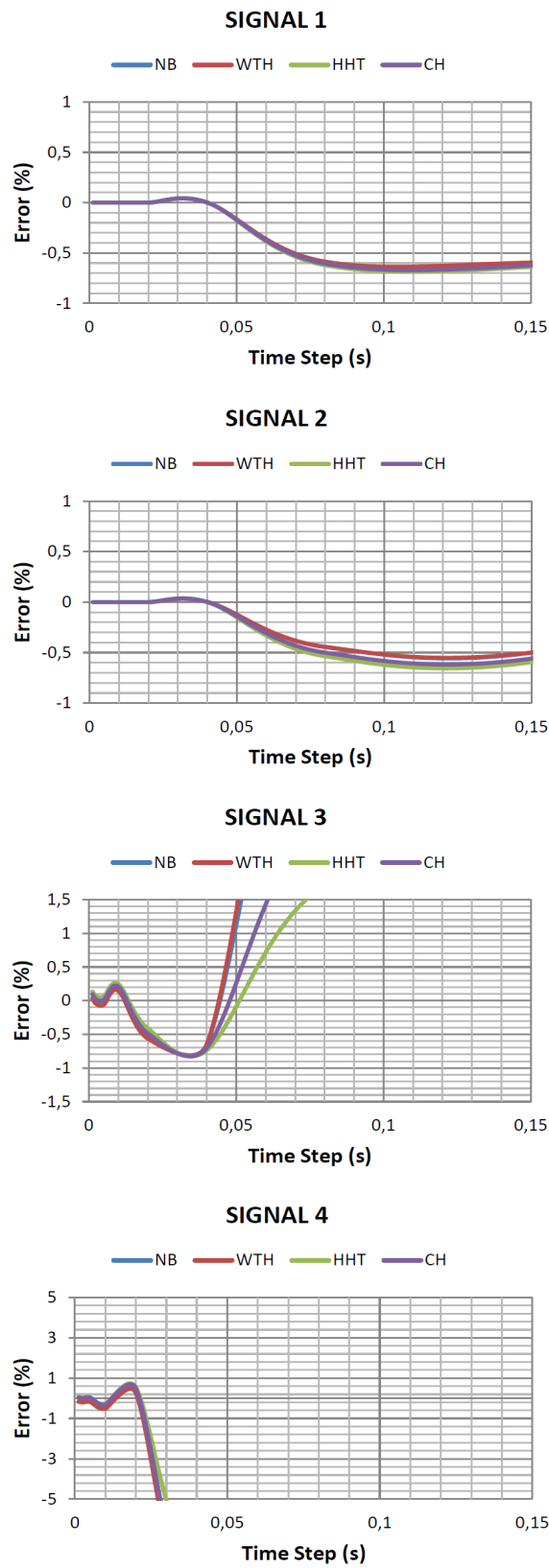


Figure 3.17: Energy error analysis. Model B Influence of time step size. Damping ratio=2%.

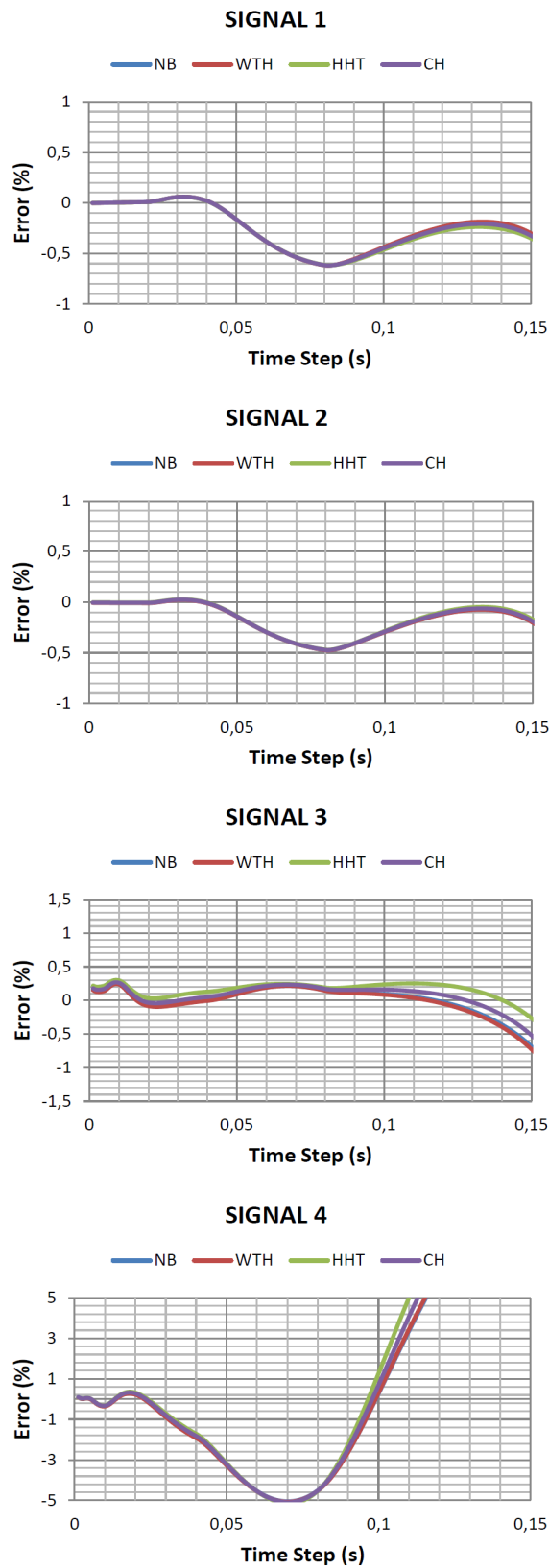


Figure 3.18: Energy error analysis. Model C Influence of time step size. Damping ratio=2%.

3.3.7.- Numerical results: Influence of the damping ratio.

It should be noted that the damping considered in our experiments is of an external nature, given the fact that no material non-linearities have been taken in consideration.

The corresponding Rayleigh mass and stiffness coefficients defined in equation (3.24) were obtained according to reference [ADH2000]. Figure 3.19 shows the relationship of these values with the models used in the study.

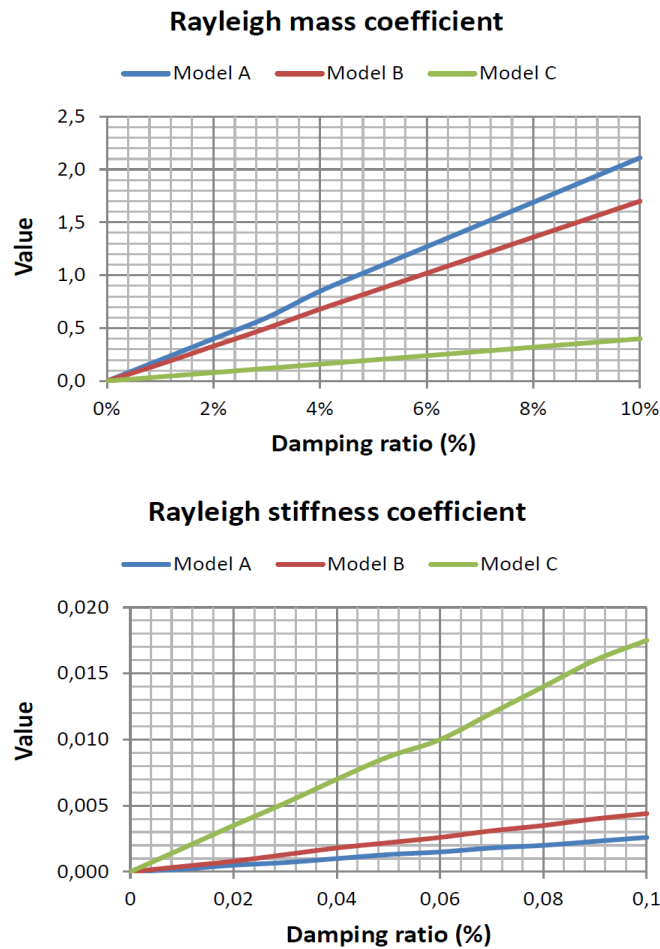


Figure 3.19: Rayleigh damping coefficients. The values are directly proportional to the value of the chosen damping ratio. For higher frequencies of the model, the value of the mass coefficient is higher, and vice-versa for the stiffness coefficient.

The sensitivity of the numerical methods to variations in the damping ratio is presented in 3 figures 3.20 to 3.22. For all three models the range of study was fixed between 0% to 10% of critical damping. In general, this is sufficient for all the methods to reach their asymptotic limit in almost every simulation. For models A and B a value of 2% of damping suffices to achieve stable behaviour with an error of less than 0.3%, which can be considered very acceptable.

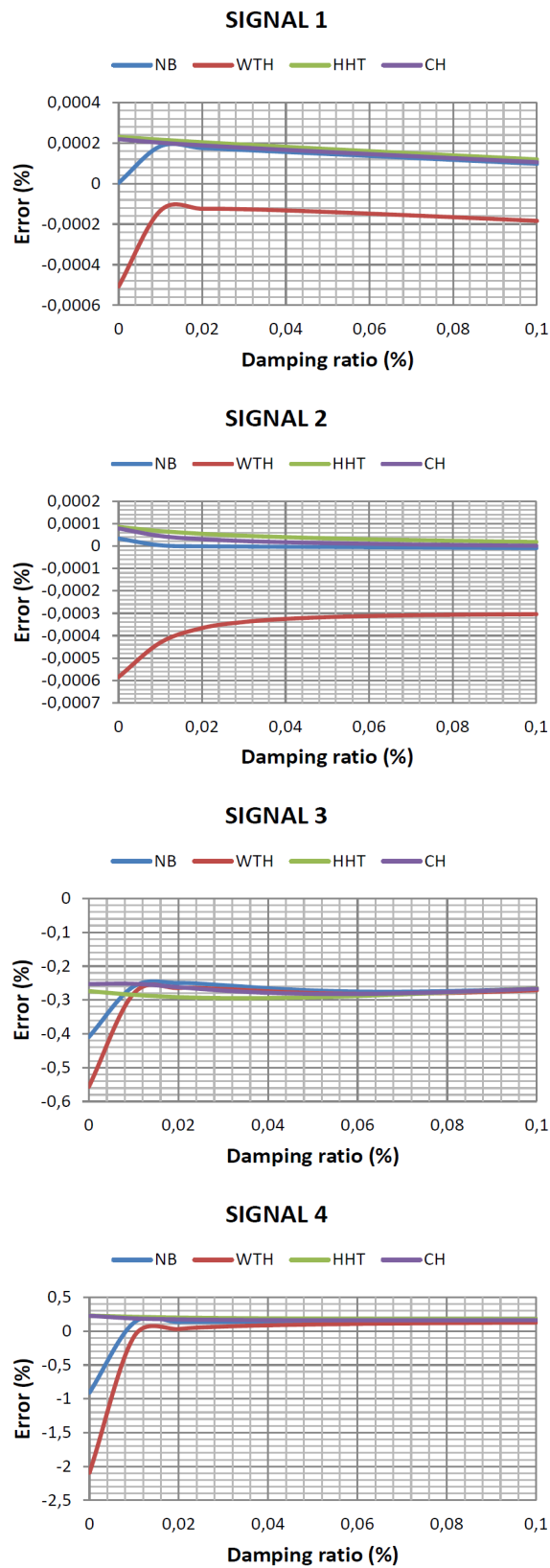


Figure 3.20: Energy error analysis. Model A. Influence of damping ratio. Time step=0.01 s.

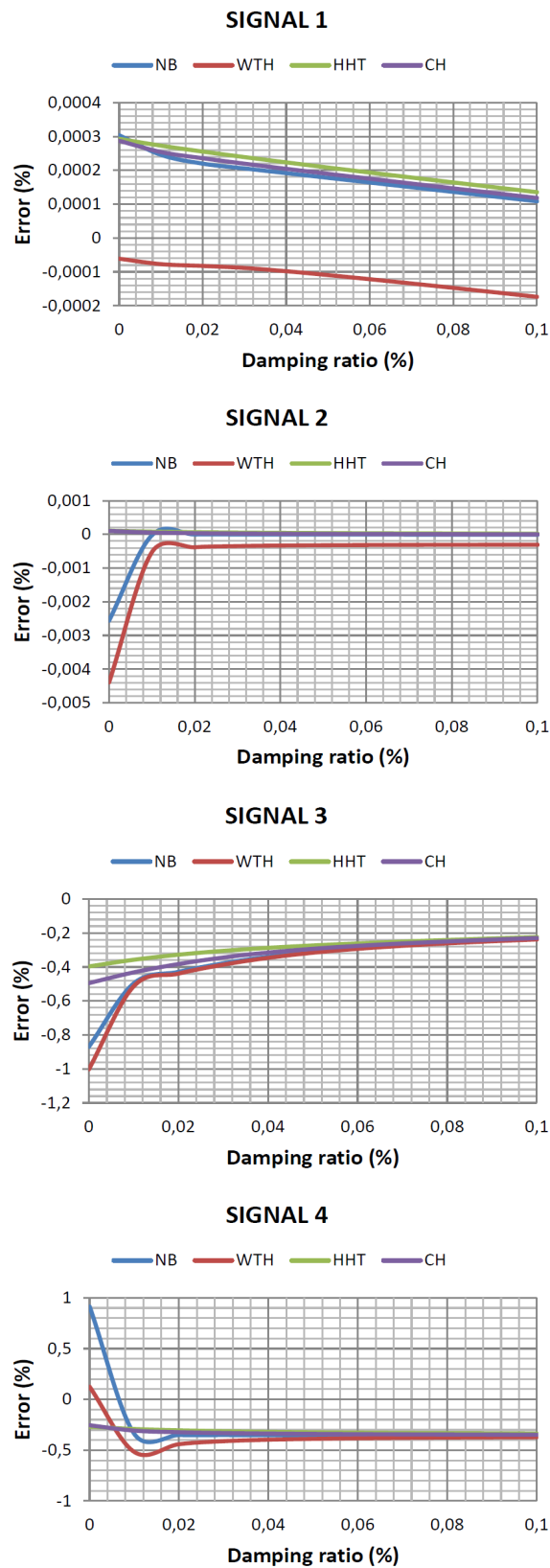


Figure 3.21: Energy error analysis. Model B. Influence of damping ratio. Time step=0.01 s.

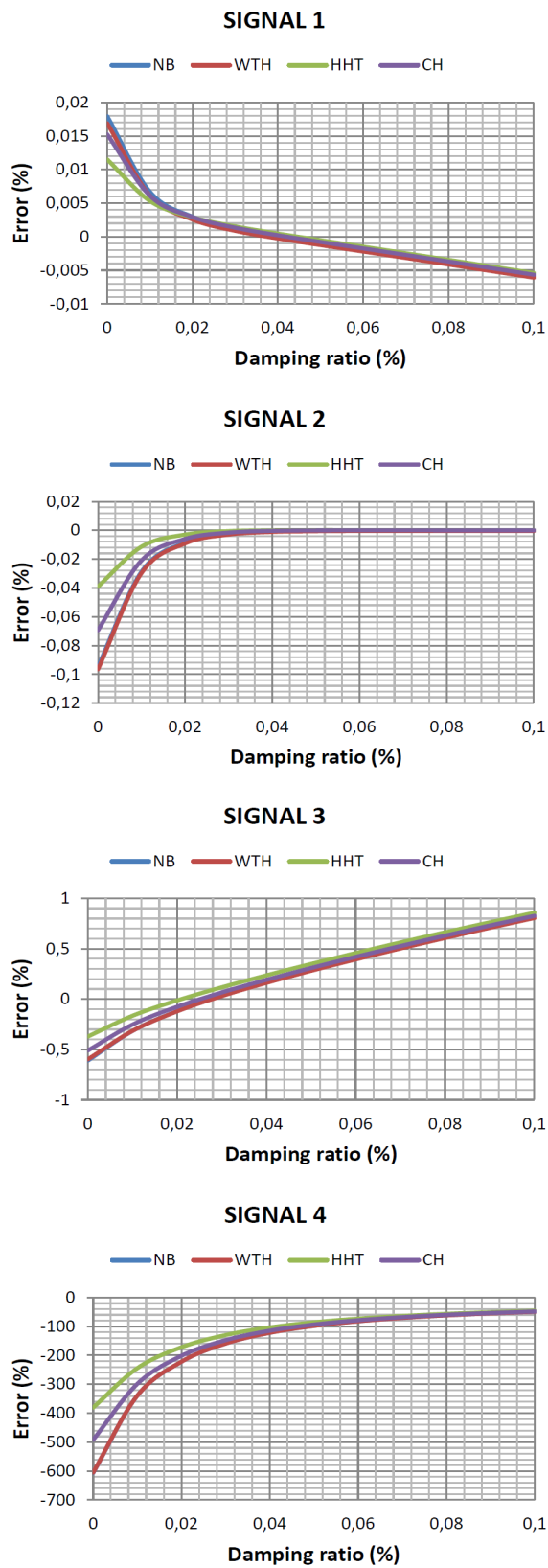


Figure 3.22: Energy error analysis. Model C. Influence of damping ratio. Time step=0.01 s.

3.3.8.- Numerical results: Influence of the number of integration points for matter integration methods.

For the study of the matter integration techniques a similar approach based on the variational principle of action was adopted. However, here the definition of a reference parameter W_{ref} was not required as the analytical solution for beam elements is available applying the concepts of section 3.2.4.

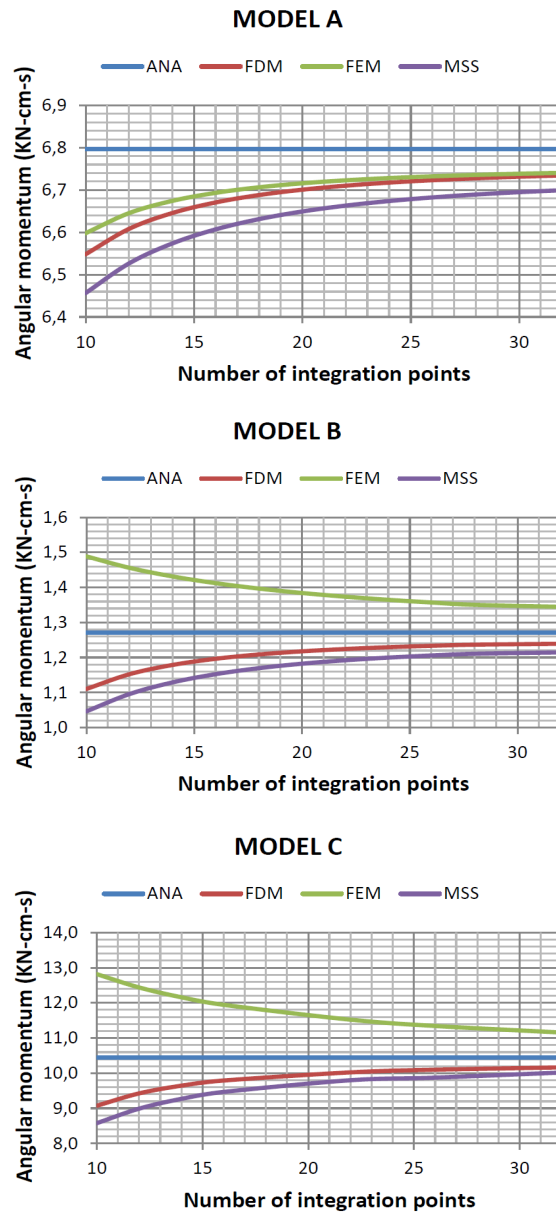


Figure 3.23: Comparison of angular momentum computation for matter integration methods against number of integration points. Analytical (ANA) vs Finite Differences (FDM) vs Finite Element (FEM) vs Mass Spring System (MSS).

Instead, we computed a global action term, whose units are also those of angular momentum. It is defined as:

$$S = \int_t U_{elas}(t) dt \quad (3.36)$$

The charts in figure 3.23 were made by computing the instantaneous value of internal work corresponding to each different numerical method, and averaging it over time. The applied transient force was signal 1.

The measure of the error was computed as a percentage of the difference to the analytical value. A positive error indicates numerical spurious dissipation of energy, whereas a negative error stands for artificial energy creation.

As expected, for an increasing number of integration points the methods converge towards the analytical value. However, they do it in an asymptotic fashion, reaching an almost flat parallel value after about 25 integration points. In general, the obtained error values remain below 5% for all the methods, which is completely acceptable in practice.

Interestingly, FEM presents the best behaviour only for the simple cantilever beam, creating spurious strain energy for the other two models.

FDM and MSS tend to dissipate energy in all cases, which means that, in general, they result in an underestimated value of displacement by about 2%, remaining on the unsafe side.

3.4.- Discussion

It was proven how methods of different nature and concept can be compared using the same theoretical background, in particular the variational principle of Least Action of Lagrange and Hamilton.

It was shown how variational principles and an energetic norm can be employed in an easy and efficient manner to benchmark and assess the accuracy and stability of different implementations. The accuracy and good performance of time and matter integration methods is generally taken for granted, as it is difficult, in the displacement domain, to assess it stringently.

The total Hamiltonian actions of three systems under transient loadings have been computed for each possible combination of methods. A comparison was made on the basis of energy principles.

The scheme provided, tested in three simple examples, is trivially extensible to more complex systems where more elements are present. The advantage of this approach is that it allows for the monitoring of the global behaviour by means of one simple scalar. No further algebraic artifacts, common in benchmarking, seem to be necessary, which greatly simplifies the assessment not just of a simulation, but of any method in general.

4.- State of the art: non-deterministic methods for structural design

4.1.- Introduction

The purpose of this chapter is to present the main tendencies in probabilistic design applied to the particular case of structural design and its potential benefits. It is not intended to be an exhaustive overview but an introduction to the topic, emphasizing the difference between non-deterministic optimization and non-deterministic analysis.

This differentiation is important as new stochastic methods are constantly being proposed under the common umbrella of probabilistic design. However, these methods can be oriented towards the treatment of the inherent uncertainty of the design process or as search algorithms to obtain better designs.

The next section explains how, by shifting from deterministic criteria to the definition of reliability targets, the parameters involved in the analysis (applied loads, material strength, manufacture defects, etc.) are researched and measured in order to give a statistical definition. With this data, a probabilistic analysis model can be made for the whole system and a set of failure probabilities can be obtained.

This serves to explain the analysis step within the design process and the three main approaches to account for uncertainty within it: fully deterministic, semi-probabilistic and fully probabilistic. At the end of the chapter, an example is given to illustrate the main characteristics of each approach and to allow for methodological comparison.

It is highlighted how, with the knowledge of the contributions of each parameter to the overall risk of failure, the designer is enabled to find those points where reliability is improved. Design objectives other than safety such as economy, quality, functionality, etc. can then be improved as a consequence of applying probabilistic methods.

The third section is then dedicated to introduce the most commonly-used optimization techniques and their potential and drawbacks as tools for assistance in the design.

4.1.1.- *The origins of deterministic structural design*

In the two previous chapters of this thesis, emphasis was made only on the deterministic analytical part of structural dynamics. However, simulations generally are made with a purpose. In the fields of Biomechanics, Molecular Dynamics or Graphics Animation, this purpose is commonly self-contained. The analyst devises a model and its simulation for better understanding of a given phenomenon or just to visually represent an interesting sequence.

However, in engineering disciplines (Civil, Aeronautics, Automotive, Robotics, etc.), the final result is a material object and the virtual simulation is only an intermediate step in a longer process of design. Traditionally, the realm of Physics in this subject is considered to reach as far as the definition of models

goes. In this chapter and the next, however, it will be shown how also in the empirical side of their trade designers can be assisted by a physicist's mentality.

“Physics is defined as the scientific discipline that studies the properties of matter and energy, considering only those attributes that can be measured”. In this manner, physicists design and perform experiments that allow them to observe and analyse phenomena. With these, they attempt to unveil the laws that describe future events and behaviours. Before that is achieved, an intense work of abstraction and detection of patterns is needed, often challenging their own intuitions. The target is, then, the description of unobserved behaviours of phenomena. The limits imposed to the task are no less than those of the already known laws of physics, which must be observed by any new theory. The employed language is that of mathematics, and the main sources of uncertainty in their job are methodological errors or inaccuracies in the measures.

Analogously, design is the process of creation of specifications intended to accomplish the goal of construing an object. Designers need to make a series of abstractions that will eventually lead to the creation of tangible objects. To such end, they specify relationships between elements subject to a given set of limitations. The similarity with physics appears more obvious when one sees that the target is also the description of (yet) unobserved things, subject to limitations (regulatory, economic, cultural, etc.), explained with a given language (not only graphic but often also mathematical) and liable to endless sources of uncertainty (material properties, manufacture defects, applied actions, modelling errors, etc.).

In the previous chapters of this thesis we presented some concepts of Physics that stretched the boundaries of Newtonian Mechanics and how they can be effectively employed in modern analyses of structural systems. In short, these are based on the treatment of energy as a functional and how by minimizing this functional we have a powerful tool to solve many problems of Physics.

This minimization process is called calculus of variations, hence the term Variational Mechanics. It was introduced late in the 18th century by Euler, Lagrange, Maupertuis and others and perfected in the first half of the 19th century by Hamilton. Together with the laws of Thermodynamics, these advances led to a highly prolific period of discoveries of natural phenomena that could be explained theoretically. When theoretical knowledge failed to explain the observations, it was common practice to attribute the failure to lack of accuracy of the instrumentation or errors in the methodology.

During this period, cause and effect were intrinsically connected by the laws of nature and this idea prevailed in most doctrines. The beginning of the 20th century, however, brought serious doubts about the completeness of Classical Mechanics, as not even Maxwell's principles could accurately predict the results of the experiments in black body radiation or the photoelectric effect.

The theories presented by Louis de Broglie solving the first, and the work of Einstein explaining the

second, undermined definitively those beliefs and Modern Physics was born on the foundations of Quantum Mechanics. The works of Heisenberg, Born, Jordan, Pauli, Dirac, Schrödinger and Planck established a series of principles that denied the possibility of fundamental causality, replacing it with probabilistic relationships between discrete states of the elementary subatomic particles.

As it is common case when a change of paradigm occurs, there was initial reluctance from many parts to accept the new perspective of things. Einstein himself refused the probabilistic approach by asserting that “God does not play dice with the universe”. As a result of this controversy, two sides were created. The supporters of Classical Mechanics kept maintaining that future events could be “determined” if enough data about past events (causes) is provided. This led to the coining of the term “determinism” and was presented in opposition of the “probabilistic” philosophical counterpart.

In parallel with the enormous advances in science of the 19th century, industry and commerce began the implementation of standards, which became one of the cornerstones of the Industrial Revolution. By implementing standards, engineers maximized key objectives of their designs such as compatibility, interoperability, safety, repeatability and quality. Naturally, the redaction of those standards happened under the strong influence of the aforementioned determinism. This influence, still persistent throughout the whole 20th century, has only been challenged lately with the extensive use of digital computers and the widespread development of the numerical methods introduced in chapter 1.

The particular case of safety, which is a key component of structural design, has seen some evolution in this aspect, as it is directly linked with the concept of uncertainty. Initially, the process of structural design was almost based entirely on empirical knowledge. Safety was achieved by repeating already tested solutions or by doing small increments in scale.

Once material science and the theory of structures gained some confidence, design guidelines were implemented in the form of standards. Initially, uncertainties were taken care of by means of a safety factor. Later on, as different circumstances and failure modes were detected in the lifespan of structures of all kinds (ships, aircraft, buildings, bridges,...), the notion of limit state design, a semi-probabilistic approach to the same problem, refined a bit on the matter.

The concept of using the probability of failure as a criterion for structural design can be credited to the Russians N. F. Khotsialov and N.S. Streletskii who presented the idea in the late 1920s. However, it was the works of Emil Julius Gumbel, Ernst Weibull, Alfred Freudentahl (not to be mistaken with the mathematician Hans Freudentahl) and Maurice Frechet later in the 1950s century, that opened the doors to the theories of probability and risk assessment to structural design in Western countries. In the present day most design codes of any engineering discipline have abandoned the crude safety factor approach in favour of the slightly more refined limit state design practice. However, this approach is still subject to

criticism as the choice of the values of the factors remains somewhat arbitrary.

4.1.2.- *The iterative process of structural design*

The design of structural systems is an iterative routine in which different configurations of elements are first proposed and then tested for their suitability in any aspects the designer considers adequate (safety, comfortability, cost, ...). The final purpose of these iterations is to achieve an optimized version of an object in which all or most of the design requirements are satisfied. This definition of design applies with equal accuracy to the discipline of physics, where the target is not the specification of characteristics of objects but those of laws of Nature. Both require the iteration of an *a priori* reasoning – *a posteriori* contrasting and the use of inference to measure, in the first case, the validity of a proposed design, and in the second, that of a given theory.

One can easily observe many steps in the process of structural design. However, we will highlight basically four:

1. Definition of the function of the structural object (bearing loads, protect against wind, etc.)
2. Definition of the structural concept employed (frame-like, shell, etc.)
3. Optimization of the design (according to cost, weight, strength, performance, etc.)
4. Definition of details (constructive, aesthetic, etc.)

In the first two stages, a series of properties and characteristics of the system are defined (geometric configuration, materials, etc.), composing a prototype that can be either physical or mathematical. These will define the capacity of the design product. In this stage also, circumstantial and environmental requirements are presumed, composing the demand. The definition of both capacity and demand involves a series of assumptions and simplifications which are the first source of uncertainty regarding the final result of the design.

Once an initial set of characteristics and solicitations is defined, they can be tested against each other. The testing procedure is called analysis, and it basically serves to contrast the demand against the capacity. This can be made under a deterministic or under a non-deterministic perspective, and is repeated as many times as it is necessary throughout the whole optimization process.

In itself, the optimization process can be regarded as *indirect* or as *direct*. The first type is characterized by an inherent resource to intuitiveness, in which the designer modifies the original pre-design according to his/her own epistemologic understanding of what the optimal result will be. The second type, also known as mathematical optimization, involves the definition of design and static variables and of objective functions, leading to purely logic-based decisions regarding the design.

In synthesis, as optimization (be it direct or indirect), is the sub-process within design where the best elements are selected according to functional and conceptual criteria, analysis is the sub-process within optimization where compliance with the requirements is investigated. The other three steps suffer a great influence from societal and cultural inputs, and are the ones that make necessary the figure of the designer as an interpreter of the inputs and the outputs in the process.

The distinction made here between design, optimization and analysis is necessary in order to clarify fundamental differences that unfortunately too often, appear mixed in the literature, even in official regulations. The scope of this thesis is fundamentally the application of variational and probabilistic methods to the analysis of structural systems. One must not be misled by the abundance of research made in the application of probabilistic and stochastic methods to structural optimization. The following is a brief outline of both concepts:

4.1.2.1.- Structural optimization

When structural optimization is dealt with in a direct, mathematical manner, there are mainly three types of problems that can be solved: size problems, shape problems and topology problems. Size problems refer to those in which the cross section of the structural elements is iteratively modified until the best possible ratio of capacity/demand is achieved subject to a set of given constraints. Shape optimization aims for the same target, but updating the boundaries of the structural system. When not only the shape but also the interconnections between elements is allowed to change, the problem becomes a topology optimization one.

The mathematical techniques to solve such problem range from calculus of variations, linear, non-linear or stochastic programming to game theory, simulated annealing, genetic algorithms or neural networks. Although the whole mathematical optimization discipline is beyond the scope of this thesis, a short outline of the employed methodology will be given here.

A mathematical optimization problem has the form:

$$\begin{aligned} & \text{minimize } f_o(x) \\ & \text{subject to } f_i(x) \leq b_i, \quad i=1, \dots, m. \end{aligned} \quad (4.1)$$

where the vector x is the optimization variable, the function f_o the objective function, the m functions f_i are the constraint functions and the constants b_1, \dots, b_m are the limits, or bounds, for the constraints.

In synthesis, an optimization problem is composed of:

- Design variables, which is the set of parameters describing the system (material properties, size, loads,...)
- An objective function, whose purpose is to give a benchmarking as to which design is better than

other (deflection, weight, cost,...)

- Design constraints, within which the system must perform and that can be influenced by the system (maximum and minimum limits that the design variables, or combinations of them, can adopt).

The key of a well formulated optimization problem is the correct identification of the design variables. A minimum number of independent definitions is needed in order to obtain a solvable formulation. These variables are represented as elements of a vector x .

The objective function $f_o(x)$ is a scalar value depending on the vector x , and it is common practice to choose in such a way that the solution of the problem is that of finding a minimum for it. One can also encounter problems in which more than one objectives need to be achieved: these are called multi-objective functions.

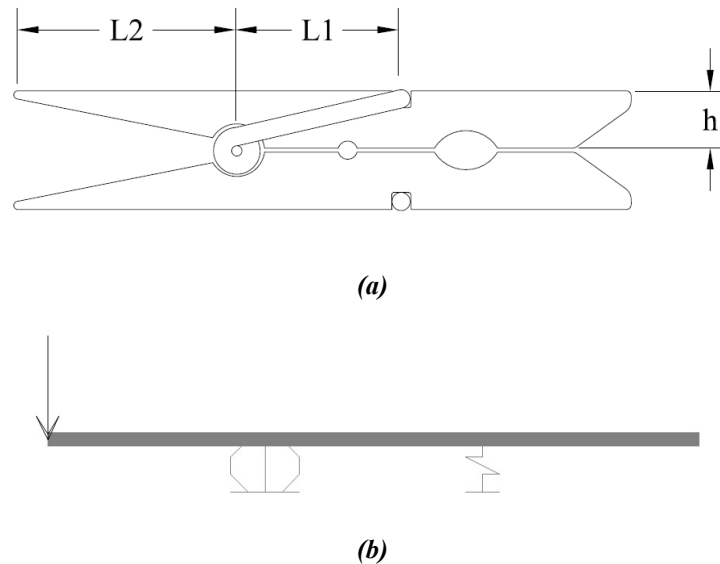


Figure 4.1: Schematic of a clothespin and simplified modelization in a structural design application. The geometrical dimensions are shown in (a), with the design variables h , $L1$ and $L2$. The simplified model shown in (b) is based on beam elements. Symmetry is applied to halve the computational effort.

A design meeting all the requirements is called a feasible design. If one or more constraints are not met, then the design is infeasible or unacceptable. These constraints can come in the form of linear or non-linear equations that, themselves, can also be equalities or inequalities.

The standard optimization model, given the definition of equation (4.1), takes the following form:

$$\begin{aligned}
 & \text{minimize } f_o(x) = f(x_1, x_2, \dots, x_n) \\
 & \text{subject to:} \\
 & \text{(a) } g_i(x) = g_i(x_1, x_2, \dots, x_n) = 0, i=1 \text{ to } m \\
 & \text{(b) } h_j(x) = h_j(x_1, x_2, \dots, x_n) \leq 0, j=1 \text{ to } p
 \end{aligned} \tag{4.2}$$

Where $g_i(x)$ is the set of m equality constraints and $h_j(x)$ is the set of p inequality constraints.

Let's illustrate the idea by means of a simple optimization problem: that of the section of a wooden clothespin body depicted in figure 4.1. Given that these are manufactured by the thousands, every savings in material can have a large repercussion in the long run. The functioning mechanism is very simple, as can be seen in the synthetic model of figure 4.1(b). The spring acting in one third of the body compensates the action of any applied load in the extreme, rotating around the axis of the peg whenever the load is larger than the force of the spring. The amount of rotation is limited to the angle of the edge of the body as long as the body behaves as a rigid solid. For lower stiffness, the action of the force applies only to deformation of the tip, hence eliminating the functionality.

The design variables for this particular problem can be enumerated in several ways. We will choose the following:

$$\begin{aligned}
 x_1 &= K_s \text{ (spring's force)} \\
 x_2 &= L_1 \text{ (spring's lever arm)} \\
 x_3 &= F \text{ (applied force in the tip)} \\
 x_4 &= L_2 \text{ (force's lever arm)} \\
 x_5 &= E_{wood} \text{ (wood's elastic modulus)} \\
 x_6 &= h \text{ (height of the peg's body)} \\
 x_7 &= I \text{ (moment of inertia of the body's section)} \\
 x_8 &= \delta \text{ (displacement of the tip)}
 \end{aligned} \tag{4.3}$$

With these parameters, it is possible to describe a set of relationships between them.

First, we will describe those constraints that are defined by equalities. The force exerted by the spring (x_1), the spring and the force's lever arms (x_2 and x_4) and the modulus of elasticity of the wood (x_5), can be taken as a fixed value, defining the following set of functions:

$$\begin{aligned}
 g_1(x) &= K_s = x_1 = 5 \text{ N} \\
 g_2(x) &= L_1 = x_2 = 20 \text{ mm} \\
 g_3(x) &= L_2 = x_4 = 30 \text{ mm} \\
 g_4(x) &= E_{wood} = x_5 = 500 \text{ N/mm}^2
 \end{aligned} \tag{4.4}$$

By equilibrium of forces, we can define another equality function relating the spring force and the applied load:

$$g_5(x) = K_s \cdot L_1 - F \cdot L_2 = x_1 \cdot x_2 - x_3 \cdot x_4 = 0 \tag{4.5}$$

And the relation between moment of inertia, area and the height of the section:

$$g_6(x) = I = \frac{bh^3}{12} = \frac{A \cdot x_6^2}{12} \quad (4.6)$$

Secondly, we can define the conditions with inequalities, such as the tension in the section should not exceed the strength capacity of the material and the geometric constraint, mentioned above, that limits the amount of displacement of the tip to the amount of opening being equal to the height of the body:

$$h_1(x) = \sigma = \frac{My}{I} = \frac{F \cdot L_2 \cdot h}{2 \cdot I} = \frac{x_3 \cdot x_4 \cdot x_6}{2 \cdot x_7} - \sigma_{ywood} \leq 0 \quad (4.7)$$

$$h_2(x) = \delta = \frac{FL_2^3}{3EI} + \frac{FL_1}{K_s L_2} = \frac{x_3 \cdot x_4^3}{3 \cdot x_5 \cdot x_7} + \frac{x_3 \cdot x_2}{x_1 \cdot x_4} - x_8 \leq 0 \quad (4.8)$$

This allows us to formulate the problem as that of finding the minimum average area for the cross section, leading to the following description of the problem in standard form:

$$\begin{aligned} & \text{minimize } f_o(x) = f(x_1, x_2, \dots, x_n) \\ & \text{subject to:} \\ & \text{(a) } g_i(x) = g_i(x_1, x_2, \dots, x_n) = 0, \quad i = 1 \text{ to } m \\ & \text{(b) } h_j(x) = h_j(x_1, x_2, \dots, x_n) \leq 0, \quad j = 1 \text{ to } p \end{aligned} \quad (4.9)$$

Given that the only variables whose value is not pre-defined are the moment of inertia and the height of the section (x_6 and x_7), we can make the objective function dependent on them as per equation (4.6), leaving the objective function as follows:

$$f_o(x) = f(x_1, x_2, \dots, x_n) = A = \frac{12 \cdot I}{h^2} = 12 \frac{x_7}{x_6^2} \quad (4.10)$$

A plot of the objective function can be seen in figure 4.2. The selected variable for depicting the iterative approach was the section's height (x_6). The objective function, as the relation between the area and the moment of inertia, can be seen as a straight line, whereas both the non-linear constraints $h_1(x)$ and $h_2(x)$ define lower bounds of the design space. Any point of the green region is a valid design. However, the optimum lies in the intersection between $f_o(x)$ and $h_2(x) < 0$, for being this a minimum of $f_o(x)$ still larger than the condition imposed by $h_1(x)$ and $h_2(x)$.

In our case, with a 5kg strong spring, a height of 4 mm should provide the body of the clothespeg with enough rigidity to open the other end without bending, hence rendering useless. This condition is visibly much more restrictive than that of resisting a given amount of tension, as the plot of $h_2(x)$ reveals.

4.1.2.2.- Structural analysis

An elementary step in the design process is the determination of the effects of the environment on the designed object and its components: the analysis.

As explained earlier in this chapter, prior to this point an estimate of specifications of characteristics such as geometry, material properties, expected cost etc. must be provided for each element. These specifications will account for the capacity of the design.

On the other hand demand, in structural design, is generally defined by a set of loads of different nature (permanent, variable, accidental, etc.) each of them with a different degree of associated uncertainty. An initial estimate of their values and characteristics is also needed to begin with the analytical process.

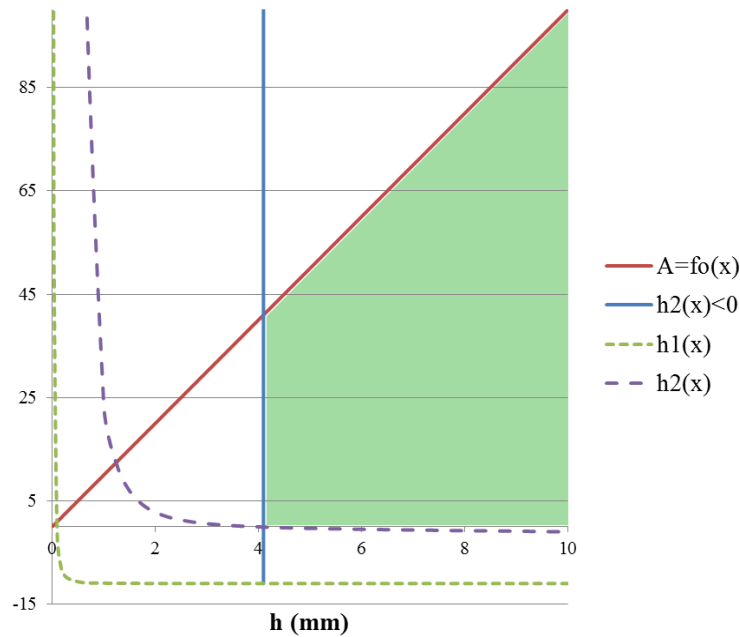


Figure 4.2: Plot of the objective function and the inequality constraints. The feasible design is contained within the green area. The optimum, in the intersection of the blue line ($h_2(x)<0$) and the red line (objective function).

The very definition of an analytical model is in itself a source of uncertainty, given that a big amount of assumptions and simplifications needs to be made. The necessity of those simplifications has many origins: computational efficiency, mathematical limitations, insufficient knowledge about the simulated phenomenon, etc.

In the process of analysis, the balance between demand and capacity is examined in order to detect the potential sources of failure of the design. To such end, the structural system is decomposed into isolated parts that are studied according to the basic physical principles and natural laws. In general, this procedure is applied recursively until an acceptable level of equilibrium between both demand and capacity, subject to a set of requirements or constraints, is achieved. This iteration was introduced in the previous section as the optimization process.

It is not uncommon to find in the literature the concepts of optimization mixed with those of the analysis, given that both share a great deal of common mathematical tools. However, as it was shown, there are substantial differences between them and their respective importance within the globality of the design process. Analysis is the elementary subroutine within optimization, which in itself is one step of the design process. In the example given above, each of the points of the given curves was the product of one complete analysis. In this case, it could be simplified as two single functions ($h_1(x)$ and $h_2(x)$), but in general analytical models acquire very high degrees of complexity.

4.2.- The process of analysis in structural design

Despite the rigorous scientific methodology involved, there are many sources of uncertainty that arise in this part of the design, namely computational error (of the physical model, of discretization, of programming, round off errors...), material properties, random nature of the loads, manufacture defects or unexpected final usage.

Given the potentially catastrophic results of structural failure (not only economic, but also fatal), there have been, historically, countless efforts in the attempt to contain such uncertainty. In its most primitive form, uncertainty was restrained within the boundaries of a “safety factor”. With the development of applications of probabilistic methods of risk assessment in the 1950s, more sophisticated semi-probabilistic approaches were possible that led to the current Load and Resistance Factor Design / Limit States Design (LRFD/LSD) methodologies. In the past three decades, however, those approaches have also been challenged and fully probabilistic procedures to deal with uncertainty are being proposed, replacing the concept of structural safety with that of structural reliability.

4.2.1.- Deterministic analysis: working stress approach

A deterministic design process is characterized by the a priori assumption that there is only one optimal designed object to cover a given need (or demand) under the set of given limitations (or capacity). Accordingly, demand and capacity themselves are considered to be deterministically foreseeable and predictable. Making an analogy with physics, this is equivalent to say that the trajectory of an object can be accurately described by averaging the time-history of its maximum and minimum possible locations at each time step. Before the advent of Quantum Mechanics, this assert was generally accepted in the belief that the span between the observed maximum and minimum, given the right time to improve the measures, would become zero and the average would be coincident with the real trajectory.

In order to account for the many sources of uncertainty, a deterministically minded designer increases the capacity of the designed object and decreases the expected demands by means of safety factors whose values are given either by past experience or by convention. In the deterministic approach, uncertainty is not considered inherent to the designed object or the observed phenomenon, but an intrinsic flaw of the observation, hence subject to replaced by confidence and safety.

The term safety factor has many different usages among engineers of different disciplines and a precise definition of it is not possible in a general manner that satisfies all disciplines. In the particular case of structural design it refers to a measure of the reliability of a particular design.

Although deprecated worldwide in modern standards of practice, the value of this measure is commonly convened by means of standards and codes maintained by the respective industry the structural object

might be designed for (aircraft, building, bridge, etc.).

This value is normally symbolized as γ and can be obtained in a straightforward manner by dividing the maximum load at which the structure is expected to fail (its capacity C) by the expected load the object will be submitted to (the demand D):

$$\gamma = C/D > 1 \quad (4.11)$$

The rationale underlying this methodology is simple and straightforward: the larger the value of the factor γ , the higher the safety achieved.

If, for example, a structural configuration can withhold the maximum expected wind load demand for its given lifetime it will, most certainly, resist any other wind loads because they will be of lower intensity.

In design practice, however, the value of the capacity is unknown a priori as neither the object is built or a final model is set. Hence equation (4.1) has to be treated as the following inequality:

$$D < C/\gamma \quad (4.12)$$

In this manner, an iterative process can be performed in which, departing from an initial configuration whose capacity can be estimated, one reaches the point where the condition imposed by equation (4.12) is accomplished.

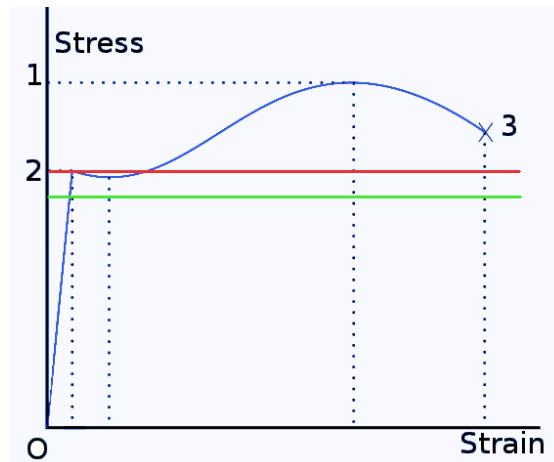


Figure 4.3: Stress-strain diagram for a generic material. Capacity is defined according to the limits established in this curve. Point 1 is the ultimate strength limit. Point 2 is the elastic limit. The green line is the design limit.

A second a priori assumption of this approach must also be mentioned: the measure of demand is based on the amount of stress the members of the object are subjected to (hence the denomination working stress design). In this way, demand is calculated element by element by means of the numerical methods described in the first chapter. This happens as a result of the traditional definition of capacity provided by the science of resistance of materials, by virtue of which it can easily be defined by load-displacement

curves such as that of figure 4.3. Its convenience relies on the possibility of stating a nominal value, generally within the elastic limit (point 2 in figure 4.3), that can be factored by the γ safety factor to obtain the design limit.

In the working stress approach, average values from several essays are considered acceptable as parameters for the definition of both capacity and demand.

4.2.2.- *Semi-probabilistic analysis: Load and resistance factor / Limit state approach*

Load and resistance factor analysis (LRFA) is also known as limit state analysis (LSA). It is globally accepted as a more refined version of the safety factor approach and is currently enforced by most regulations worldwide.

In this approach, the predictability of the demand (applied loads) and the variabilities of the capacity parameters (resistance parameters) are accounted for separately. In the case of the loads, each can have a different factor according to whether their nature is permanent or variable in time. Moreover, their simultaneities are also studied thoroughly in order to find a worst case scenario. For the results of outranging the capacity, a series of “limit states” are defined: ultimate if the result is collapse, serviceability if the result are minor defects (generally excessive deformation or vibrations), fatigue if the result is a wearing off due to cyclical loads or accidental if the demand is originated by explosions, fire, collisions, etc. Note that both fatigue and accidental limit states are actually defined by the nature of the demand. However, in the regulations they are considered to affect the capacity.

This leads to a new interpretation of equation (4.11):

$$\sum D_i \cdot \gamma_D < \sum C_i / \gamma_C \tag{4.13}$$

The load (demand) and strength (capacity) factors are different for each type of loading and strength. The higher the uncertainty associated with a load or a strength parameter, the higher the corresponding load factor. The factors are probabilistically defined so that they correspond to a prescribed safety level.

It is considered a semi-probabilistic approach because it maintains the basic assumption of the existence of a single optimal solution but both the values of capacity and demand are based on the extreme value theory introduced by Gumbel, Frechet and Weibul in the middle of the 20th century. Figure 4.4 illustrates the sequence that leads to a Gumbel-like probability distribution in the case of wind speeds.

In a similar manner, the capacity can be associated with properties of the material that constitute the structure (mechanical, geometrical, etc.).

These properties are also subject to statistical analysis. figure 4.5 shows the probability density function, superimposed to its histogram, of the compressive strength of concrete. Although in both cases the values

are obtained by means of statistical and probabilistic analysis, the methodology remains deterministic in the sense that it only studies one possibility, be it the average or that with the highest probability.

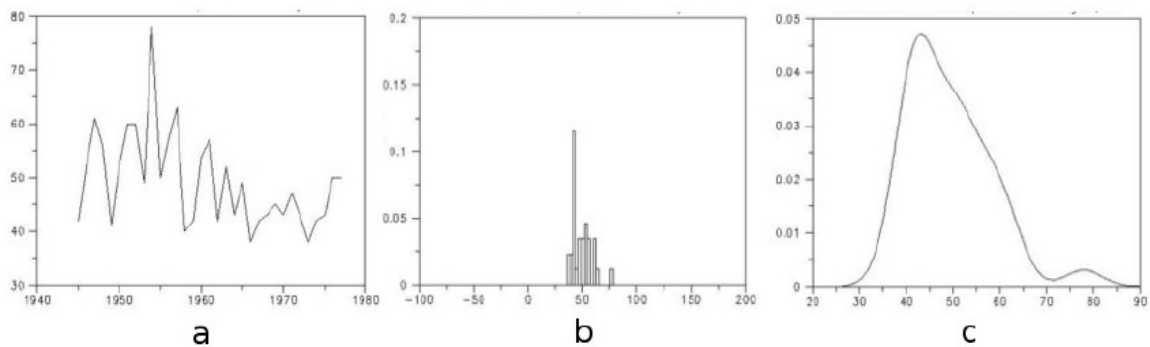


Figure 4.4: Analysis of raw data for wind speed in Washington. The extreme value theory gives the probabilities of occurrence of the maximum and minimum wind speeds. a) maximum annual wind speeds against time. b) histogram of relative frequencies for each recorded speed c) Gumbel-like probability density function.

The semi-probabilistic approach has the advantage over the fully deterministic one in the fact that ultimate limit states are checked against factored load combinations whereas in the working stress approach only one safety factor is employed. This allows for more economical designs with equivalent level of reliability by scaling the probabilities of exceeding failure modes. Also, the second-order geometric effects resulting from deformation and material behaviour can be considered in a straightforward manner at the load levels associated with failure.

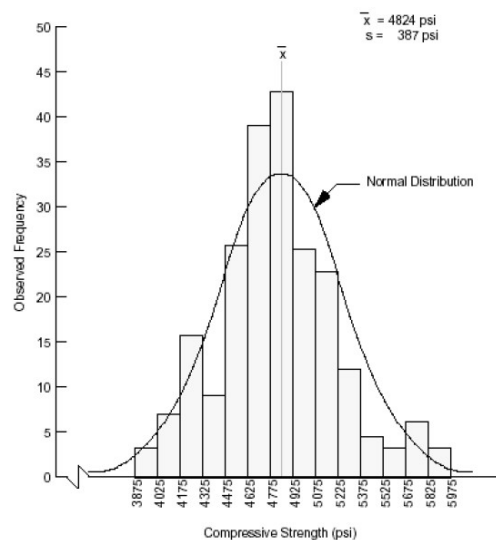


Figure 4.5: Bell curve, superimposed over a histogram of pavement concrete compressive strength data. The average value has the highest probability of occurrence.

4.2.3.- Fully probabilistic analysis: Reliability assessment approach

The semi -probabilistic approach defined earlier, however, does not allow for a direct evaluation of the probability of failure. By means of defining the reliability of a design iteration it is possible to achieve a more global and comprehensive understanding of the failure or safety violations.

However, to use this approach one needs to consider the multi-random variable input governing both capacity and demand, whose analytical mathematical solutions required to determine the design point can become very difficult, if not impossible to formulate.

To such end, reliability analysis methods use stochastic procedures to model both the variability in the demanding loads as in the properties characterizing the capacity: the variables are treated as probability distributions instead of single values. This replaces the notion of a safety factor with a probability of failure, leading to a probabilistic reinterpretation of equation (4.11):

$$P_f = P \{C-D \leq 0\} < P_D \tag{4.14}$$

Where P_f is the probability of failure, conditioned to be smaller than a given design probability, P_d .

Figure 4.6 depicts the conceptual approach showing how both the capacity of the system and the demand are understood as bounded histograms of the cumulative probabilities of the corresponding input variables. The probability of failure is a 3-dimensional region where capacity is smaller or equal to the demand.

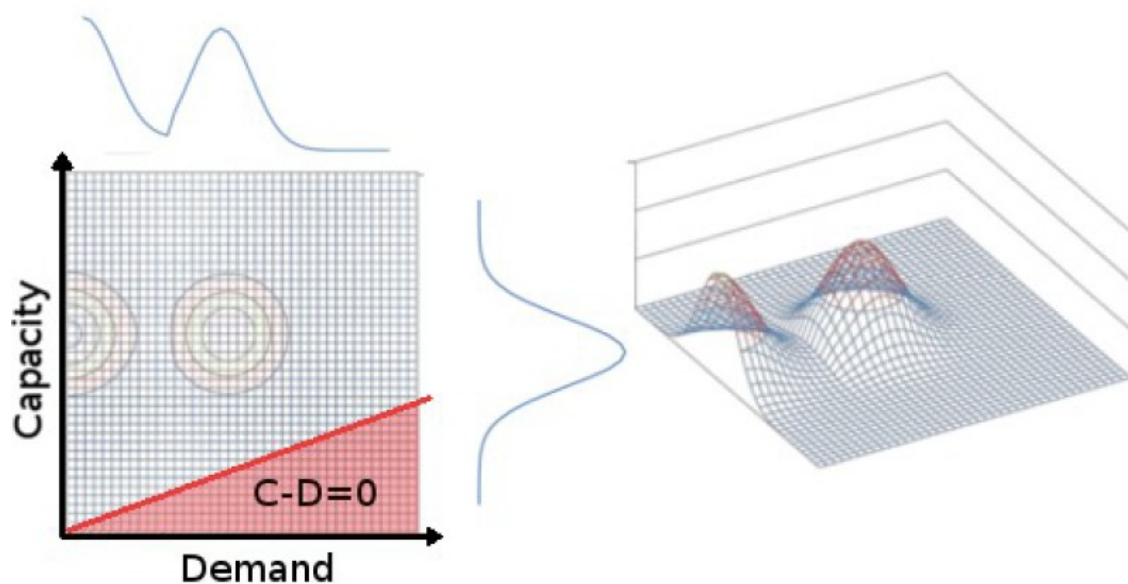


Figure 4.6: Graphical representation of a probability region for a given structural system. Both capacity and demand are treated in a fully probabilistic way by means of bounded histograms. The red color covers the failure region where the ratio Capacity / Demand is bigger than unity.

The two most common-approaches used in structural reliability analysis are the group of reliability index

methods (first and second order) and simulation methods (Monte Carlo).

In the category of reliability index, a limit state function is defined out of equation (4.14) as:

$$g(x) = C - D \quad (4.15)$$

Whether the function $g(x)$ is linear or non-linear, the analysis reduces to the calculation of the minimum distance of the line representing $g(x)$ to the origin. In the example of figure 4.4, where the problem is linear, First Order Reliability Method (FORM) is of application. When the limit state function is non-linear, more complex recursive algorithms are used, such as in Second Order Reliability Method (SORM).

Regarding simulation techniques, once defined the limit state function of equation (4.15) it is possible to formulate the probability of failure in the following manner:

$$P_f = \int_{g(x)=0} f_x(x) dx \quad (4.16)$$

where $f_x(x)$ is the joint probability density function of the random variables X . Stochastic simulation methods such as Monte Carlo, although computationally much more intensive than the previously mentioned ones, are particularly suitable for approximating integrals. They are mostly used when the limit state function is not differentiable or when several design point contribute to the failure probability.

A thorough study of those methodologies is beyond the scope of this thesis. However, it seems in order to clarify here their applicability only to the analysis part of the design. There is a certain amount of confusion in the literature, particularly under the Reliability Based Design Optimization publications, where the procedures above outlined are sometimes mistakenly presented as actual optimization techniques. The optimization part of design is treated in the discipline of mathematical programming, and involves objective functions instead of limit state functions. A particular application of optimization solving technique will be presented in the next chapter.

4.2.4.- The limits of accuracy: uncertainty quantification in numerical simulation

Both in the deterministic and the semi-probabilistic approaches there is a common flaw regarding the ubiquitous presence of uncertainty: it is treated in the same manner as errors. However, they are not the same thing.

While an error is an identifiable deficiency either in the model or in the introduced parameters, uncertainty is a potential deficiency due to lack of knowledge. Errors have their origin in the mathematical characteristics of the posed problem. Uncertainty in the other hand can be either epistemic (incertitude) or aleatory (variability), and is rooted in the very description of the physics involved.

In order to tackle errors, common deterministic practice relies on the increasing control of the

mathematics, i.e., increase of the accuracy of the measures, floating point precision, reduction of the round off error, mesh refinements, etc. But lack of knowledge or aleatory behavior can not be treated in that manner because there is no way to know beforehand what is needed to be reduced. Regarding the epistemic uncertainty, it is still possible to treat oversimplified assumptions in a more rigorous manner, defining new sets of parameters that help to match better the analysis results with the observed experiments. Material properties, operation conditions, manufacture tolerances and other sources of variability can not, however, be better foreseen by increasing the number of, for example, strength tests, if in the end only the average result will be employed.

In order to account for the degree of uncertainty associated with a given design function, we must first define the degree of uncertainty of its defining parameters. When no prior information about the parameters or their relationship can be established, the measurement of a function and its maximum combined uncertainty is given by

$$f(x_1, x_2, \dots, x_n) \pm U_f = \left| \frac{df}{dx_1} \right| U_{x_1} + \left| \frac{df}{dx_2} \right| U_{x_2} + \dots + \left| \frac{df}{dx_n} \right| U_{x_n} \quad (4.15)$$

where U_f is the total associated uncertainty to the function and $U_{x_1}, U_{x_2}, \dots, U_{x_n}$ are the associated uncertainties of the particular parameters.

As an example, let us consider the calculation of the axial rigidity of a structural element, given by the analytical formula:

$$K = \frac{AE}{L} = f(x_1, x_2, x_3) = \frac{x_1 \cdot x_2}{x_3} \quad (4.16)$$

where A is the area of the section, E is the modulus of elasticity of the material and L is the length of the element. In equations (3.11) to (3.14), this value would be regarded as a parameter describing the capacity of a given structural system (a vertical column, for example), and A , E and L its sub-parameters.

Inserting equation (4.16) into equation (4.15) leads to:

$$f(x_1, x_2, x_3) \pm U_f = \left| \frac{df}{dx_1} \right| U_{x_1} + \left| \frac{df}{dx_2} \right| U_{x_2} + \left| \frac{df}{dx_3} \right| U_{x_3} = \frac{E}{L} \cdot U_A + \frac{A}{L} \cdot U_E + \frac{A \cdot E}{L^2} \cdot U_L \quad (4.17)$$

with the U_A , U_E and U_L values being respectively the associated uncertainties of area, modulus of elasticity and length.

Table 4.1 gives nominal values for each parameter and its associated example uncertainties. For the sake of simplicity, we have use standard deviations in percentage as a measure of their particular variability. In the particular case proposed in the table, the final uncertainty obtained for the design parameter K would be exactly the sum of the three uncertainties, 11%, which is lower than that of 25% given in deterministic

steel codes.

Table 4.1: Design parameters of a column and their associated uncertainty

Parameter	Value	Uncertainty
Area (cm ²)	144	4%
Length (cm)	300	2%
Modulus of elasticity (kN/cm ²)	21000	5%

Figure 4.7 illustrates the linear relationship between the variation of the total added uncertainty and that of a particular parameter. In more complex functions, a sensitivity analysis of the influence of each parameter gives valuable information regarding the importance of their contributions to the total uncertainty. This allows the designer to take informed decisions as to how to minimize the epistemic uncertainty and also, to better understand the modeled physical reality.

Uncertainty quantification and sensitivity analysis can be carried away regardless of the deterministic or non deterministic character of the design approach. However, a probabilistic approach deals with them in a straightforward manner as parameters are given already in the form of distribution functions instead of single average values.

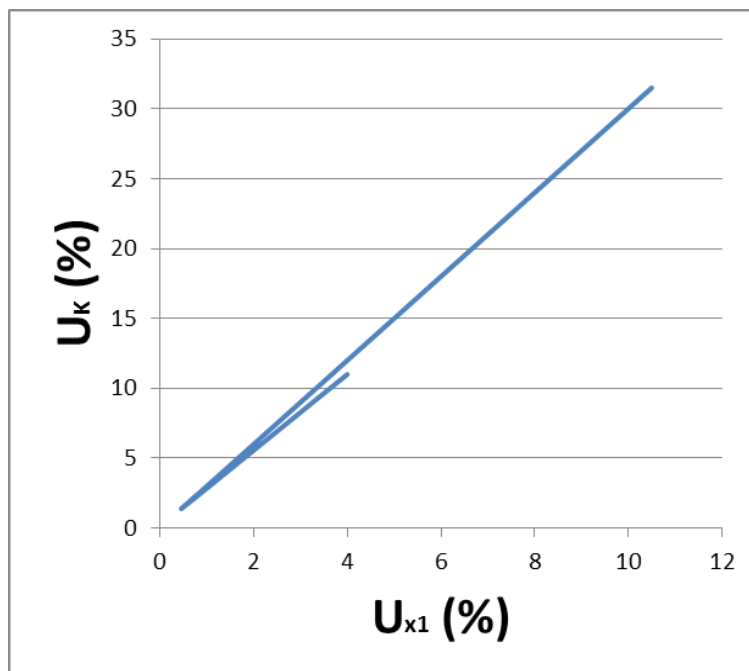


Figure 4.7: Variation of the uncertainty of the axial stiffness function with respect to the variation of its variables A , E and L . The total uncertainty of the function increases linearly at a rate almost three times its composing variables, given that it is three of them contributing equally. Sensitivity analysis allows for the characterization of the degree of influence of the variables in the final total uncertainty of a model.

4.3.- The process of optimization in structural design

In the introduction to this chapter the mathematical modelling of the optimum design problem was presented. From the very definition of the problem in equation (4.1), it is fairly obvious that the possibilities for formulating it are quite vast. There are, however, some practical limitations to the applicability of rigorous mathematical implementations given mostly their degree of abstraction. This has led to two main approximations that can be found in the literature, one using mathematical programming and other the so called optimality criteria.

4.3.1.- Mathematical programming techniques

Mathematical programming, or mathematical optimization, in the discipline that studies the solution of problems by systematically choosing input values from within an allowed set and putting them in an objective function, whose value is to be maximized or minimized.

Optimization problems in the field of mathematics have many applications, from logistics to economics, and originated also in the work of Lagrange and Fermat. Actually, the Lagrange Multipliers method described in Chapter 2 of this thesis is one of them. The methods presented in the present chapter differ from the ones introduced previously in that they are “constrained”, which requires extra analytical effort and modifies slightly the approach taken to solve them. The term “programming” in this context is inherited from its use in military “programs” referring to training and logistics schedules of the U. S. Army in the first half of the 20th Century, and is not related to the contemporary notion of “computer programming”.

In general, they represent search algorithms that compute the gradient of the objective function and iterate from an initial point to a following point. The condition for “moving” into the next consecutive point is that the value of the design variables remains larger than a given threshold, terminating otherwise.

In the particular case of structural design, a few of these techniques have been employed with success. The following is a non-exhaustive list that, nonetheless, covers most of the approaches found in literature: Sequential Linear and Quadratic Programming (SLP and SQP), Penalty Function Methods (PFM) and Gradient Projection Method (GPM).

- SLP: in a geometric sense, this group of algorithms compute a line or a plane tangent to the curve or surface defined by the objective function in the current iteration point. Given that, in structural optimization, the constraints are normally non-linear, this method uses Taylor expansion series to transfer the non-linear programming problem into a linear programming one. It is also known as “cutting plane method”. SQP, on the other hand, approximates the original non-linearly constrained problem with a quadratic sub-problem and successively solves this sub problem until

convergence. It has proven to be quite effective in solving large scale structural models.

- PFM: in this group of algorithms the techniques for unconstrained minimization described in chapter 1 of this thesis are employed. The idea is to replace the constraint equations with penalty values on constraint violations so that the efficiency advantages of unconstrained optimization can be exploited. Conceptually, it only involves problems regarding the inequality constraints because the penalty can only apply to constraint violations. They have been proven reliable for structures of moderate complexity.
- GPM: in this method, iterations follow the boundary defined by the objective functions until the constraints are met. To such end, a gradient vector is computed and decomposed in its tangent and a normal components. Its values are then used in a series of Newton iterations to find the next feasible point.

Despite all their theoretical generality, none of the above listed methodologies succeed in effectively solving all kinds of structural problems. Besides, they are mainly counterintuitive for the engineering practitioner as these methodologies are originally developed in other disciplines and contain a high level of mathematical abstraction. The fact that, commonly, their implementations are laborious and their use is very computational expensive does also not help to make them attractive to the structural engineering community despite their intellectual elegance.

4.3.2.- Optimality criteria techniques

Given the aforementioned limitations, in the late 1960s a method for optimal plastic design was proposed by Prager and subsequently extended to several elastic and plastic design problems. Optimality criteria are conditions which must be fulfilled at the solution of an optimal design problem. Their enunciation is dictated by actual experience in the field of structural design and can contemplate from regulatory constraints to minimum strain energy or combined stresses located in a section. In the numerical experiments section of this chapter an example using constant average strain energy criterion will be shown. The current research work on structural optimization based on optimality criteria is an extremely prolific one and will not be reviewed here. The reader is referred to the excellent work of Saka and Geem [SAK2013].

In general, the optimality criteria approach tends to yield efficient optimization algorithms regardless of the complexity of the structures. They have proven useful in the optimum design of linear elastic, non-linear elastic and elastic-plastic structures.

However, whether one chooses any of the above approaches to solve a design problem, it must be considered that the practical realization of structural objects involves a discrete set of possible

constructive solutions dictated by industry requirements. Whether beams, columns, walls or any other elements are made of aluminium, steel, wood or any other material, eventually the potential advantages of a refined optimized model can get diluted due to crude restrictions in the availability of a given section or profile. Although possible, adapting the deterministic approaches to contemplate discrete possibilities is algorithmically cumbersome. This explains the increasing popularity of stochastic search methods.

4.3.3.- Techniques of stochastic optimization of structures

Historically, the deterministic approach explained earlier has prevailed, originated in the search of finding solutions for problems of optimality as explained in the first chapter of this thesis. From the second half of the past century however, stochastic methods have proliferated also in the field of optimization thanks to their versatility and algorithmic simplicity.

Stochastic methods, or statistical simulation methods, are a general family of numerical techniques that employ sequences of random numbers to perform a simulation. As opposed to the “conventional” methods described in chapter 2, stochastic methods simulate physical processes directly, without explicit need of differential equations.

Largely three groups of methodologies have found application in the field of structural optimization: evolutionary algorithms, simulated annealing and particle swarm strategies. For introductory purposes they are briefly described below:

4.3.3.1.- Evolutionary algorithms

The underlying analogy of these methods is that of Darwin's theory of evolution and survival of the fittest. On each iteration, a set of solutions called individuals, candidates or phenotypes is generated. For such generation, the vector of random variables is populated with random valid values that define a feasible solution. This vector is called genome or chromosome. A new individual is obtained by simply changing one of the values of the vector. The fitness of each individual of an iteration set or generation is checked against a defined optimality criteria. Once the fittest is found, the next iteration is made taking it as a basis for the generation of all the following individuals.

Depending on how the chromosome is treated to pass the information to the following generation, we have different types of algorithms. The most popular among them are the so-called genetic algorithms, where techniques of crossover, mutation and recombination are used.

4.3.3.2.- Simulated annealing

This technique iterates through the space of feasible designs to find a global minimum even when the objective function has several local minima. It employs the analogy with the metallurgic process of

annealing, where the properties of a given material are improved by adding a large amount of energy in the form of heat and slowly cooling of it. Algorithmically, the slow cooling means a narrowing of the probability of acceptance for consecutive solutions which are worse. Worse solutions are needed in the process as they allow for a more extensive search for the optimal solution.

At each step, the simulated annealing algorithm considers some neighbouring state s' of the current state s , and decides between moving the system to state s' or staying in state s . To do so, it calculates an acceptance probability based on the current state and, if satisfactory, it keeps the value. Otherwise a new value is randomly generated and the iteration is made again. The process terminates when the temperature function reaches a predefined value. In our numerical experiments this technique is illustrated and applied to a structural optimization problem in combination with a statistical mechanics approach to the analysis.

4.3.3.3.- Multi-agent systems

This type of techniques involves a number of “particles” that move freely over the objective function. The “particles” or “agents” are actually candidate solutions that “move” over the search space according to a given set of rules. These “agents” communicate to each other in such a way that those located in poorer positions are “attracted” towards the position of those with higher values. Coordinated collective behaviours emerge from relatively simple interactions between the group and the individuals. Each single particle is programmed to respect certain restrictions regarding the locality, collision avoidance, velocity matching and centering in the flock.

Larger communities require higher computation effort, but also they scan faster the search space. This makes this kind of algorithms very interesting for parallel computation. Depending on how the interactions of the individuals between each other and the search space are coded we have mainly two types of techniques:

- Particle swarm: in this case the search space is associated to a continuous 2-dimensional euclidean space where the particles have a position and velocity according to their fitness. This is defined by a fitness function that takes into account one or several optimality criteria. Taking into account the restrictions to their movement mentioned earlier, the particles swarm over the search space and the values associated to the fittest individual are retrieved after a number of iterations.
- Ant colony: for this methodology the search space must first be assimilated to a graph over which the particles jump from node to node, looking for cheaper paths. Using the analogy of pheromone traces employed by ants in their search of optimal paths, individuals “mark” each node according to a probability defined by the fitness function. It has some advantages over simulated annealing and genetic algorithms in what the graph is allowed to change dynamically as the procedure can run continuously and adapt to changes in real time.

In the following sections of this chapter a methodological procedure combining the energy principles explained in chapter 3 with the simulated annealing technique will be presented. The choice of such technique was dictated by its straightforward analogy with the thermodynamics principles, its claimed numerical superiority according to several authors and its algorithmic simplicity.

4.4.- Discussion

In this chapter, it was explained how structural design is a process involving decisions based on a rigorous scientific methodology within which optimization is one subroutine that incorporates itself several iterations of the process of analysis. This important distinction between optimization and analysis as processes within design was also made. It is frequent to find published work where these two concepts are not discriminated, leading to potential misconceptions on the topic.

It was also remarked how, both in the deterministic and the semi-probabilistic approaches to analysis, uncertainty is commonly disregarded and treated as errors, although they are not the same thing. By increasing the accuracy of the measures, implementing floating point precision, refining meshes, etc. can only account for the uncertainty originated in error.

However, lack of knowledge or aleatory behavior can not be treated in that manner because there is no way to know beforehand what is needed to be reduced. The tools of uncertainty quantification and sensitivity analysis were used to demonstrate how a probabilistic approach deals with them in a straightforward manner as parameters are given already in the form of distribution functions instead of single average values.

An example was made illustrating the methodological aspects for all three approaches to the analysis (deterministic, semi-probabilistic and probabilistic). The increasing degree of sophistication and computational effort from one approach to the next was made evident. Particularly with regard of the computational effort where, for large structural systems, it is not feasible to use probabilistic approaches despite all of their advantages.

Regarding the optimization part, the main tendencies in deterministic as well as in stochastic techniques we presented. This should serve to contextualize the simulated annealing algorithm employed in the next chapter.

5.- A Statistical Mechanics framework for structural systems

5.1.- Introduction

In the previous chapter the intrinsic relationship between structural analysis and structural optimization was described and, more importantly, the fundamental differences between both concepts were drawn and illustrated.

Being analysis an iterative subroutine within optimization, if the notions of probabilistic design are not introduced correctly in their respective segments of knowledge it is easy that they lead to confusion. Such is the case found in many research works, where stochastic routines are attributed to optimization techniques when they are actually considering them only in the analysis part, and vice versa.

A novel approach to structural analysis will be introduced based on statistical mechanics and thermodynamics. This framework will serve to explore the practical implications of the variations of the different energy parameters involved in the deformation of structures. The variables will be treated from the scope of thermodynamics and will be later on employed for the rigorous definition of an energy-based objective function. This objective function will be introduced within the context of a Simulated Annealing optimization algorithm.

Although based on deterministic static analysis, the Simulated Annealing approach must be regarded as stochastic as the algorithm uses random variations of the inputs to search for an optimized configuration.

It must be noted that no reference will be made to probabilistic analysis techniques, as the field itself is sufficiently explored elsewhere [MAY2008].

5.1.1.- Assessing a structural system in terms of energy

The next section will serve to describe a methodology for the quantitative characterization of structural systems in terms of performance, stability, resilience, robustness and other design objectives. These parameters are obtained from quantities traditionally associated to thermodynamics and statistical mechanics (temperature, heat, entropy) and applied only to nanoscopic or microscopic systems.

The necessary conceptualizations to make them usable also in a macroscopic level will be presented, with the double purpose of expanding the reach and understanding of such powerful disciplines and also for providing with yet another field for their practical applicability.

We have resourced to a general purpose finite element application, and applied the aforementioned bridging concepts to yield substantially more valuable information about the modelled structures than merely the internal stresses and displacements relationships.

In the context of structural design, it is important to count on qualitative variables such as robustness, resilience or stiffness applied with a global perspective to the behaviour of the entire system. Moreover,

the availability of a quantitative methodology to compare different designs makes them even more attractive. Robustness is here understood as the ability of the system to resist change without deforming. Resilience, its ability to absorb energy when deformed elastically. Stiffness is treated in a global sense, not just the ratio between applied force and produced displacement of one single point but for the whole structure. Statistical mechanics are widely used for the simulation and definition of material properties in many scientific disciplines. It is generally applied on the molecular level, where the amount of elements, N , has the order of Avogadro's number. In models of structural systems, however, if one gives to N the value of the amount of interconnecting nodes, such value never exceeds the million and is most commonly within the tens of thousands. In this discipline, the elements are molecules or atoms represented as point masses connected to each other by means of potential functions. These functions, together with the velocities, allow for the computation of the potential and kinetic energetic states from which statistical data can be obtained and be used to characterize macroscopic behaviours.

From the engineering practice perspective however, the most extended discretization methods are those that replace the simulated matter with interconnected pieces interpolating the expected material behaviour (deformation, heat, etc.) between a series of nodes. Such are the techniques of Finite Elements, Finite Differences or Boundary Elements among many others. Commonly used, these methods divest the nodes from information and focus primarily on the links or "elements" between them (i.e. rods, beams, tetrahedra, etc.). Nevertheless, their mathematical description relies strongly in the construction of matrices defined by the nodes of the system. For this reason, as the technique of our choice is the Finite Element Method, we have resourced to a series of conceptual and numerical adaptations in order to retrieve the relevant information and have it "lumped" in the nodes. This will permit us to use the techniques of statistical mechanics.

From the point of view of statistical mechanics, a further conceptualization arises due to the previously mentioned number of involved particles, N . Being it so relatively small, we find ourselves in the particular case of non-asymptotic thermodynamic ensembles, where Boltzmann's equation for the definition of probabilities doesn't apply. Hence, for our definition of the value of Entropy, S , and more specifically for the calculation of the probabilities we have had to resource to a frequency based model adapted from references [NIV2009a] and [NIV2009b].

Statistical thermodynamics seek to relate microscopic properties of individual particles to the bulk properties of the sample that contains them. Analogously, if a structural system is treated as a set of interconnected nodes, global characteristics of its behaviour can be found when using probabilistic and statistical techniques.

By defining thermodynamic parameters for a structural system and establishing relationships between them it is possible to expand our understanding of it in a more global manner. Instead of merely

monitoring internal tension distributions of particular beam elements or the displacements of a defined node, one can achieve a general view on how the whole system responds to a set of loads by computing, for example, its “structural heat”, which summarizes in a single parameter both internal stress distribution and displacements.

In the present section the following thermodynamic variables have been computed:

- Number of nodes, N
- Internal energy, dU
- Internal strain energy, δW
- Added heat, δQ
- Entropy, dS
- Temperature, T
- Internal kinetic energy, KE

By defining the proper relationships of thermodynamic variables, it is possible to infer whether the behaviour of a structure under a given set of loads will be more or less robust than another, its degree of global stiffness or how much resilient it will be. These parameters are extremely valuable for the proper design of structures of any kind. For the sake of simplicity, we have limited to simple Timoshenko beam configurations in simple frame-like structures. Nevertheless, this scheme is general and admits any kind of structure and other types of discretization, as long they have a consistent means to transfer the internal energies to the nodes.

We have used four different structures of variable complexity under a simple lateral load. Their description was based on a widespread seismic regulation as it provides with an empirical basis to test our framework.

We have explored the space of possible states by means of random iterations over the magnitude of the applied load. These variations allow for the observation of particular tendencies and correlations between the variables previously enumerated. The range of calculated values of these variables (KE , W , S) are shown as a function of the total applied energy (dU), so that an outline of their behaviour can be observed. Our experiment aims to illustrate the purely elastic behaviour. In this case the emerging ratios of change with respect to the applied energy for all variables are expected to be linear. However, the slopes of the lines will be different for each model, representing unique properties of their configurations.

5.2.- Statistical Mechanics of structural systems

Thermodynamics is mainly concerned with the *changes* that occur in internal energy of a system. Hence, the first law of thermodynamics is an equation of change:

$$dU = \delta Q - \delta W \quad (5.1)$$

where dU is the change in the internal energy of the system, dQ is the heat *added to the system* and dW is the work *performed on the system*.

In statistical mechanics, which is a slightly younger discipline, thermodynamic systems are conceived as assemblies of smaller units which relate to each other in such a way that these changes can emerge.

Within the proposed framework of this chapter, the systems which are under study consist of sets of interconnected Timoshenko beams under the effect of static loads. By means of a general purpose Finite Element application, the linear equations which yield the displacement vector are solved, and the corresponding internal stresses and tensions are obtained. This allows us to compute the related internal energies of the beams and their particular contribution to each node.

5.2.1.- Internal energy, dU

As the presented mechanical system is considered to be thermodynamically closed, the value of the change in the internal energy is computed from the actual value of external work. Given the solution of the displacement vector and the applied force vector, it can be stated that:

$$dU = \frac{1}{2} \{F\}^T \cdot \{x\} \quad (5.2)$$

where $\{F\}$ is the vector of the applied forces and $\{x\}$ represents the displacement of each degree of freedom. This value is equivalent to the expression involving the stiffness matrix $[Kg]$:

$$dU = \frac{1}{2} \{x\}^T \cdot [Kg] \cdot \{x\} \quad (5.3)$$

as the displacement $\{x\}$ is the solution of the system of equations defined by $[Kg]$ and the vector $\{F\}$.

In figure 5.1 an interesting feature of this quantity is presented. It shows how the total internal energy is only inversely proportional to the stiffness while quadratically dependent on the applied force. As a result, flexible structures are capable of dissipating a large amount of applied energy in the form of displacements. If such systems are only slightly more rigid, however, their dissipative capacity is rapidly reduced and must resource to other mechanisms in order to balance the energies.

5.2.2.- Internal work, dW

In classical thermodynamics, this internal form of energy is associated with the mechanical part of the changing process. For the particular case of ideal gases or any non-viscous fluid, this term of the equation of change is generally assumed to be:

$$\delta W = - p dV \tag{4.4}$$

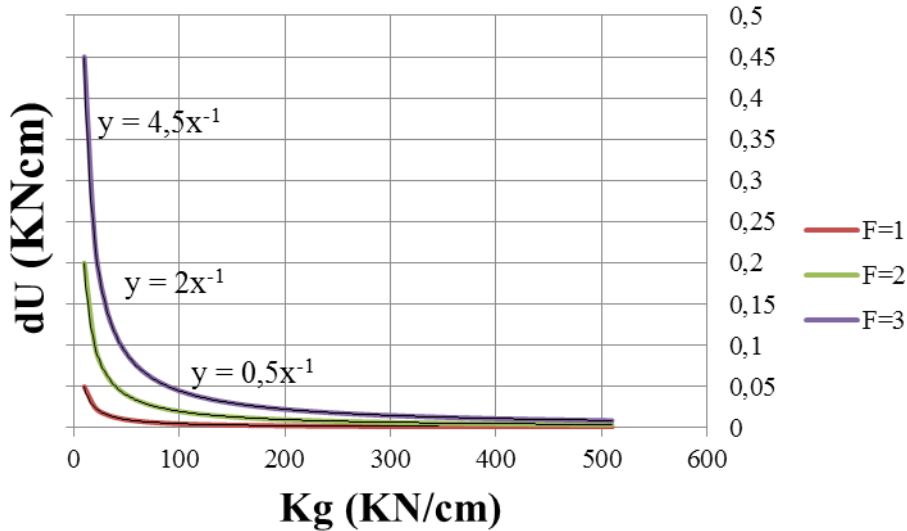


Figure 5.1: Total internal energy versus the stiffness of a system with a single element. This quantity is a quadratic function of the applied force and varies inversely proportional to the stiffness.

where p is the pressure applied to the system and dV the change in volume. For an elastic medium, however, this mechanical energy term must consider the work done by the internal stresses and the strains [LAN1986]. This means that our definition of the work performed on the system is:

$$\delta W = -\frac{1}{2} \int_V \sigma \cdot \varepsilon dV \tag{5.5}$$

where s represents the internal stresses and e the internal strains, integrated over the whole volume of the structure, V . The direction of this work is opposed to that of the total internal energy, hence the negative sign. In order to assimilate the above concepts to a structural system, where several elements are combined and attached in N nodes, it is proposed that a straightforward connection be made between the nodes, acting as atoms or molecules, and the beam elements, taken as bonds between them. The formulae given in table 3.1, either as a function of the internal beam strains or as a function of the internal stresses [AND2013], can be used to such effect. Within the scope of our framework, the internal stresses (axial A , bending M , shear S and torsional T) are commonly available from a general purpose Finite Element

Method application. The stress-based integrals of table 3.1 can then be used in discrete form as a sum through the defined integration stations of each element. The degree of accuracy is higher for a smaller size of the stations, so the value of ds becomes a trade-off between computational effort and precision [MOR2008].

The final nodal internal energy was approximated by summing the contributions of half of each connected beam. The total internal energy of the system is then computed as:

$$\delta W = - \sum_{i=1}^N \sum_{j=1}^{b_i} \frac{1}{2} (W_{Ab} + W_{Mb} + W_{Sb} + W_{Tb}) \quad (5.6)$$

where b_i denotes the number of beams attached to the i th node and W_{Ab} , W_{Mb} , W_{Sb} and W_{Tb} are the respective internal energies of each beam as calculated from table 3.1.

5.2.3.- Added Heat, dQ , Temperature, T and entropy change, dS

The heat added to a system is directly related to the amount of movement of its particles, which are in our case represented by the nodes of the investigated structure. Thus it involves the entropy gained by the system in the process and its temperature:

$$\delta Q = T \cdot dS \quad (5.7)$$

When dealing with the microscopic level, solids are treated as regular lattices of atoms, tied together with bonds which can't vibrate independently (see Einstein and Debye models for simple examples). In order to account for the energy associated with the movement of these atoms, the vibrations take the form of collective modes which propagate through the material. Such propagating lattice vibrations can be considered to be sound waves, whose speed is the speed of sound in the material. The average of this energy is characterized by the temperature, T , while dS , the increase in entropy, parameterizes the “quality” of such energy, i.e. its degree of order.

On a macroscopic structural model, the heat magnitude, Q , tells us how much of the work done by the external force is not absorbed internally by the structure. It is closely linked to the value of kinetic energy, which is described in the following section of this chapter.

In order to compute the value of the heat change we simply proceed to substitute the values of dU and dW previously obtained through equations (4.2) and (4.6), yielding:

$$\delta Q = dU + \delta W \quad (5.8)$$

In an idealized situation where only elastic changes occur and all of the applied work is absorbed by the system without extra displacements or internal stresses, the value of the internal energy, dU , and the performed work on the system, δW , are exactly the same. As the sign of δW is negative, this yields a null

value of δQ . A more common case occurs when δW is slightly smaller than dU in a normal elastic deformation process. In this case, a certain amount of entropy is produced implying that some of the internal strain energy is reallocated through the structure. As long as all the bonds of the structure remain within the elastic regime, this variation of entropy is a constant regardless of the magnitude of the external work. In other words, when dealing with an elastic regime, the distribution of the internal strain energy to the nodes depends only on the configuration of the structural system (i.e. its stiffness and topology). In the case of a more extreme situation, when plastic dissipative processes are studied, dU and δW depend on each other to a lesser extent. As plastic joints begin to appear, the structure loses stiffness and the possible displacements become larger, so that the value of the kinetic energy is increased. As a consequence of this, the temperature of the system must also increase. Whereas the entropy of the system remains more or less constant under a constant value of the applied force, the temperature must increase in order to compensate for the larger amount of heat energy available to the system.

Another term involved in equation (5.7) is entropy, S . Traditionally, it is considered to be an intrinsic property of a system. However, recent treatments of this quantity have revealed that could be more correctly understood as a property of *the description of the system* [TSE2002]. From this point of view, and taking into account the many available definitions of entropy, we decided in favour of an interpretation which is closer to the approach provided in thermodynamics.

In this way our measure of entropy should be a monotonic function of the temperature, and be related to the mass of the nodes and to the internal energy, increasing as the mass increases and decreasing as the internal energy increases [TSE2002]. In order to compute the increase of entropy dS a frequency-based approach was adopted for the computation of the probabilities [ALE1976], [KNU2006]. First, each of the

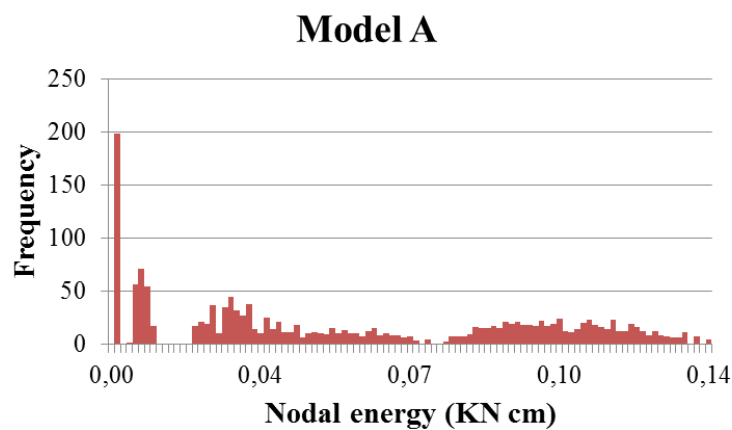


Figure 5.2: Histogram for one of the studied models with the frequency of energy states of all the nodes after 1000 simulations The lowest group of values gets the most of occurrences.

N nodal internal energies δW_i was calculated, as defined in the previous section.

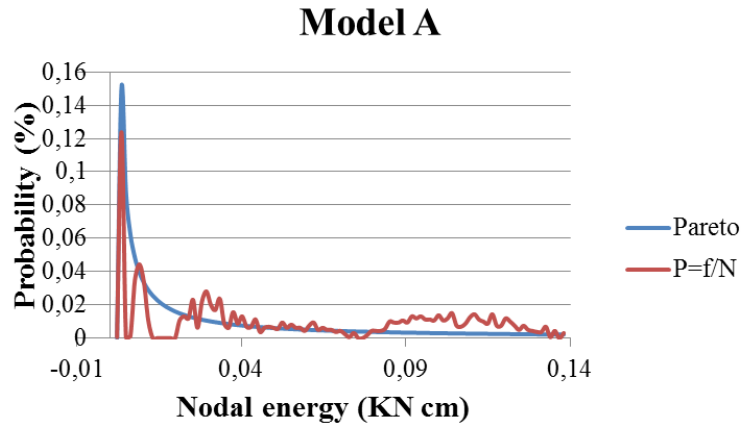


Figure 5.3: Probability mass function and Pareto probability density function of nodal energy states for one the studied models. The PMF is obtained by normalization of the frequency. The PDF is approximated as a long-tail Pareto law.

Then a constant sized bin histogram representing the nodal energetic states could be created for each model out of a number of simulations sufficiently large. As an illustrative example, figure 5.2 shows the histogram corresponding to Model A, which is further described in the next chapter. The discrete probability of a node to be in an energy state δWi is then defined as:

$$p_{discr} = \frac{freq(\delta Wi)}{N_{tot}} \quad (5.9)$$

where N_{tot} is the number of nodes of the structure, N , times the number of simulations (in our case 1000 was considered to be enough). In statistical terms, this value of probability is just the frequency with which the value δWi is found in a population of N_{tot} nodal energy states, normalized to the total number of nodal states of the model.

Already in the case of 1000 simulations it is possible to observe the long-tail behaviour of the distribution. In our case this distribution is best approximated by the well known Pareto law. In figure 5.3 the probability mass functions for the same example model A has been plotted with a superimposed Pareto law as explained in [KAF2009], which can be described by the equation:

$$freq(r) = \frac{\ln(1 + \frac{1}{r})}{\ln(R+1)} \quad (5.10)$$

where r is an integer value between 1 and R , the total number of bins between the largest and the smallest

value of nodal energy for all the simulations. With this expression of the frequency it is now possible to recalculate, for each nodal state, the corresponding continuous probabilistic value as:

$$p_{icont} = \frac{freq(r)}{N} \quad (5.11)$$

The probabilities can then be obtained for each node after each simulation iteration. Using the node's energy state from the density function from the fitted Pareto distribution, it was then possible to retrieve the continuous value of probability, p_{icont} . The increase in entropy was then iteratively computed as:

$$dS = \sum_{i=0}^{i=N} p_{icont} \ln p_{icont} \quad (5.12)$$

The value of the entropy given in equation (5.12) provides us with a measure of how much a particular configuration of a structural system under applied forces affects its capacity to absorb heat. It increases linearly with the number of nodes of the structure, N , and is related to the existence of disparities in the distribution of the internal strain energy.

Figure 5.4 illustrates the evolution of dS for the different possible values of p_{icont} . The highest possible value that a node could, any case, contribute is that of 0,367 units of entropy in and that would be so if the value of its probability were 37% regardless of the structural configuration the node would be immersed in. For a structural system, this means that unevenly shared stresses lead to concentrate high values of strain energy at certain points and low in others. According to the Pareto law of figure 5.3 this results in a lower value of the global entropy because both high and low nodal energies have, respectively, very low and very high probabilities.

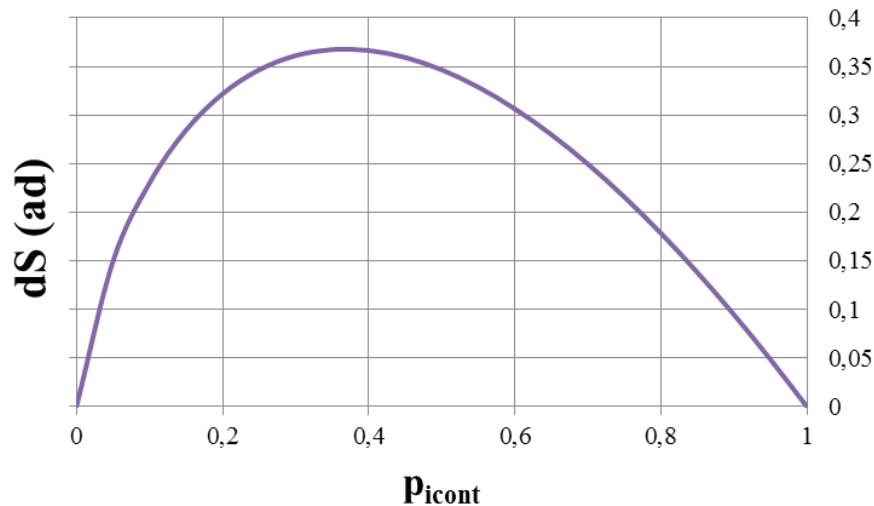


Figure 5.4: Evolution of the values of entropy with the probability. Higher values of probability do not necessarily imply higher entropy. In fact, the highest entropy of the system would be achieved if the probabilities of all the nodes were in the vicinity of 37%.

It must be noted here the omission of Boltzmann's constant, k_b , in the definition of equation (5.12). This happens as a consequence of the low number of entities involved, far below Avogadro's number, that makes the bulk scaling unnecessary. This also renders our definition of entropy dimensionless, as it is only a function of probabilities.

The remaining quantity involved in the description of a system's internal agitation is the temperature. In our case this value is not available as an element of the given data, and its definition for structural systems is not straightforward. However, it is easy to calculate from the definition given by classical thermodynamics in equation (5.7):

$$T = \frac{\delta Q}{dS} \quad (5.13)$$

This value of temperature can be understood as a measure of the tendency of a structural system to dissipate applied energy by displacement instead of concentrating it internally. Some authors define it as a measure of the quality of a state of a system [BRY1907], while others refer to it as the degree of "hotness" of a system [MAR2011]. In our case, higher values of temperature imply global deterioration of the static behaviour, whereas at lower values the system shows a higher degree of stiffness. This is directly related to the value of kinetic energy, and varies quadratically with it, as will be shown in the numerical examples provided. As follows from equation (5.13), and the fact that our definition of entropy has no dimensions, its units are those of energy.

5.2.4.- The kinetic energy of a system, KE

In our framework, the simulations represent quasi-static processes, where changes are homogeneous throughout the system, and slow enough as to maintain a constant state of equilibrium. Nevertheless, from the available data of a static simulation, using a general-purpose Finite Element application, it is possible to derive the following expression for the computation of the kinetic term:

$$KE = \frac{1}{2} \{\dot{x}\}^T \cdot [M] \cdot \{\dot{x}\} \quad (5.14)$$

Where the superscript dot denotes derivative with respect to time and the mass matrix [M] is assembled by simple addition of each beam elements' particular masses to their concurrent nodes (i.e. lumped mass matrix). In our case, however, this expression presents two problems:

- Stochastic methods lack an objective definition of time.
- The quasi-static approach implies that the inertia forces and kinetic energy, respectively, are neglected in the equations of motion and energy balance.

Still, a unitary time step can be selected for every iteration, yielding:

$$\{\dot{x}\} = \frac{d\{x(t)\}}{dt} = \frac{d\{x(t)\}}{1} = \{x\} \quad (5.15)$$

which means that we can dismiss the time dependency of the structural response and obtain information purely related to the inertia of the system, and its resistance to change in its motion. With this simplification it is now possible to rewrite the quasi-static equation for kinetic energy:

$$KE_{qs} = \frac{1}{2} \{x\}^T \cdot [M] \cdot \{x\} \quad (5.16)$$

This approach is necessary given the two limitations mentioned earlier, but will prove to be a good trade-off between computational demand and valuable information.

In figure 5.5 the quasi-static kinetic energy is presented against mass. As occurred in Figure 5.1, between the stiffness Kg and the total energy dU , the relationship is inversely proportional to the displacement and quadratically dependent on the applied force, so that light structures tend to have much higher values of kinetic energy. It is worth noting that in both figures 5.1 and 5.5 the lines of the isoforces follow the same paths, since both dU and KE_{qs} are functions of the same displacement. In both charts, different structures would have different constant stiffness (when limiting to elastic regime) or different mass, and when the same force was applied would give a different value along the isoforce line.

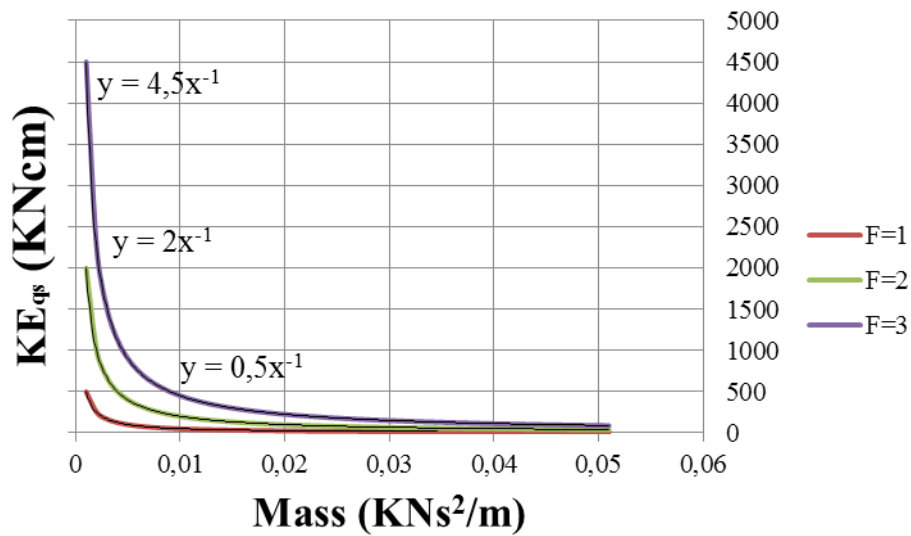


Figure 5.5: Quasi-static kinetic energy versus the mass of a structural system consisting of a single element. The kinetic energy defined here is a quadratic function of the applied force and varies inversely proportional to the mass. It is worth noting the equivalence to the plotted lines in Figure 1, as both dU and $Keqs$ are quadratic functions of the displacement.

5.2.5.- Rayleigh's quotient

A very interesting function of the elastic potential energy defined in equation (5.3) and in the kinetic term of equation (5.16) is commonly known as Rayleigh's quotient or the Rayleigh-Ritz ratio:

$$R = \frac{dU}{KE_{qs}} = \frac{\{x\}^T \cdot [Kg] \cdot \{x\}}{\{x\}^T \cdot [M] \cdot \{x\}} \quad (5.17)$$

This parameter is more commonly used in iterative numerical techniques for the computation of eigenvalues and eigenvectors in many mathematical and engineering problems, assuming that $\{x\}$ is a mode shape. In our case, given that the Rayleigh quotient is well defined regardless of this condition [PAR1974], this ratio between energies also tells us about how much of the applied energy is involved in the actual displacements, or, inversely, how much energy is stored elastically by the structural configuration.

Large values of this parameter imply either a large total energy dU or a small kinetic energy KE . As has been depicted in figures 5.1 and 5.5, this happens when the stiffness is small, even in situations when the mass is not necessarily very large. As it will be shown in the following numerical examples, global stiffness can be achieved either by means of beams with larger sections (hence more massive), or by a correct geometric disposition and nodal interconnection.

Rayleigh's quotient is complementary of heat as yet another measure of the amount of movement, but it omits information relative to the degree of disorder. Instead, Rayleigh's quotient gives an idea of the influence of the relationship between the connecting bonds (i.e. the beams' deployment) and the inertia of the system (i.e. the beams' masses). When this ratio is bigger then we have the case of stiffness dominated structures. For smaller ratios, the inertia of the system dominates the behaviour.

5.2.6.- Simulated annealing of structural systems

A straightforward application of the present framework is in the optimization of frame structures by means of simulated annealing. An algorithm was developed where the above concepts were implemented together with those of the first section of this chapter to solve a size optimization problem.

As it was explained earlier, simulated annealing allows for a stochastic search within the space defined by the objective function and the constraints. In engineering practice, an optimal structure is that whose weight is a minimum, as it implies minimum use of material which, ultimately, is in direct relationship with its cost. Adapting equation (5.1) to our current description of the problem in terms of nodes instead of beam elements:

$$\begin{aligned} \text{minimize } f_o(x) &= \sum_{i=1}^N \sum_{j=1}^{b_i} \frac{1}{2} w_j = \sum_{i=1}^N \sum_{j=1}^{b_i} \frac{1}{2} A_j \cdot L_j \cdot \rho_j \\ \text{subject to } f_1(x) &= A_j = \{\text{Values from a profiles table}\}, \quad j=1, \dots, b_i \end{aligned} \quad (5.18)$$

where w_j is the weight of each beam element concomitant to the i th node, b_i is the number of these beam elements and N is the number of nodes. A_j , L_j and ρ_j are, respectively, the area, length and density of the aforementioned beam elements. It must be noted here how, in this application of a stochastic methodology to an optimization problem the parameters are considered in the analysis from the deterministic point of view. This means that we are only using their average values instead of treating them as probabilistic random variables. This leads to a formulation of the constraint $f_i(x)$ only dependent on the areas, as L_j and ρ_j are treated as geometrical and material constants.

Nevertheless, equation (5.18) is difficult to solve other than by exhaustive iteration over all the values within the given profile table and the given beam elements. Even a stochastic approach for exploration of the whole design space would be computationally cumbersome.

To overcome this difficulty, we will combine the optimality criterion developed in [VEN1968], by means of which it can be stated that an optimum structural design is that where the average strain energy density is a constant throughout its elements. The evaluation of this quantity could be made in a probabilistic manner by including another sub-iteration within the analysis. For the sake of clarity, however, we will utilize only the deterministic value.

The definition of average strain energy density, once the parameters of the previous section have been introduced, is quite straightforward: it is the ratio of the internal work of a node, δW_i , to the total volume V_i of its concurrent beam elements. It can be understood as a measure on how close to the elastic limit the node is, or more precisely, to what extent the available energy capacity is used.

The energy capacity of a node can be calculated as:

$$\delta W_{ui} = \sum_{j=1}^{b_i} \frac{\sigma_{ui}^2}{2 E_i} \cdot V_j \quad (5.19)$$

where σ_{ui} and E_i are generally constant throughout a structure as material properties so the only variable affecting each node is the volume of its tributary beam elements. It is trivial to realize that the energy capacity of a node is then only dependent on its volume. The strain energy density, which depends on the state of deformation, can adopt different values for each node depending on the structural configuration. Unless the adopted beam's discretization is an infinitesimal value, the strain energy capacity is always many times larger than the strain energy density. Nevertheless, structures where the strain energy density varies little among nodes, i.e., the overall variance is small, utilize better the material than those with high fluctuations. This is in consonance with the previously explained notion of entropy, which is related to this variabilities, as a measure of the capacity to absorb heat.

Once the concept of nodal strain energy density has been introduced, it is possible to enunciate equation

(5.18) again considering yet another constraint that includes the strain energy density in the equation:

$$\begin{aligned} \text{minimize } f_o(x) &= \sum_{i=1}^N \sum_{j=1}^{b_i} \frac{1}{2} w_j = \sum_{i=1}^N \sum_{j=1}^{b_i} \frac{1}{2} A_j \cdot L_j \cdot \rho_j & (5.20) \\ \text{subject to} & \\ f_1(x) &= A_j = \{\text{Values from a profiles table}\}, \quad j=1, \dots, b_i \\ f_2(x) &= \text{stdev}(\delta W_{uj}) \leq \epsilon, \quad j=1, \dots, b_i \end{aligned}$$

The solution of this problem is now possible and efficient by means of deterministic optimization procedures such as Lagrange Multipliers [VEN1968], but these are algorithmically quite involved and still require the constraint $f_i(x)$ to be treated as a continuous range of values instead of taking discrete fixed values from a profiles table.

A solution to both the algorithmic complexity and the discrete value assignment is made possible using the Simulated Annealing approach. In pseudocode, this algorithm can be expressed in the following manner:

$s = s_0; H_k = H_k(s)$	//Initial state, nodal strain energy's standard deviation
$s_{best} = s; H_{k_{best}} = H_k$	//Initial best solution
$k = 0$	//Energy evaluation count
<i>while</i> $k < k_{max}$ and $H_k > H_{k_{max}}$	//While there is time and solution is not good enough
$T = \text{temperature}(k / k_{max})$	//Calculate temperature
$s_{new} = \text{neighbour}(s)$	//Pick some random neighbour
$H_{k_{new}} = H_k(s_{new})$	//Compute the energy state
<i>if</i> $\text{Probability}(H_k, H_{k_{new}}, T) > \text{random}()$ <i>then</i>	//Is it good to adopt this neighbour's state?
$s = s_{new}; H_k = H_{k_{new}}$	//Yes, change state
<i>if</i> $H_{k_{new}} < H_{k_{best}}$ <i>then</i>	//Is it a new best?
$s_{best} = s_{new}; H_{k_{best}} = H_{k_{new}}$	//Store this new state as new best
$k = k + 1$	//One more evaluation done
<i>end while</i>	//Repeat the procedure
<i>return</i> s_{best}	//Return the best solution found

Table 5.1: Pseudocode for the Simulated Annealing algorithm

Given that all the variables of the algorithm have been defined in the previous section, only the value of $\text{Probability}(H_k, H_{k_{new}}, T)$ needs to be characterized. We have used the original acceptance probability function given by [KIR1983]:

$$\text{Probability}(\delta W, \delta W_{new}, T) = e^{-\frac{H_k - H_{k-1}}{T}} \quad (5.21)$$

where H_k and H_{k-1} are respectively the current and the previous step measures of statistical dispersion of the nodal strain energy density. We have chosen the standard deviation at each iteration step as it is more adequate for single evaluations than entropy, which would require several sub-iterations to be properly characterized.

It must be remarked here how the limit states constraints defined in chapter 4 are not explicitly included the Simulated Annealing optimization algorithm. Moreover, the Capacity-Demand notions intrinsic to the analysis part of design have not been included. It is trivial, though, to establish a null probability value for those states whose capacity were estimated below a given demand threshold. This makes this approach suitable not only for deterministic analysis techniques but also for probabilistic ones.

In the numerical examples provided in the next section, the limit state constraint has been explicitly defined to make it more illustrative.

5.3.- Numerical experiments and results

In this chapter the results of some numerical experiments are presented, together with some detailed observations. Four different specimens were tested, and the thermodynamic quantities described earlier computed using a general purpose finite element application. Their configurations were adopted from the seismic regulation Eurocode 8 (EC-8), where a behaviour factor q is defined for several different kinds of structural arrangements [ECS2004]. This behaviour factor serves, in a simplified calculation of the non-linear response of a structure, to reduce the design forces obtained from a linear analysis. Higher values of this factor imply the assumption of better behaviour in the event of plastification of the elements. In other words, the behaviour factor accounts for the ability of the structure to dissipate energy by yielding.

In order to avoid excessive complexity, the specimens were treated as 2D models and kept within the elastic range, considering the shear effects to make a negligible contribution towards the deformation. Also for the sake of simplicity, geometrical non-linearities were omitted from the analyses.

Two types of experiments were carried out: modification of the applied force in order to account for the energetic behaviour of the different configurations and modification of the sections using the simulated annealing scheme.

5.3.1.- The studied specimens

The material and section properties shown in Table 5.1 are common in engineering practice, with values similar to those corresponding to a 200x200x2 mm hollow extruded steel bar.

The geometric configuration of each model is displayed in figure 5.6.

Table 5.2: Properties of the beam elements composing the specimens

Parameter	Value
Number of nodes, N	47
Area (cm ²)	144
Modulus of inertia (cm ⁴)	7872
Modulus of elasticity (kN/cm ²)	21000
Shear modulus (kN/cm ²)	8076,92
Material density (kN/cm ³)	7.892E-8

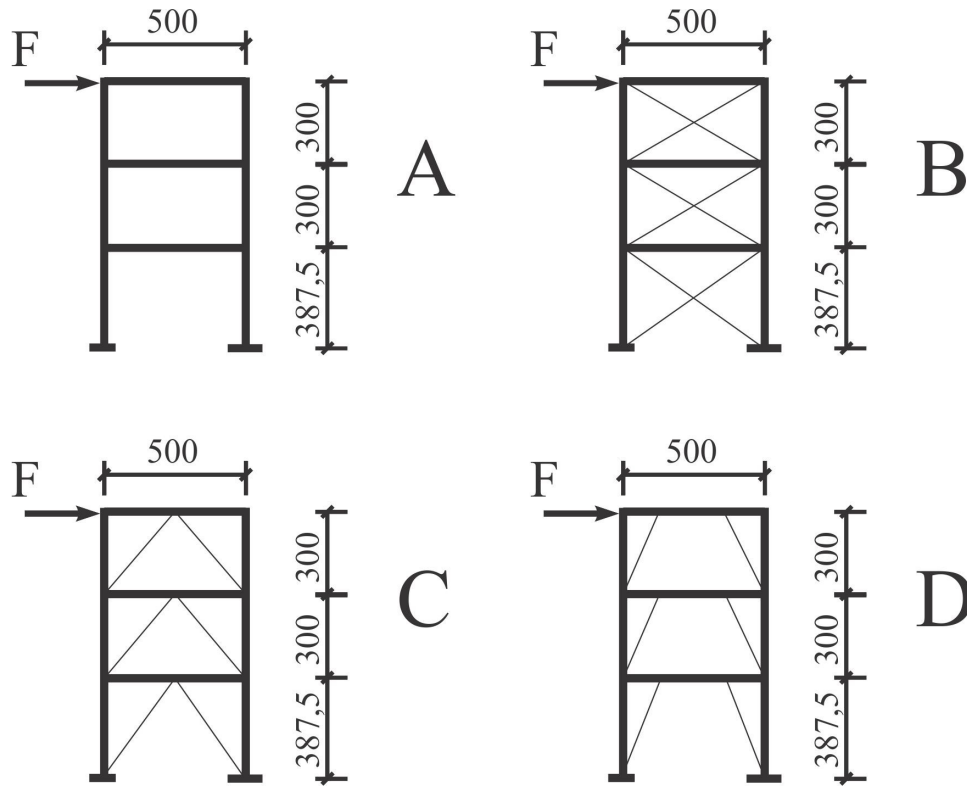


Figure 5.6: Schematic distribution of the nodes and beams which were the subject of the study. The behaviour of each model varies with the disposition of the braces as described in the seismic regulation Eurocode 8.

Some characteristic properties of the sample models, such as volume, mass, and moments of inertia, were calculated and are provided in Table 5.2. The total volume was computed by multiplying the section area given in Table 5.1 by the added length of every beam. Mass was obtained as the product of the volume and the material density (structural steel).

The inertia of an assembly of masses is given by the expression:

$$I = \sum_{i=1}^N m_i r_i^2 \tag{5.22}$$

where m_i is the lumped mass of each node and r_i the distance of the node to the centre of gravity of the system. For the computation of the values of inertia only the XZ plane was of interest.

Table 5.3: Properties of the studied specimens

Parameter	Model A	Model B	Model C	Model D
Volume (cm ³)	500256	1078080	857808	833328
Mass (kNs ² /cm)	0,0392	0,0798	0,0672	0,0653
Inertia XZ(kN cm s ²)	5866	48235	33735	31916

5.3.2.- Experiment 1: Modification of the applied force

The value of the applied force F was randomly modified around an initial value F_0 by means of an exponential function:

$$F_t = F_0 \cdot e^{\frac{-\rho \cdot \alpha}{F_0}} \tag{5.23}$$

where ρ is a random value between 0 and 1 and α is a control parameter that was fixed as equal to 5. This leads to a random oscillation of the value of F_t , when $F_0=100$ N, between 0 N and 100 N.

As no probabilistic assumption can be made regarding the outcome of the samples, no rejection condition was defined for a Metropolis algorithm. All the calculated samples were in the elastic regime, so the outcome is purely deterministic. In fact, the choice of a random function for the definition of F_t was based on the practical advantage of the Montecarlo method for the exploration of larger search spaces more efficiently.

Figures 5.7 to 5.13 show the relationships of the parameters described in the previous chapter. In the elastic regime described in this experiment, all the variations are visibly linear and homogeneous, with differences between the models that support the explained concepts. Given the large differences in internal energy between the models, which are particularly relevant in Model A, in some cases the ordinate axis has to be shown on a log10 scale.

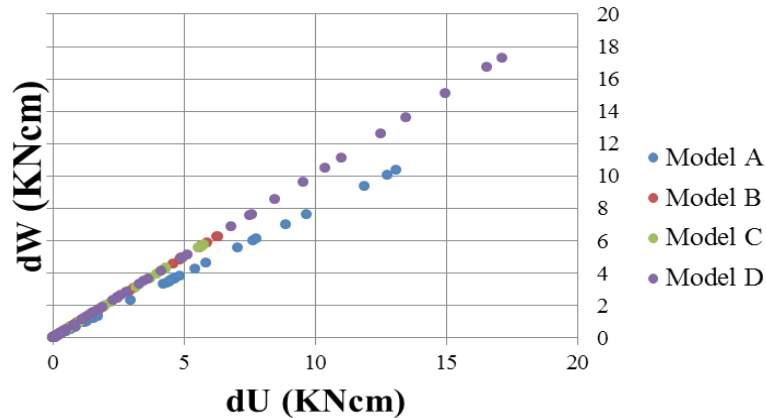


Figure 5.7: Variation of internal elastic energy with respect to total applied energy. Robust configurations have a short span of values in the horizontal axis as they oppose to changes in total energy dU . Although shortened for graphical clarity, the line for Model A reaches values as high as 500 kNcm. Models B and C, however, have much shorter trails and, for the same range of forces, oscillate only between 0 and 8 kNcm.

In Figure 5.7 the internal elastic potential energy δW is compared to the total applied energy, dU . In all

the models the ratio between δW and dU is constant. Nevertheless, there are some differences between the systems with regard to the span of internal energy that they can develop. In particular, model A reaches levels of internal energy that are orders of magnitude larger than the rest as a consequence of its much lower stiffness (it has no bracing whatsoever). On the other end of the scale, model C shows not only lower values in this case, but also a narrower span of possible values of total energy. Robustness, described as the persistence of a system to maintain a certain behaviour under changes, can be understood as the difference between the maximum and minimum values of dU in this and subsequent charts. The more robust a system is, the narrower is the span.

From Figure 5.7 it is apparent that dU and δW : are proportional, so that:

$$\delta W = -\gamma dU \quad (5.24)$$

where γ has a value close to one. As seen earlier in equations (5.2) and (5.3), dU is also proportional to the square of the force and inversely proportional to the stiffness, which leads to:

$$dU = \frac{1}{2} F^T \cdot Kg^{-1} \cdot F \quad (5.25)$$

from which it is possible to conclude that:

$$\delta W = \frac{-\gamma}{2} F^T \cdot Kg^{-1} \cdot F \quad (5.26)$$

This means that, regardless of the γ ratio, stiff systems will show lower values of δW than more flexible ones. Figure 5.8 depicts the relationship defined in equation (5.26). The quadratic dependence on the applied force makes the differences between models even more clear.

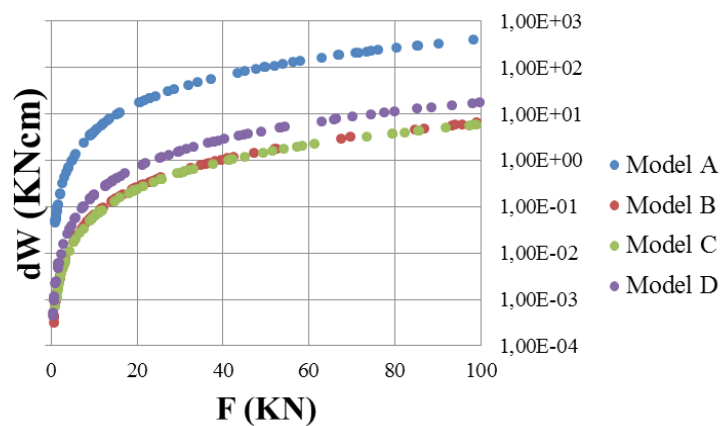


Figure 5.8: Variation of the internal elastic energy with respect to the force applied to the system. The ordinates presented by means of a log10 scale. In the linear regime, the internal work varies quadratically with respect to the applied force.

Figure 5.9 shows variation of entropy with respect to applied force. The curves present a very interesting parallel decreasing behaviour, indicating that a rise in the energy in the system leads to a reduction of its entropy. Mathematically this means that, for lower energy states of the system, the individual probabilities of each nodal state are higher. This makes the distribution more homogeneous, leading to a higher entropy. Assuming the existence of an elastic regime, the share of internal energy stored in the nodes of a structure does not change, only the quantity that they store. In other words, although the individual nodal elastic energy levels δW_i may change from one value of the external forces to another (i.e. between simulation iterations), the relative internal ratio between them remains a constant.

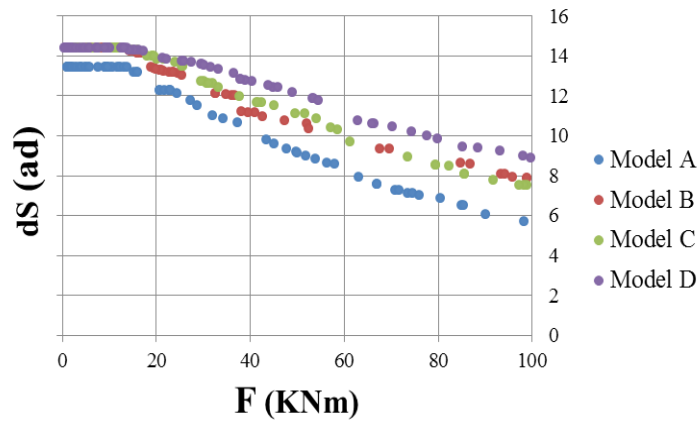


Figure 5.9: Variation of entropy with respect to the force applied to the system. A higher force results in a higher total energy dU . As dU increases, the individual nodal energies reach higher values, whose probabilities are lower according to the Pareto law. This leads to lower values of the entropy.

When the available energy is higher for all the nodes, these must also increase their energy and the difference in probabilities from one another increases. This causes the entropy to decrease as, from the definition given in equation (5.12), the maximum value of the entropy is achieved for a system in which all the nodes share the available energy equally, and are equally probable. This maximum can be observed in the upper section of each curve, where flat behaviour is present. In a case of much disparity and the predominance of high values, the entropy tends to a minimum as the majority of the nodes have high values whose probability is lower according to the Pareto law. As defined in our work, the quantity dS is dimensionless. Structurally, it provides information about the degree of evenness in the distribution of the internal work, which is directly related to the internal distribution of the tensions. A higher value means a lower likelihood of concentrated tensions. The chart shown in figure 5.10 is also interesting as it summarizes much of the information provided by both figures 5.8 and 5.9. The value of δQ expresses how close the values of the internal elastic energy δW and the total energy dU are. In other words, how

far from unity the ratio $\gamma = \delta W / dU$ is. In the elastic regime, γ is constant regardless of the amount of total energy. For model A, dU is 25% larger than δW , whereas for the rest of models the ratio remains very close to 1. Negative heat, i.e. a ratio smaller than 1, is present in models C and D. If, as explained earlier, higher entropy is associated with a more even distribution of the nodal energy, the reason why models C and D show a value of internal work δW larger than the total energy dU can only be derived from their particular beam configurations.

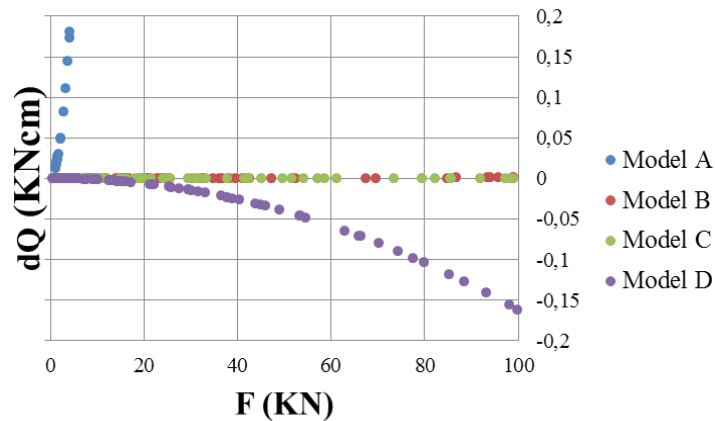


Figure 5.10: Variation of heat with respect to the force applied to the system. The large values of dQ represent big differences between the internal work dW and the total energy, dU . When positive, they reflect dissipative behaviour; when negative, internal accumulation in the nodes.

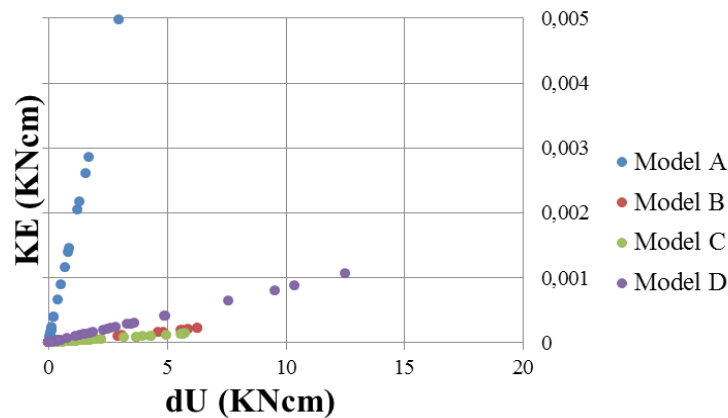


Figure 5.11: Variation of quasi-static kinetic energy with respect to force applied on the system. The slope of the line is the inverse of Rayleigh's quotient. Steeper lines indicate higher flexibility, flatter lines, higher stiffness.

Keeping in mind the fact that all four models have the same number of nodes, whose topological relationships are dictated by the interconnecting beams, a larger number of connected nodes means also a more even redistribution of the internal work among them. This explains the difference not only in the

internal work but also in the entropy between the models. Negative values of δQ indicate internal adsorption of the applied energy, whereas positive values indicate dissipation by means of displacement.

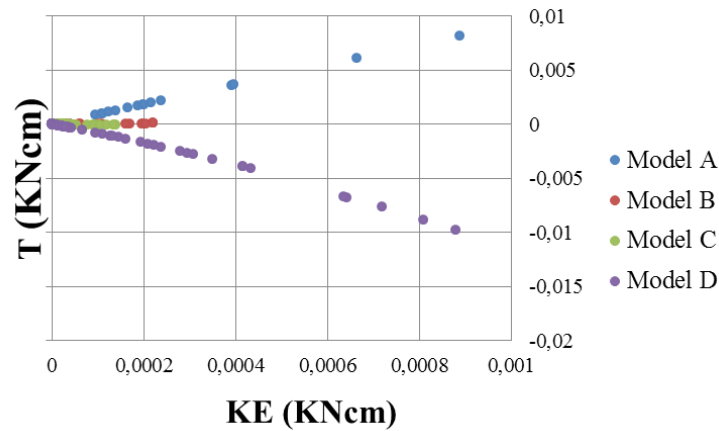


Figure 5.12: Temperature vs Kinetic energy. The quadratic relation between T and KE can be linearized to obtain the parameter τ when kinetic energies are low.

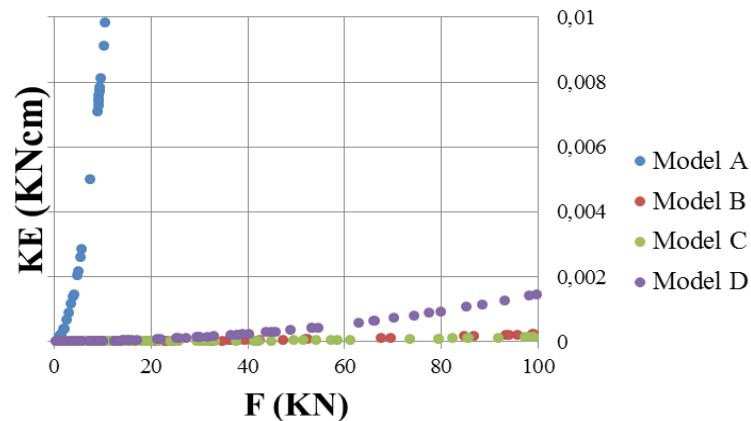


Figure 5.13: Variation of quasi-static kinetic energy with respect to force applied on the system. The relationship between kinetic energy and applied force is quadratic. Flexible structures present narrow paraboles.

The magnitude of this characteristic is given by the absolute value of δQ .

The plot of figure 5.11 reveals yet another interesting characteristic of a structure's behaviour: the relationship between its global stiffness and its inertia. Model A, despite having much less mass to oppose in the direction of the applied force, has a much larger kinetic component as a result of its greater flexibility. However, comparing the other specimens whose values range closer to one another, the higher mass of model B dominates over the effect of its smaller displacements. This can be perceived as a line above that of model C, with lower inertia but also lower mass.

In the chart of figure 5.12 the same values of quasi-static kinetic energy are presented against the applied force. This case is similar as that of δW and δQ in that there is a linear relationship with the total energy dU and, by virtue of equation (5.21), a quadratic dependence on the force applied. Summarizing, the kind of information that can be extracted from the values of KE_{sq} is related to whether a structure's behaviour is dominated by the mass of its elements or by their beams' distribution.

Figure 5.13 shows a plot of the temperature against kinetic energy for all four models. Here it is possible to observe the quadratic dependence between these two variables although they were computed from mathematically independent relationships. In this situation, a linear approximation can be made in order to describe this relationship between temperature and kinetic energy. If the linear dependence is characterized as a value τ , and substitutes in equation (5.13):

$$T = \frac{\delta Q}{dS} \approx \tau \cdot KE \quad (5.27)$$

that leads to:

$$\tau = \frac{\delta Q}{dS \cdot KE} \quad (5.28)$$

replacing heat by its definition from equation (5.8):

$$\tau = \frac{dU - \delta W}{dS \cdot KE} \quad (5.29)$$

which is the coefficient that combines the independently obtained parameters dU , δW , dS and KE . This coefficient summarizes most of the characteristics described above independently for each of the parameters. Its positive or negative value indicates a predominance of internal work over total energy, meaning a nodal energy distribution which is even. A larger average absolute value stands for a higher degree of flexibility, which, as we have seen earlier, means a larger difference between the internal work and the total energy (i.e. a larger heat), being the kinetic energy compensated by the entropy in the denominator.

In figure 5.14, the deformed shapes of the four structures are shown. It is possible to see how models A and B maintain the same number of connected nodes, whereas C and D "activate" the rotational degrees of freedom of extra nodes, increasing not only their internal energy but also their entropy. It is also interesting to note how, since all four models have the same arrangement of points with different nodal connections, the range of dS is very similar in all cases.

As the total energy dU increases, if the value of δQ remains close to zero this means that the relation established in equation (5.13) gets closer and closer to zero unless the entropy, dS , also decreases

correspondingly. Given that the entropy is fairly similar between the configurations, this forces the temperature, T , to vary. However, in the case of model A, δQ is a sensibly large number compared to the others. As the temperature and kinetic energy are dependent on one another, this increment of temperature leads to a higher degree of nodal displacements. We can therefore establish that, in the case of similar and comparable values of the entropy, larger absolute values of heat also imply a lower degree of stiffness.

In table 5.4 a summary is made for comparison of all four models and the average values yielded after 100 iterations of the experiment (only for entropy was given the maximum). The values provided in the Eurocode 8 for the behaviour factor q of each structural configuration are also added for convenience. Interestingly, and despite their completely different behaviours, models A and D are given the same value. Also, they are favoured in the code as q is considered a factor of reduction of the applied loads.

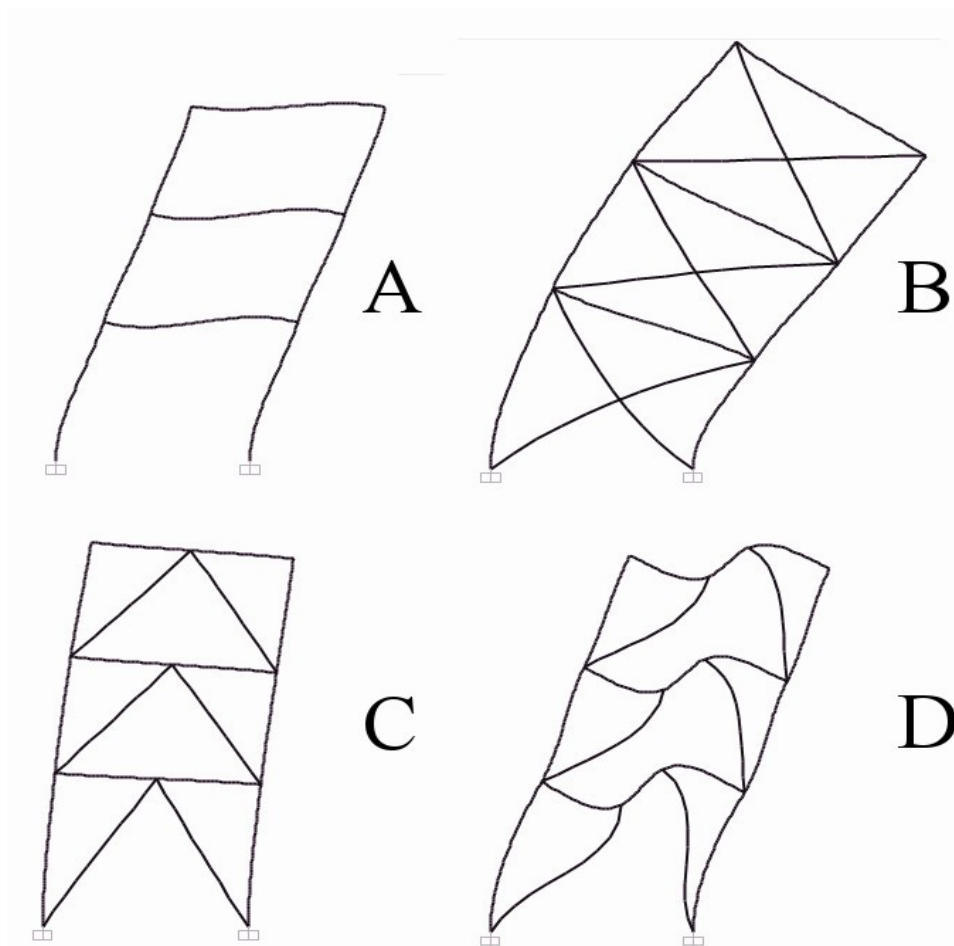


Figure 5.14: The deformed shapes of the models under the applied load. Model A was magnified by a factor of 1000, whereas models B, C, and D were magnified by a factor of 10000. Models A and B have the same amount of connected nodes, although B presents a much lower kinetic energy. C and D have more connected nodes that explain their negative heat as they store energy internally instead of dissipating it.

Table 5.4: Summary of the average values after 100 iterations.

Parameter	Model A	Model B	Model C	Model D
$\langle dU \rangle$	115,6	1,45	1,36	3,92
$\langle \delta W \rangle$	91	1,45	1,36	3,95
$\langle \delta Q \rangle$	24	0,00016	-0,00007	-0,03
dSmax	13,45	14,38	14,38	14,38
$\langle KE \rangle$	0,19	0,00005	0,00003	0,0003
$\langle T \rangle$	7,4	0,00005	-0,00002	-0,01
$\langle R \rangle$	595	28607	41321	11797
$\langle T \rangle$	12,7	0,26	-0,18	-8,99
EC 8 Behaviour factor, $q^{(*)}$	5	4	2,5	5

(*) The values of q are for a given ductility classification. For more details see [ECS2004].

5.3.3.- Experiment 2: Modification of the cross sectional properties

As it was explained in the point 4.1.2.1, the optimization procedure can take place mainly as three types of problems: size problems, shape problems and topology problems. This exercise will focus on the first type, applying it to the Model A.

By modifying the sizes of the beam elements' sections, the optimization problem reduces to an iterative procedure such as the one described by equation (5.18). We have adapted the Simulated Annealing algorithm provided in table 5.2 to make use of the parameters described in this chapter, namely:

- The ratio of nodal internal work δW_i against the nodal volume V_i as the strain energy density and its variance throughout the structure.
- The structure's notion of temperature as calculated in equation (5.13).

On each iteration, the state of a structure is defined by the height, width and thickness of the beam elements that integrate it. Table 5.5 gives the available sections from a commercial provider that were used to constraint the possible states of the structural configurations. The table was simply input in the program as a selection matrix. Provided that each element can adopt any type of sections from the table, the design space spans $2,5 \times 10^9$ possible states. In this manner, the neighbouring configurations would be selected by retrieving random indexes of the matrix until a valid profile would be returned for all the sections of the structures.

In figure 5.15 a population of 10000 specimens was randomly generated. The mass of each state is depicted against the standard deviation of the nodal strain energy density. An optimal solution is that where, respecting the feasibility conditions, a minimum mass is obtained. The feasible design space has

been defined by those structural configurations whose tip deflection is less than 1/500 of the height of the structure. This limit is given in the regulations as a serviceability limit. Regarding the the minimum, it must be located in the boundary of the surface created by the possible points. It is interesting to note how the design space in this case is not continuous but presents itself as a grid of clustered solutions. This is a result of the discrete nature of the possible element sections given in table 5.5 and has obvious advantages from the practical point of view over the gradient-based methodologies described in the point 4.1.1.

Table 5.5: Available profile sections used in the Simulated Annealing optimization procedure

tw\bxh (mm)	50	50	60	60	70	75	80	90	100	100	120	120	150	160	200	250	300	400
	x	x	x	x	x	x	x	x	x	x	x	x	x	x	x	x	x	x
	25	30	30	40	40	50	40	50	50	60	60	80	100	80	100	150	200	200
2,00	.																	
2,50	.	.																
3,00									
3,50								.		.	.							
4,00												
5,00							
6,00							
6,30													.			.		
8,00											
10,00												
12,50														

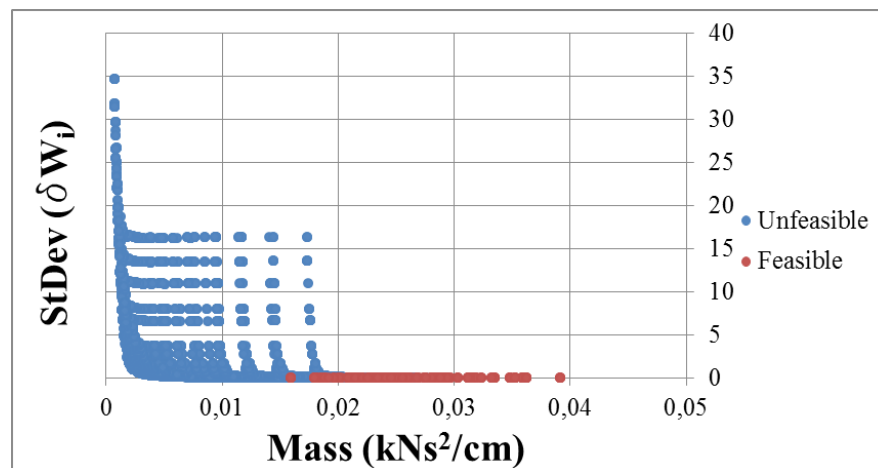


Figure 5.15: Structure's mass vs standard deviation of the nodal strain energy density for a random population of 10000 specimens. The design space is a surface of 2,5x10⁹ points. The optimal is a minimum in the boundary of this surface. Feasible and unfeasible designs are selected according to the maximum displacement serviceability limit state.

Figure 5.16 shows the results for the same population, but comparing the relationship between the standard deviation of the nodal strain energy density and the total energy of the system. The total energy,

in this particular experiment, is itself linearly dependent on the displacement, given that there is only one point of application of the force. The different solutions are banded in lines following a quadratic tendency. This makes the standard deviation a better tool for measuring the optimality as it has a more straightforward interpretation than the entropy, requiring less computational effort. The main difference between both measures is that, while entropy focuses in the actual energetic states of each node and their relationship to the total structure, the standard deviation of the nodal strain energy density gives a single value for the whole structure measuring the degree of solicitation of each node with respect to its capacity.

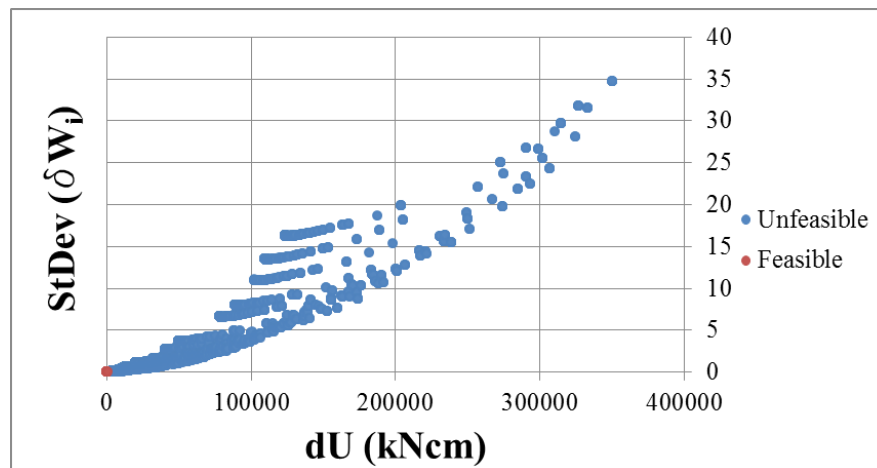


Figure 5.16: Structure's total energy vs standard deviation of the nodal strain energy density for a random population of 10000 specimens. The standard deviation of the nodal strain energy density is a more effective measure of the dispersion of the nodal energy than the entropy as it only requires one calculation per state.

The chart in figure 5.17 gives the comparison between mass and temperature for the same random population depicted earlier. As expected, larger masses imply lower capacity of movement hence lower values of temperature. By means of the Simulated Annealing algorithm, the value of our computed temperature intervenes as a control variable in the search. When the mass of the structure is small, its members have less stiffness hence it is subject to more displacements and its temperature is higher.

When the structure is more massive, it has lower temperature. It is clearly visible in the feasible region where the displacement constraint is very strict and the range of possible temperatures is very narrow. Simulated Annealing employs the temperature as a control parameter for the selection of the neighbour.

The higher the temperature, the larger the leap to a next state. This emulates the cooling effect in real annealing.

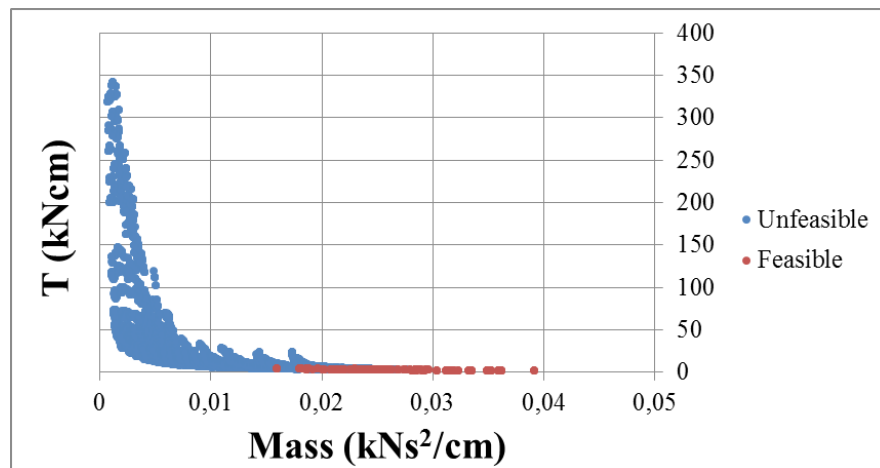


Figure 5.17: Structure's mass vs temperature for a random population of 10000 specimens.. Larger masses imply lower capacity of movement hence lower values of temperature. By means of the Simulated Annealing algorithm, the value of our computed temperature intervenes as a control variable in the search.

In figure 5.18 the result of 50 iterations in our Simulated Annealing algorithm is presented. The global minimum for the standard deviation of the nodal strain energy density is quickly found and can be identified as the point from which most other iterations are tried. The optimum however is that whose mass is a minimum while its nodal strain energy dispersion is a minimum. As can be seen in figures 5.16 and 5.18, these conditions are mutually incompatible and some intermediate solution must be adopted. Clearly, it is up to the designer to choose what criterion is most adequate to the particular application of our method.

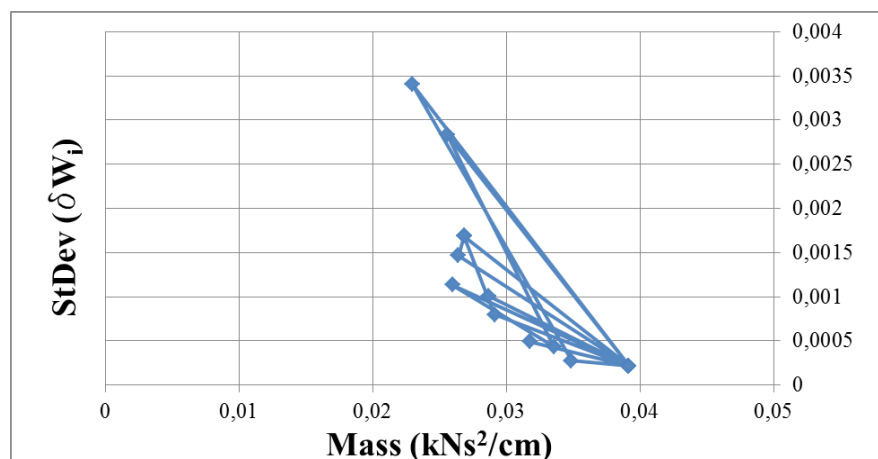


Figure 5.18: Structure's mass vs standard deviation of the nodal strain energy density. 50 iterations in the Simulated Annealing algorithm. The design space is constrained to a much smaller line of exponential nature.

5.4.- Discussion

In this chapter a series of quantities from statistical mechanics have been used to describe and compare the properties of a set of structures. The values of these quantities were obtained by assimilating certain structural systems to an aggregate of interconnected nodes undergoing a quasi-static process of thermodynamic change. In this manner, it was also possible to define:

- The number of nodes, N , as the size of the assembled matrices,
- The internal energy, dU , as the amount of work done by the forces on the structural system,
- The internal strain energy, δW , as the amount of such work mechanically stored in the nodes,
- The added heat, δQ , as the energy dissipated in the form of displacements,
- The entropy, S , as a measure of the degree to which δW is evenly distributed throughout the nodes.
- The temperature, T , as the ratio between the added heat and the entropy,
- The internal kinetic energy, KE , as a measure of the influence of the mass of the system,
- The Rayleigh quotient, R , as the ratio between the internal energy and the kinetic energy.

At the same time, a series of qualitative properties of the investigated structural systems was determined and observed within the scope of the above-listed quantities. These properties are the following:

- Robustness, or the persistence of a system's characteristic behaviour under perturbations, characterized by a small span of the possible values of dU ,
- Resilience, which is complementary to the above, is the capacity of a system to absorb energy elastically, which is characteristic of systems with large values of dU ,
- Stiffness, or the resistance of an object to deform, which is also related to a small span of dU and a δQ which is close to zero,
- Flexibility, as opposed to stiffness, being the ability to deform elastically, and indicative of systems with large and positive values of δQ .

These properties have been identified in a group of four structural configurations obtained from the seismic regulation Eurocode 8. The choice of a structural engineering reference provides our framework with a sound background for the establishing of comparisons and, more importantly, a handy factor, q , which is called a "behaviour factor".

A coefficient τ which relates the temperature to the kinetic energy has also been defined. This coefficient provides more information about the behaviour of a structural system as it includes not only a magnitude but also a direction (positive or negative), and can indicate whether a design is dissipative or cumulative.

The framework has also been proven a valuable tool for structural optimization. Employing both the notions of nodal strain energy density and temperature, it has been applied in a straightforward manner to the implementation of a Simulated Annealing algorithm. Although this technique has been applied before for the optimization of structural designs, the physical foundations of its application appear to be quite vague in the literature found. With this work a more solid theoretical background is given.

It was concluded that the techniques developed for analysing systems from the point of view of statistical mechanics work very well with structural systems.

Within the framework presented in this chapter, it is possible to determine whether a structural system will require from its elements the ability to store applied energy or to deform in order to dissipate it, and to what extent. A numerical value associated with qualitative variables such as robustness or stiffness can be chosen matching those of total internal energy or heat, respectively.

We have also presented a novel application of entropy in order to define the degree to which internal energy is evenly distributed within a structure. Uniform distribution of this energy, being dependent on internal stresses, means a lower likelihood of encountering overstressed points while underutilizing others. Structures with high values of entropy are less likely to present local failures and will do so only after resourcing all of its available elements. From our experiments, more flexibility also means lower entropy. However, a more flexible structure can also respond to a much wider range of applied energies. It is the trade-off between material economy, energetic capacity, and entropy which makes a good structural design. To complement the notion of entropy, the standard deviation of the nodal strain energy density was introduced as another measure of dispersion. In this case it refers to the ratio between the theoretical energy capacity of a node and its real demand. The lower this value, the higher the efficiency with which the material is being used.

6.- Development of a computational environment for probabilistic structural design

6.1.- Introduction

The experimental results shown in this thesis required a significant amount of computational effort due to the number of involved specimens, the iterative nature of the researched methods and the purposed amplitude of the parametric studies. In total, over 500 hours of processor time were used only in the calculations in an Intel ® Core ® 2 CPU 6600 at 2,4GHz each, with 1GB of RAM. Such job could only be completed by resorting to automation of the process of assigning values to the studied parameters. Otherwise, human error and lack of time would have rendered the results unreliable.

On an initial stage of the research, attempts were made to implement a fully comprehensive Open Source application that contained most of the numerical methods defined in the previous chapters. The task soon proved itself to be overwhelming and alternative solutions had to be found. A main concern of this research was to provide with a didactic yet useful environment that narrowed the current gap between engineering practitioners and the concepts of physics. Eventually the option of adapting main stream applications to such purpose seemed optimal. One of the most common problems in design when it comes to experience new software is the familiarity with the interfaces.

In order to minimize such problem, the final solution was to develop an application that combined three main areas: CAD, Structural Analysis and Data Management.

For the CAD part, the package of choice was Robert McNeel and Associates' Rhinoceros ®. It is a NURBS (Non Uniform Rational B-Splines) based CAD application common to industrial, architectural and automotive design. Among other, this software has the decisive characteristic of embedding a visual programming plugin named Grasshopper ®. This makes it unique for the graphical representation of the developed code and serves ideally the didactic purpose of this thesis.

The main benchmarking tool for validating our Structural Analysis results was the commercial general purpose software SAP2000 ©, for which a free research license was obtained. Other options were studied (OpenSees, Autodesk Robot) but none provided the ability of straightforward linking with other Windows-based programs via an available API. Despite being a proprietary solution, SAP2000 © met all our requirements of reliability and, most importantly, of familiarity. Also, it came with CSI's OAPI (Computers & Structures, Inc. Open Application Programming Interface), that allowed for the linking of the data with other software and the automation of some critical processes.

The data produced by the software was then processed by means of the proprietary spreadsheet application Excel and then treated with GIMP, the Gnu Image Manipulation Program. In this process, at least three different applications were combined by manual operations which led to considerable expense of research time.

As a result, the central piece of our empirical research were three purpose-made open-source applications that combined several other proprietary solutions to collect, process and display the experimental data. For chapter 3 the simulation data was generated by means of an embedded application developed in the Rhinoceros' Grasshopper development environment. For chapter 5, model data was generated with SAP2000. This data was collected into an spreadsheet connected via its API.

To make this possible, the underlying software technology had to be based on the Microsoft Corporation's Windows operating system. Unfortunately, in the moment of writing this thesis the applications common to Structural Engineering practice are almost invariably based on such platform. Although a number of Open Source applications for structural engineers are being developed in the recent years, with equal or superior performance and characteristics, historical and practical reasons are imposed. It is yet difficult and time-costly to trust such delicate matter as structural analysis to potentially untested applications.

6.1.1.- The .NET framework

The low-level technology that enables the interconnection between applications used in this research was Microsoft's .NET Framework. It is a development kit of classes, interfaces and value types designed for building applications in Windows, Windows Phone, Windows Server and Windows Azure. It is currently in version 4.5.1.

The .NET Framework library copies mostly the Open Source Java platform, which is available as an implementation called OpenJDK. Basically, the idea consists on creating a body of routines (classes, methods and interfaces) that give access to the developers to the core operating system controlling the different hardware. The part in charge of doing this is named Java Runtime Environment (JRE) in the Java framework and, interestingly, Common Language Runtime (CLR) in .NET's. Unlike Java, .NET is available only for the Windows operating systems enumerated above. As a sort of compensation, it can be written in a number of different languages, including Visual Basic ®, and Visual C# ®, whereas Java programs can only be written in Java language.

According to Microsoft documentation, the .NET Framework enhances the practical development of applications by giving access to the following services of the operating system:

- Memory management, so the programmer does not have to allocate and release memory as it is automated by the CLR.
- A common system of types to all languages, so the compiler can always be the same regardless of the chosen programming language.
- A well documented and extensive class library that covers from access to different hardware devices to process parallelization and threading.

- Version compatibility of programs regardless of the installed .NET Framework version.

Software applications developed for the Windows platform, including those enumerated above, make use of this framework. In many cases, these programs also expose an Application Programming Interface (API) that permits the linking between them. It is possible due to the fact that low-level Operating System structures are available to all of them.

6.1.2.- Integrating multiple software applications via .NET

In order to compute the results presented in the different chapters of this thesis, a set of applications was developed linking the different APIs of the aforementioned computer programs: Rhinoceros's Grasshopper, SAP2000 and Excel.

Each of them exposes a series of classes that permit the automation of the processes programmatically at any degree of complexity. Instead of accessing them via their Graphic User Interfaces (GUIs) and being limited by predetermined work flows, we could iterate our different experiments several hundred times and extract the necessary data in a much more efficient way.

6.1.2.1.- RhinoCommon .NET SDK and Grasshopper

Although the main application itself is of proprietary code, Rhinoceros is based on the openNURBS initiative. Perhaps for this reason, it still shows some degree of consideration for the developers which contribute and give feedback for the improvement of their core program. The whole Rhinoceros ® development package is a complex set of libraries fully accessible from many languages and IDEs.

In this philosophy, the Rhino Software Development Kit (SDK) is an Open Source tool accessible from the .NET Framework and also Mono, the Open Source adaptation of the .NET Framework. In the moment of writing this document it is delivered as RhinoCommon.dll and can be obtained from the Open Source repository GitHub [RHI2011].

By means of the RhinoCommon .NET SDK it is possible to extend and customize Rhino. This SDK can be included in other IDEs as a DLL in the form of a container for a set of identifiers or namespace. This namespace contains fundamental types that define commonly-used value types and classes used in Rhino.

One excellent example of this extensibility is the visual programming interface Grasshopper. This extension allows for the seamless creation of geometry within the CAD application by means of interconnected blocks of code that can be dragged on a canvas, known as components.

Particularly interesting is the component that allows for running custom sequential code written either in C# or in Visual Basic within Grasshopper. It was used as an IDE itself, since it offers immediate compilation of the code as well as automatic code-completion. Other custom components are also

possible using more powerful IDEs like MonoDevelop or Visual Studio. For this thesis a set of these were implemented in order to be able to access both SAP2000 and Excel APIs. In this manner, model data was created iteratively from the structural analysis application and managed and presented using spreadsheets in a seamlessly

6.1.2.2.- The SAP2000 API

The SAP2000 API allows third-party products to integrate with SAP2000 such that users may create custom engineering applications. SAP2000.exe is an Activex control which external applications may reference [CSI2014]. It is named CSI OAPI (Computers And Structures Inc. Open Application Programming Interface), and currently is in version 16. Being .NET based, it can be programmed in several different languages, including the popular C# and Visual Basic.

In order to be able to use the OAPI it is necessary to be in possession of a functioning licence of the SAP2000 program and the required classes are automatically installed in the system as a Dynamic Link Library (DLL). The customized code can be easily implemented by means of an Interactive Development Environment (IDE) such as Visual Studio or, as Open Source alternatives, the one included in the OpenOffice.org Basic, SharpDevelop, xacc.ide or MonoDevelop.

It has an extensive documentation that covers examples of usage for every exposed function. This comes in a SAP200_API_Documentation.chm file containing the full list of all provided functions with their exact syntax, detailed description of arguments and commented examples of usage [SEX2011].

6.1.2.3.- The Microsoft Excel API

The same degree of customizability is possible in the Microsoft's office suite. It comes with a language independent API which allows to program it by means of different programming languages. Moreover, by default it also includes its own Visual Basic for Applications (VBA) IDE. However, VBA compiles to an intermediate language exclusive of Microsoft called P-code, which is executed in a virtual machine. This makes the process less efficient from the point of view of computing speed.

For this reason, the interface of choice was once again Grasshopper using the access provided by the Office API. Analogously as SAP2000, all that is required to be able to use the Excel API is a functioning license of the Excel program and the required library becomes available within the very Excel executable. The accessed assembly is the Microsoft.Office.Interop.Excel library, and allows for the manipulation of all the objects normally present in Excel: worksheets, cells, ranges, rows, etc.

In this case, not only the documentation is exhaustive but also a large online users base is of assistance at any point of the development process.

6.2.- Visual programming implementation of routines for variational mechanics

As it is explained in the introduction, one of the objectives of this thesis is to narrow the gap currently found between the disciplines of structural design and computational physics.

A first problem often encountered in bridging them is the different degrees of abstraction and approach to the mathematical modeling of the concepts. Graphical tools that give a visual perspective of the problem can be of great help in these circumstances. Fortunately, in the recent years a number of visual programming IDEs has been developed that are currently mature enough to allow for the fast development of useful yet easy to understand applications.

Another problem is the prolificacy of the computational methods that, as it is shown in chapter 1, exist in great number making it difficult to follow the actual improvement that one contributes over the previous. The main point of chapter 3 is to resort to Variational Mechanics to have a benchmarking tool that allows for their neutral comparison in terms of accuracy and reliability, while presenting a significant number of them in a structured manner so their interactions can be understood.

In order to tackle both problems at once, we have resorted to the aforementioned Grasshopper[®] IDE included in McNeel and Associates' Rhinoceros[®]. In this chapter we are showing how it can be employed intensively both for didactic as well as for practical purposes. Figure 6.1 gives a global view of the complete program that enabled the comparison of all combinations exposed in chapter 3. As it can be seen, the modularity and procedural sequence are explicitly included in the very implementation, making this programming approach both functional and easy to understand.

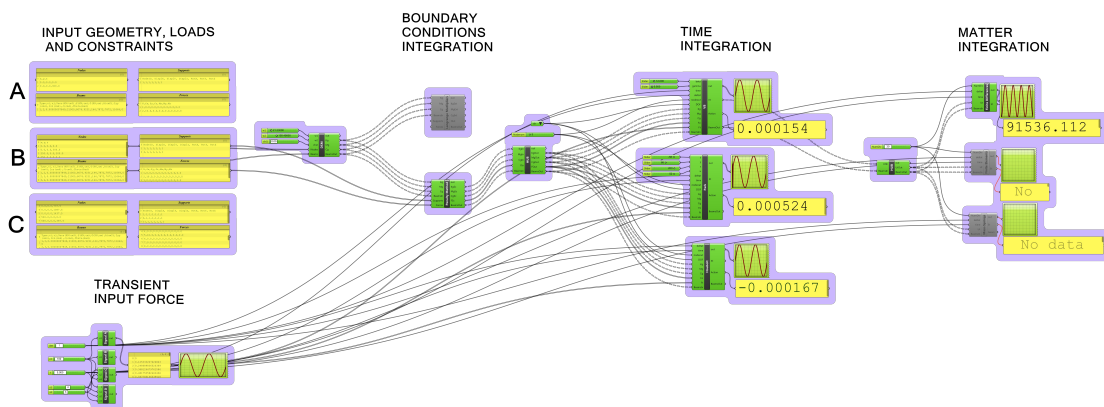


Figure 6.1: Grasshopper definition of the complete program. The visual programming interface makes it possible to have a global view of the whole process and the interconnection between elements at a glance.

6.2.1.- Simultaneous comparison of numerical methods

This first application shown in figure 6.2 contains all the modules required to obtain the data used in our numerical comparisons of section 3.3.7.

INPUT GEOMETRY, LOADS AND CONSTRAINTS



Figure 6.2: Close-up of the group of input panel components used to define model characteristics. Each model is completely defined by four blocks of information: node positions, beam section characteristics, support boundary conditions and force magnitude.

It can be read from left to right how first input data is prepared for each of the A, B and C models.

Then the stiffness, mass and damping matrices are created by means of the Direct Stiffness Method so the boundary conditions can be applied by means of either the Penalty Method or the Lagrange Multipliers.

Only then the time integration procedures can be iterated over the constructed matrices, being here examined the Newmark-Beta, the Houbolt and the Park's methods.

Eventually, the actual matter integration methods of Finite Elements, Finite Differences and Mass Spring System receive the nodal coordinates and discretize the defined beams according to their mathematical criteria.

Figure 6.3 is a close-up of the input panel components employed to collect the necessary data that defines the geometry, loads and constraints of each model of study. Each model is easily represented by four blocks of data: nodal coordinates, beam section characteristics and nodes, support boundary conditions and nodal force magnitude. The black lines are links to the next components, where they are parsed and interpreted as text strings. Linking a different set of data is what originates a different resulting model.

In figure 6.4 the different time-dependent signals are generated programmatically as iterations with different characteristics. They were custom made from the available VB:NET component. The control parameters are shown in the left and the resulting transient input values can be visualized on the right, making the debug process very easy and immediate. The linking of a different signal component to a particular numerical method component gives the possibility of making different combinations.

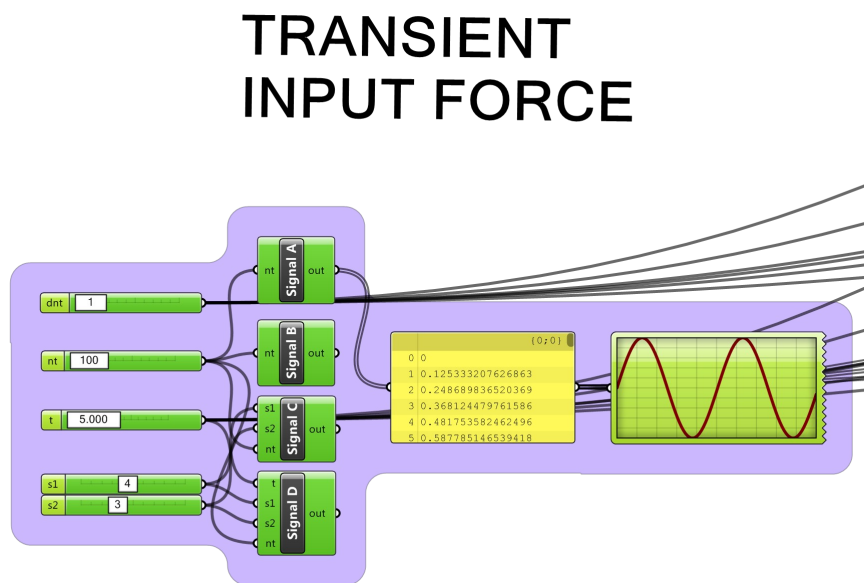


Figure 6.3: View of the transient input force generation components. The control of the parameters is made by means of slider components and the results are easily visualized both numerically and graphically.

The block presented in figure 6.5 is the Direct Stiffness Method component. It was also custom made for the purpose of this thesis using the VB.NET component available in Grasshopper®. It takes the node coordinates and beam properties defined earlier and parses them as the data from which assemble the different stiffness and mass matrices. It also takes the necessary parameters for the construction of the Rayleigh damping matrix as explained in chapter 3. The assembled stiffness matrix implements the

equations for Timoshenko beams while the mass matrix lumps the masses of the tributary beams to each node. The BeamsOut variable is the whole collection of beam properties and nodes that need also to be passed as variable to the next steps of the program.

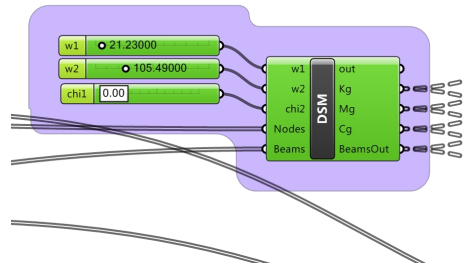


Figure 6.4: Direct stiffness matrix assembly. This module contains the code for generating the necessary stiffness, mass and damping matrices.

BOUNDARY CONDITIONS INTEGRATION

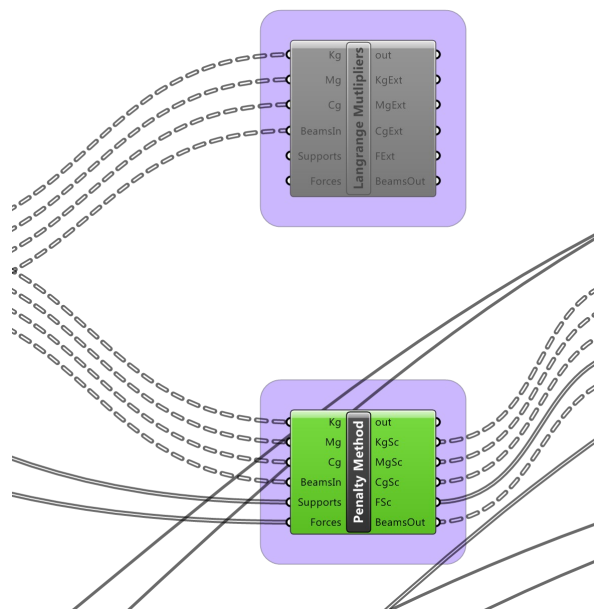


Figure 6.5: Integration of boundary conditions. It is possible to link either to Penalty Method or the Lagrange Multipliers method. In the picture, Lagrange Multiplier is deactivated for efficiency reasons.

In figure 6.6 the Penalty Method for integrating the boundary conditions is shown as linked to the time integration procedure while the Lagrange Multipliers appears as deactivated. Both take as inputs the previously assembled stiffness, mass and damping matrices as well as the collection of beams and the nodal constraints. Then they perform the necessary modifications to the matrices so that the linear systems of equations are solvable. The outputs are a new set of modified matrices and a force vector. In the case of LM, the matrix range is increased in those equations indicated by the nodal constraints, whereas by means of the PM, the respective diagonal values are “scaled” by a number several orders of magnitude larger.

In figure 6.7 a “HUB” component is presented together with the common parameters that control the time integration methods. The “HUB” component is an accessory to manage the possible combinations between numerical methods, so that the outputs of the previous component can remain fixed while switching between inputs in the next. This eases greatly the required labour of collecting results as the number of connections to make is much smaller. In essence this component takes no significant computational effort, as it just collects the beam collection and the different modified matrices and force vector and passes them unmodified.

Regarding the control parameters, they are used for debug purposes. They give the possibility of controlling the calculated transient displacement of a given node at a particular degree of freedom. They are linked to all the different methods so results can be simultaneously compared.

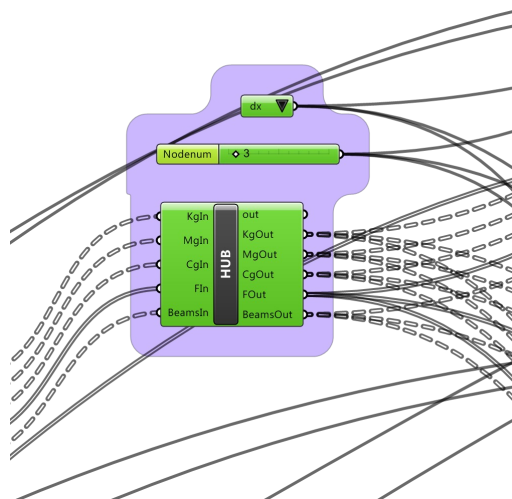


Figure 6.6: Intermediate linking component and common control parameters for time integration. In order to be able to make several combinations of methods, a connection hub was devised where links from one boundary constrain method could be fixed while switching time integration methods.

The components in figure 6.8 are those computing the results for Newmark-Beta, Park and Houbolt methods. They all take as inputs the collection of beams (BeamsIn), the transient input force (Fin), the

damping, mass and stiffness matrices (CgIn, MgIn, KgIn), the aforementioned debug controlling parameters (DOF and nodeout), the time span (time) and time step (deltat). Individually, each one is designed with a different set of fine tuning parameters that are also accessible form the Grasshopper interface.

TIME INTEGRATION

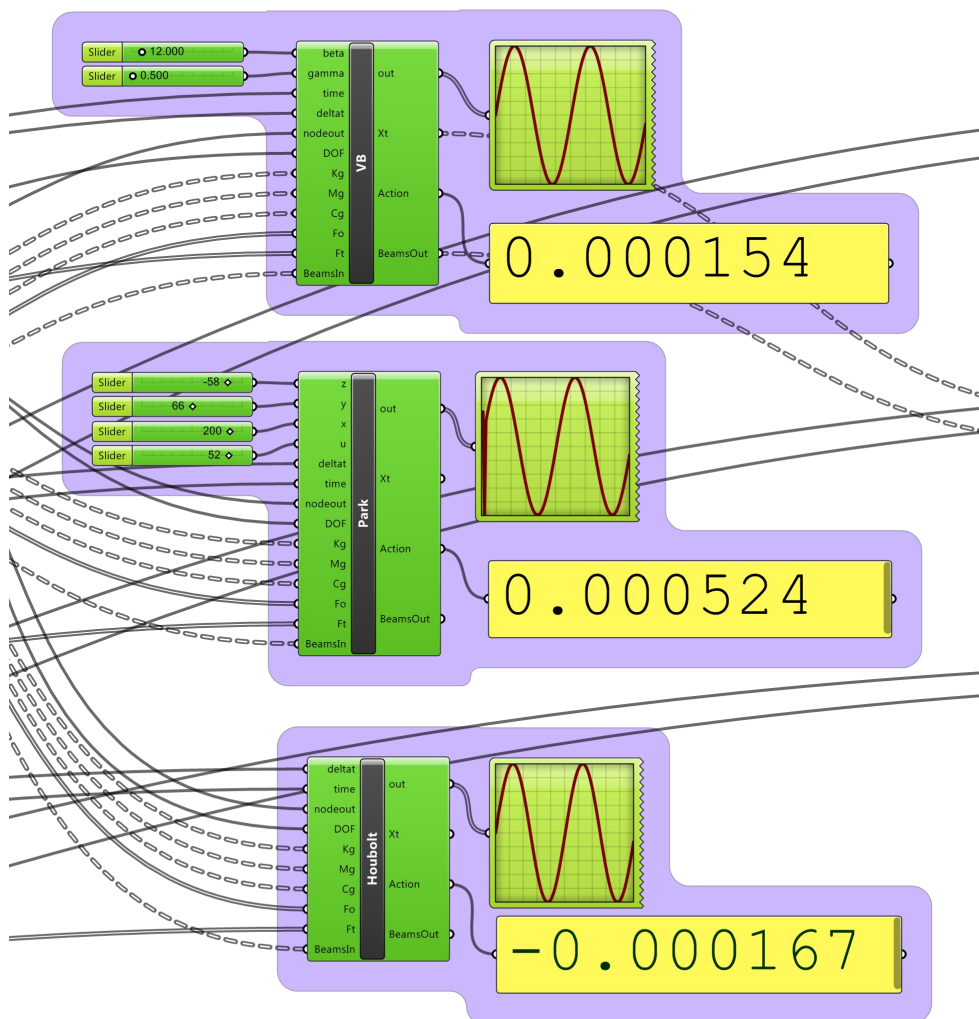


Figure 6.7: Time integration methods. It can be seen how most of the input variables are common to every method. Just a few calibration parameters differentiate the methods from one another. The time history of a selected node's displacement is presented for debug reasons. The total computed action is clearly presented and comparable.

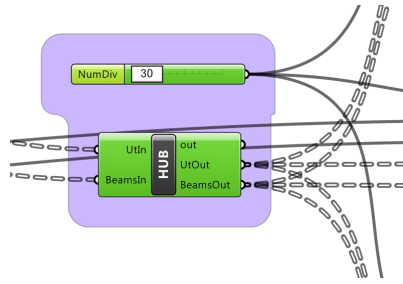


Figure 6.8: Intermediate linking component and common control parameters for time integration. In order to be able to make several combinations of methods, a connection hub was devised where links from one boundary constrain method could be fixed while switching time integration methods.

MATTER INTEGRATION

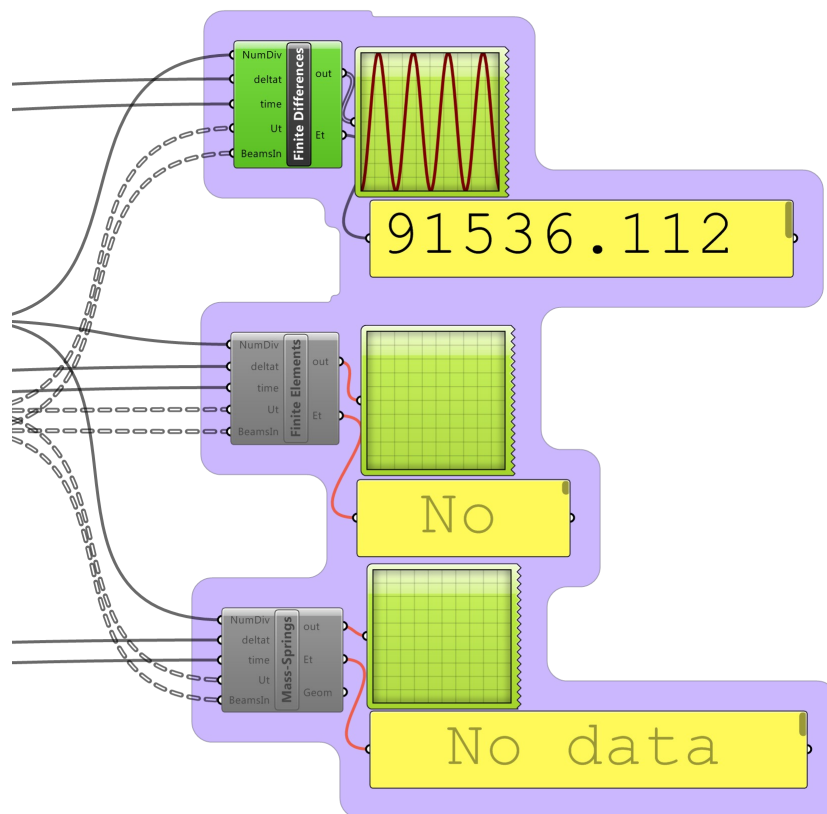


Figure 6.9: Matter integration methods. Finite Element, Finite Differences and Mass Spring System were compared. Boxes in grey are deactivated for computational efficiency.

The outcome of the resulting nodal displacement computations is easily monitored thanks to a QuickGraph component like the one mentioned in figure 6.4. Also a total value of the integrated action is given as an output and visualized in a panel component. This way coding errors and other anomalies are easily detected as the results are immediately obtained and visualized in a clear manner.

Figure 6.9 shows another switching component that was devised in order to easily study the different combinations of matter integration methods. In this case, the switching variables were only the global matrix with all the nodal displacements (U_t) and the beam collection (BeamsIn). The nodal displacements matrix contains the computed solution of the displacements for each time-step, and is passed into each matter integration method as a means to calculate the total elastic strain energy.

A common parameter controlling the number of subdivisions in the case of MSS and of interpolation points in the case of FEM and FDM appears named as NumDivs.

In figure 6.10, the last part of the program takes the computed nodal displacement history and the “global” variables of time step and time span and passes them to the matter integration methods of Finite Differences, Finite Element and Mass Spring System. The aforementioned integer value controlling the amount of subdivisions is also taken as input as well as the description of the beams properties. The total strain energy is then calculated by each component using the displacements obtained by means of the Timoshenko beams mentioned in the DSM component. These displacements are then re-oriented in the local coordinates of each beam and used as boundary conditions for integrating the respective interpolation equations that each method requires as explained in chapter 2.

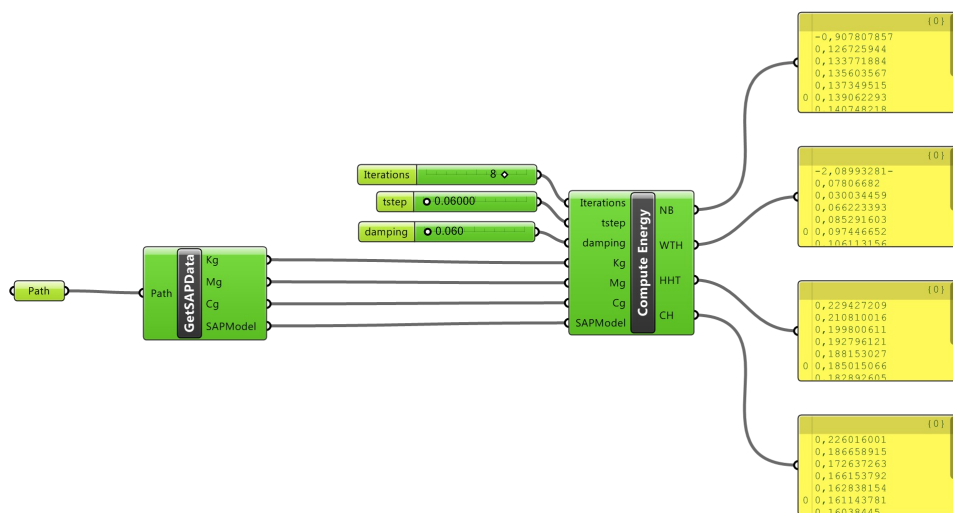


Figure 6.10: Energy balance of numerical methods for structural dynamics. The methods of Newmark Beta, Wilson Theta, hiulbert-Hugh-Taylor and Chung-Hulbert available in the SAP2000 application were seamlessly compared with two ad-hoc components. Resulting data was processed using Excel also programmatically.

6.2.2.- Energy balance study of numerical methods for structural dynamics

In order to have a benchmarking test bed for the previously described components computing numerical methods, another application was made that involved linking SAP2000 and Microsoft Excel. This was the basis for obtaining the data exposed in sections 3.3.5 and 3.3.6. The matter integration basis for SAP2000 is the Finite Element Method and no other option is available in this particular area. In time integrating, however, the program is fairly complete and offers a few state-of-the-art schemes, from which we chose Newmark Beta (NB), Wilson Theta (WTH), Hilber-Hugh-Taylor (HHT) and Chung-Hulbert for being the ones with the broadest documentation available.

Figure 6.11 shows a Grasshopper definition featuring two custom-made components: one for collecting the pre-generated SAP2000 model file, to which the necessary geometry, material, constraints and time-history data was input, and another one where the actual parametric study was carried away, gathering the results in an Excel worksheet.

The only input required for the GetSAPData component is the path to a valid working SAP2000 file. This component then opens the file and builds the stiffness, mass and damping matrices associated to this model from the outputs of the program. The program is run in the background and there is no need to show its user interface.

The second component, ComputeEnergy, receives the prepared data and the SAP2000 model and begins the connection with Excel, to which iteratively sends the results for post-processing, also in the background. It is noteworthy how the geometry of the SAP2000 model, in this case, could be arranged and linked directly to the geometry in Rhinoceros in case a different kind of study were necessary. The set of required parameters are the initial time step and damping values, but could be any other the researcher would consider of interest.

With these values, the internal routine of the component iterates over the SAP2000 model increasing linearly the value of the damping and of the time step. The results of the calculated displacements are then used to compute the energy balance as described in chapter 2 and then written in an Excel spreadsheet for its later display.

On each call to the SAP2000 time history computation the displacement vector was extracted and multiplied with the stiffness matrix to compute the internal strain energy. This matrix-vector multiplication was made employing Excel's internal methods. This was chosen over the function already programmed in the components of figure 6.8 both for convenience in the treatment of the data as much as for reliability of the final results.

6.3.- Visual programming implementation of routines for statistical mechanics

6.3.1.- Montecarlo

Adapting the previous routine to the examples in chapter 5 is fairly straightforward once the connection between SAP2000 and Excel is established. In this case, instead of submitting the model to a transient input force the values of the force are randomly modified in order to maximize the spectrum of possible states. This was made iteratively through the Grasshopper component into the SAP2000 file, that remained outputting data in the background as well as Excel, which was collecting it. In this manner, the defined statistical mechanics variables could be studied and compared for their analysis.

The GetSAPModel component was recycled and reused from the previous definition as it was the source of the SAP2000 model.

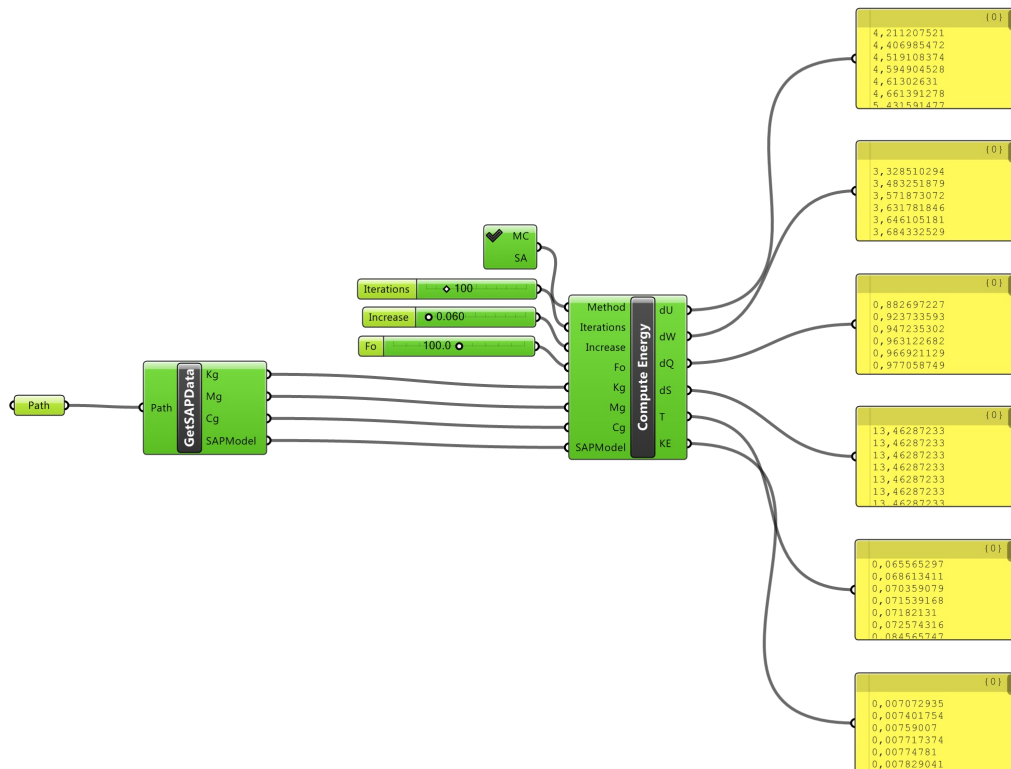


Figure 6.11: Computation of the energy parameters defined in chapter 5 by means of Monte Carlo exploration. The components used in previous research were reused when possible. In this case, time history integration was replaced with random perturbation of the input force.

The ComputeEnergy component was slightly modified, replacing the calls to the time history analysis included in SAP2000 with an iterative procedure that altered randomly the value of the applied force.

Also the newly defined parameters of chapter 5 were implemented and calculated on each iteration. Particularly important was the calculation of the internal work δW , for which the resulting internal stresses had to be retrieved for each defined beam at each integration point. The resulting values were retrieved to the corresponding Excel spreadsheet in runtime and also for convenience in the input panels as it is shown.

In order to make the component consistent within the research, a conditional input was included as input to allow to the user toggling between the different techniques exposed. Monte Carlo or Simulated Annealing.

6.3.2.- Simulated Annealing

Simulated Annealing was introduced in the chapter 5 as an efficient optimization technique when applied to structural design. In this case the random variables were the section properties instead of the applied forces. The internal functions of the component were the same as the studied output values were still those defined in section 5.2.1. When the SA value was activated, only the iterations had to be adapted to reflect the algorithm presented in table 5.2

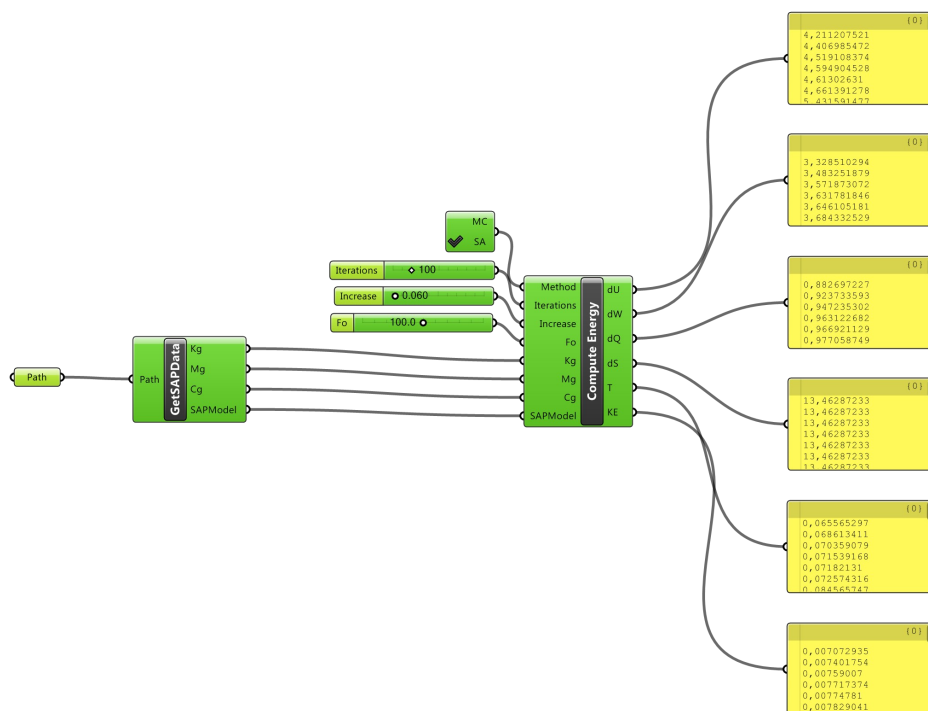


Figure 6.12: Computation of the energy parameters defined in chapter 4 by means of Simulated Annealing and optimization analysis. The random variable in this case were the geometric properties of the section of the beams..

6.4.- Discussion

Development of research software built around other existing applications was shown to be feasible and, most importantly, effective.

A tool for visual programming not only allows for a powerful combination of libraries but most importantly for a clear and step by step explanation of the involved concepts. This has an extraordinary didactic potential and greatly reduces programming errors.

With visual programming environments, all the parameters involved are instantly recognized. Besides, if the outputs are graphically appealing and agile enough, the process of debugging can be made with much less effort.

All the code employed in this thesis was created by means of a visual interface integrated in a CAD application. This code was used to link a general purpose FEM program with the CAD and a general purpose spreadsheet.

Those are all commonly-used tools that most practitioners are familiar with. This should encourage the professional community to employ the advances made in this research and further develop these pieces of code.

The programs developed in this thesis will be made publicly available under request subject to a Creative Commons GPL license.

7.- Conclusions

7.1.- Discussion

In chapter 2, a concise yet illustrative road map of the current methods of structural dynamics was provided. The purpose of this road map is to give some scope and to put together common subjects which, although available, seem too abstract and inapplicable. It was not found by the author any organized scheme for these methods in terms of tangible and engineering concepts such as time, matter and constrains.

In chapter 3, it was shown how variational principles and an energetic norm can be employed in an easy and efficient manner to benchmark and assess the accuracy and stability of different implementations. The scheme provided, tested in three simple examples, is trivially extensible to more complex systems where more elements are present. The advantage of this approach is that it allows for the monitoring of the global behaviour by means of one simple scalar. It was also shown how methods of different nature and concept can be compared using the same theoretical background, in particular the variational principle of Least Action of Lagrange and Hamilton. Accuracy and good performance of time and matter integration methods is generally taken for granted, as it is difficult, in the displacement domain, to assess it with certainty.

In chapter 4 it was explained how structural design is a process involving decisions based on a rigorous scientific methodology within which optimization is one subroutine that incorporates itself several iterations of the process of analysis. This important distinction between optimization and analysis as processes within design was also made. It is frequent to find published work where these two concepts are not discriminated, leading to potential misconceptions on the topic. The main tendencies both in optimization and non-deterministic analysis were enumerated and presented.

In chapter 5, a novel approach involving statistical mechanics was introduced. Within the framework presented in this chapter, it is possible to determine whether a structural system will require from its elements the ability to store applied energy or to deform in order to dissipate it, and to what extent. A numerical value associated with qualitative variables such as robustness or stiffness can be chosen matching those of total internal energy or heat, respectively. Also, an optimization procedure based on the stochastic method Simulated Annealing was presented and tested.

In chapter 6, the code developed in a visual programming interface was presented. It was shown how a tool for visual programming not only allows for a powerful combination of libraries but most importantly for a clear and step by step explanation of the involved concepts. This has an extraordinary didactic potential and greatly reduces programming errors.

7.2.- Revision of the working hypotheses

After all the work has been revised, the initial conceptions and misconceptions must be revisited and summarised. The working hypotheses established in the first chapter are now looked over.

A The vast body of numerical integration algorithms for structural dynamics simulation can be encompassed within an intuitive scheme that simplifies its study.

The first chapter of this thesis was devoted to the presentation of the methods for structural dynamics. A concise outline grouping them under the kind of differential equations they integrate and the physical notions they represent (ordinary, algebraic or partial for time, constraints and matter, respectively) was provided.

B Variational principles help to better understand the results of the simulations and their application gives a wider ability to analyse.

The main drawback of the legacy of Lagrange, Hamilton, D'Alembert and the rest is that it only becomes intuitive once applied experimentally. The formulations say very little about the might of these principles, and perhaps for that reason they are still considered difficult to understand. Only by carefully attending at the changes in energy rather than in position or force real comprehension of the structural dynamics can be achieved.

C Energy principles already improve the performance of structural dynamics simulations, but could also be used in combination with non-deterministic design tools. In this manner, design objective functions could be devised that accounted for optimal uses of the energetic capacity of the materials.

In our case, the performance of the simulations was not really improved but more the opposite. The software application needed to be severely tweaked in order to retrieve values in magnitudes of energy. Nonetheless, the degree of understanding of the phenomena involved in structural dynamics was greatly aided by the outputs. This understanding was interpreted in a framework which would ultimately be used for the optimization of structures.

D Theoretical advances gain value when they translate into practical and concrete tools. The research must contemplate this possibility and exploit the experimental implementations so that they can eventually reach others.

Great effort was made in this thesis to make the studied topics clear and easy to understand. The use of visualization tools to illustrate the concepts has not been limited to graphs and charts but also the very programming of code was made with a pictorial mind.

7.3.- Original scientific contributions

The task of developing this thesis was hard, intense and, in some situations, frustrating. However, the resulting work has proven very satisfactory and full of reward.

An experimental didactic methodology was put in practice in the form of weekly reports. Given the fact that the thesis was developed between Slovenia and Spain, with one mentor on each location, telematic tools were intensively used to keep track of the evolution of the research. A total of 111 reports was made giving details on a weekly basis of the different situations encountered during the research. Feedback was then discussed, also weekly, through meetings both online and in person. Further analysis of these reports will allow for deeper understanding of the study process and for recovery of potential ideas in the future.

On the initial phase of the thesis, a divulgative blog was published and maintained for two years with the aim of documenting the advances in the research (www.stochasticandlagrangian.blogspot.com). Currently, the attendance of the blog counts about 6000 annual visitors to posts related to Finite Elements and other numerical methods.

A number of articles were published in indexed international journals. Their references are given below:

- Andujar R., Roset J., Kilar V., 2011. “Beyond Finite Element Method: An overview on physics simulation tools for structural engineers“, TTEM 3 / 2011. BiH.
- Andujar R., Roset J., Kilar V., 2011. “Interdisciplinary approach to numerical methods for structural dynamics”, WASJ Vol 14 Num.8, Iran.
- Andujar R., Roset J., Kilar V., 2013 “Assessing Numerical Error in Structural Dynamics Using Energy Balance”, Advances in Mechanical Engineering, Volume 2013, Article ID 906120, Hindawi Publishing Corporation.

Another one on the topic of statistical mechanics characterization of structures, currently under revision, is expected.

Finally, the code presented in chapter 6, a total of four Grasshopper definitions, was released under a creative commons GPL license. This code is a concrete result intended to serve as basis for future research on the topic.

7.4.- Further research

As it common case in the research, many questions have been answered that have only given place to more questions. Unfortunately, many had to remain unanswered and the following is only a brief list of the possible lines of research that this thesis has opened:

- The introduction of variational time integrators in the numerical comparisons.
- The study of applications to real built structures.
- Experimentation with different laws for the fitting of the probabilities in order to see how they affect the computation of entropy.
- Exploration of the statistical mechanics framework within the plastic range.
- Implementation of other techniques of stochastic optimization than Simulated Annealing.

8.- References

- [ADH2000] Adhikari S., 2000, “Damping models for structural vibration”, PhD Thesis, Trinity College, Cambridge, UK.
- [AGU2005] Aguiar R., 2005, “Análisis estático de estructuras”, Colegio de ingenieros civiles de Pichincha, Quito, Ecuador.
- [ALE1976] Alexandrowicz Z., 1976, “Entropy calculated from the frequency of states of individual particles”, Journal of Statistical Physics, Vol. 14, issue 1, pp1-9
- [AND2011] Andujar R., Roset J., Kilar V., 2011. “Beyond Finite Element Method: An overview on physics simulation tools for structural engineers“, TTEM 3 / 2011. BiH.
- [AND2011] Andujar R., Roset J., Kilar V., 2011. “Interdisciplinary approach to numerical methods for structural dynamics”, WASJ Vol 14 Num.8, Iran.
- [AND2013] Andujar R., Roset J., Kilar V., 2013 “Assessing Numerical Error in Structural Dynamics Using Energy Balance”, Advances in Mechanical Engineering, Volume 2013, Article ID 906120, Hindawi Publishing Corporation.
- [ARG1960] Argyris J.H., 1960, “Energy theorems and structural analysis”, Butterworths Scientific publications, London, UK.
- [BAT1995] Bathe K.J., 1995, “Finite element procedures in engineering analysis”, Prentice Hall, USA.
- [BAU1972] Baumgarte J., 1972, “Stabilization of constraints and integrals of motion in dynamical systems”, Computer Methods in Applied Mechanics, 1:1-16
- [BEL1996] Belytschko T., Krongauz Y., Organ D., Fleming M., Krysl P., 1996, “Meshless methods: An overview and recent developments”, Computer Methods in Applied Mechanics and Engineering, Vol 139, issues 1-4
- [BEN2007] Bender J., 2007, “Impulse-based dynamic simulation in linear time”, Computer Animation and Virtual Worlds - CASA 2007. Vol 18 Issue 4-5
- [BLE1981] Blejwas T.E., 1981, “The simulation of elastic mechanisms using kinematic constraints and Lagrange multipliers”, Mechanism and machine theory, Vol 16 Issue 4, pages 441-445
- [BRA1998] Brank B., Briseghella L., Tonello N., Damjanic F.B., 1998, “On non-linear dynamics of shells: implementation of energy-momentum conserving algorithm for a finite rotation shell model”, International Journal for Numerical Methods in Engineering, Vol 42, Issue 3, pages 409–442.

- [BRY1907] Bryan G. H., 1907, “Thermodynamics. An introductory treatise dealing mainly with first principles and their direct applications”, B.G. Teubner, p 3.
- [BUG1991] Bugada G., 1991, “Estimacion y correccion del error en el analisis estructural por el MEF”, Monografia 9, CIMNE, Barcelona
- [BUL2004] Bullo F., Lewis A.D., 2004, “Geometric control of mechanical systems”, Texts in applied mathematics, Springer
- [BUT2008] Butcher J.C, 2008, “Numerical methods for ordinary differential equations”, John Wiley & Sons Ltd.
- [CHU1993] Chung J., Hulbert G., 1993, “A time integration algorithm for structural dynamics with improved numerical dissipation: the generalized alpha method”, Journal of Applied Mechanics, vol. 60, pp. 1562-1566
- [CRA1947] Crank J.; Nicolson P, 1947, “A practical method for numerical evaluation of solutions of partial differential equations of the heat conduction type”, Proceedings of the Cambridge Philosophical Society 43: 50–67
- [CSI2014] Computers and Structures Inc., “CSI Technical Knowledge Base”, accessed 25/04/2014 <<https://wiki.csiamerica.com/display/kb/OAPI>>
- [ECS2004] European committee for standardization, 2004, “Eurocode 8: Design of structures for earthquake resistance”
- [ERL2002] Erleben K., 2002, “Module Based design for Rigid Body Simulator”, Technical Report DIKU-TR-02/06, University of Copenhagen
- [EUL1744] Euler L. , 1744, “Methodus inveniendi lineas curvas maximi minimive proprietate gaudentes, sive solutio problematis isoperimetrici latissimo sensu accepti”, Ed. Marcum-Michaellem Bousquet & Assoc.
- [EYM1997] Eymard R., Gallou T., Herbin R., 1997, “Finite Volume Methods”, Handbook of Numerical Analysis.
- [FAL2005] de Falco D. , Pennestri E., Vita L., 2005, “The Udwadia-Kalaba formulation: a report on its numerical efficiency in multibody dynamics simulations and on its teaching effectiveness,” MULTIBODY DYNAMICS 2005, ECCOMAS Thematic Conference
- [FIT2006] Fitzpatrick R., 2006, “Computational Physics”, The University of Texas at Austin
- [GEA1984] Gear C.W., Petzold L. R., 1984, “ODE Methods for the Solution of Differential/Algebraic Systems”, SIAM Journal of Numerical Analysis, Vol 21 No 4

- [GOL2011]** Goldstein R., Wainer G., 2011, “Impulse-Based Dynamic simulation of Deformable Biological Structures”, *Transaction on Computational Systems in Biology*, XIII, LNBI 6575, Springer-Verlag, Berlin
- [HAM1835]** Hamilton W. R. 1835, "On a General Method in Dynamics", *Philosophical Transaction of the Royal Society*, Part II, pp 95-144.
- [HAN2004]** Hanc J., 2004, “The original Euler's calculus-of-variations method: Key to Lagrangian mechanics for beginners” submitted to *American Journal of Physics*.
- [HIL1977]** Hilber H. M., Hughes T. J. R., Taylor R. L., 1977, “Improved numerical dissipation for the time integration algorithms in structural dynamics”, *Earthquake Engineering and Structural Dynamics*, 5:282-292.
- [HOU1956]** Housner G.W., 1956, “Limit Design of structures to resist earthquakes”, *Proceedings of the World Conference on Earthquake Engineering*, Earthquake Engineering Research Institute
- [JAL1994]** de Jalon J. G., Bayo E., 1994, “Kinematic and Dynamic Simulation of Multibody Systems: the Real Time Challenge”, Springer-Verlag, New York
- [KAF2009]** Kafri O., 2009, “The distributions in nature and entropy principle”, *Computer Research Repository – CORR*, Vol. Abs/0906.5
- [KAS1995]** Kass M., 1995, “An Introduction to Continuum Dynamics for Computer Graphics”, SIGGRAPH course note: Physically-based modeling, ACM SIGGRAPH
- [KEL2010]** Kelager M., Niebe S., Erleben K., 2010, “A Triangle Bending Constraint Model for Position-Based Dynamics”, *Workshop on Virtual Reality Interaction and Physical Simulation VRIPHYS*
- [KIL2010]** Kilar V., Koren D., 2010, “Simplified inelastic seismic analysis of base-isolated structures using the N2 method”, *Earthquake engineering & structural dynamics*, vol. 39, no. 9, pp. 967-989.
- [KIL2013]** Kilar V., Petrovčič S., Šilih S., Koren D., 2013, “Financial aspects of a seismic base isolation system for a steel high-rack structure = Aspectos económicos de un sistema de aislamiento sísmico de base para bastidores de acero en altura.”, *Informes de la construcción*, oct./dic. 2013, vol. 65, no. 532, pp. 533-543.
- [KIR1983]** Kirkpatrick S., Gelatt C. D., Vecchi M. P., 1983, “Optimization by simulated annealing”, *Science*, Vol. 220, No. 4598, American Association for the Advancement of Science.
- [KNU2006]** Knuth K. H., 2006, “Optimal data-based binning for histograms”, *Cornell University Library*, arXiv:physics/0605197
- [KUH1999]** Kuhl D., Crisfield M. A., 1999, “Energy-conserving and decaying algorithms in non-linear

structural dynamics”, *International Journal for numerical methods in engineering*, 45, 569-599.

[LAN1952] Lanczos C., 1952, “The Variational Principles of Mechanics” *Mathematical Expositions*, No 4, Oxford University Press

[LAN1986] Landau L. D., Lifshitz E. M., 1986, “Theory of Elasticity (Course of Theoretical Physics Volume 7)”, Butterworth Heinemann.

[LEW2003] Lew A., Marsden J. E., Ortiz M., West M., 2003 “An Overview of Variational Integrators”, CIMNE, Barcelona.

[LIU2003a] Liu G.R., 2003, “Mesh free Methods: Moving Beyond Finite Element Methods”, CRC Press, USA

[LIU2003b] Liu G.R., Liu M.B., 2003, “Smoothed particle hydrodynamics: a meshfree particle method”, World Scientific Publishing Co. Pte, Ltd., Singapore

[MAR2011] Mareš J. J., 2011, “Hotness manifold, phenomenological temperature and other related concepts of thermal physics”, in the book “Glassy, amorphous and nano-crystalline materials”, pp. 327-346, Springer Netherlands

[MAR2009] Marschner S., 2009, “Backward Euler Method, Lecture Notes for the course Introduction to scientific Computing CS3220”, Cornell University

[MAR1999] Marsden J. E., West M. 1999, “Discrete Mechanics and Variational Integrators”, *Acata Numerica*, Cambridge University Press.

[MAS1999] Mase G. E., Mase G. T., 1999, “Continuum mechanics for engineers”, CRC Press.

[MAY2008] Maymon, G, 2008, “Structural Dynamics and Probabilistic Analysis for Engineers”, Butterworth Heinemann.

[MIR2007] Mirtich B.V, 2007, “Impulse based simulation of rigid body systems”, Ph.D. thesis, University of California, USA.

[MOR2008] Morris A., Rahman A., 2008, “A practical guide to reliable finite element modelling”, John Wiley & Sons, Ltd.

[MUL2006] Müller M., Heidelberger B., Hennix M., Rattcliff J., 2006, “Position based dynamics”, *Proceedings of Virtual Reality Interactions and Physical Simulations*

[NAY1992] Nayroles B., Touzot G, 1992, “Generalizing the finite element method: diffuse approximation and diffuse elements”, *Proceedings in Computational Mechanics*, Vol 10, pp 307-318.

[NEA2005] Nealen A., Müller M., Keiser R., Boxerman E., Carlson M., 2005, “Physically Based

Deformable Models in Computer Graphics”, Computer Graphics Forum, Vol. 25, issue 4

[NEU2006] Neuenschwander D.E., Taylor E.F., Tuleja S., 2006, “Action: Forcing energy to predict motion” in The Physics Teacher, Vol 44

[NEW1959] Newmark N.M., 1959, “A method of computation for structural dynamics”, ASCE Journal of engineering Mechanics Division, vol 85, no EM3.

[NIV2009a] Niven R. K., 2009, “Non-Asymptotic thermodynamic ensembles”, Cornell University Library, arXiv:0807.4160v3

[NIV2009b] Niven R. K., 2009, “Combinatorial entropies and statistics”, The European Physical Journal B, Vol. 70, Issue 1, pp 49-63

[PAR1974] Parlett B.N., 1974, “The Rayleigh quotient iteration and some generalizations for nonnormal matrices”, Mathematics of Computation, Vol 28, Num 127, pp. 679-693

[PET2013] Petrovčič S., KILAR V., 2013 “Seismic failure mode interaction for the equivalent frame modeling of unreinforced masonry structures”. Engineering structures, vol. 54, pp 9-22

[PRE1991] Press W. H. , Flannery B. P. Teulosky S. A. , 1992, “Numerical Recipes in C: The Art of Scientific Computing”, 2nd ed. Cambridge University Press.

[PRZ1968] Przemieniecki J. S., 1968, “Theory of matrix structural analysis”, McGraw-Hill. Inc, USA

[RHI2011] Robert Mc Neel & Assoc, “Rhino SDK goes Open Source”, accessed 10/10/2013 <<http://blog.rhino3d.com/2011/01/rhino-sdk-goes-open-source.html>>

[ROS1987] Roset J., Isalgué A., 1987, “Aplicació del mètode de Monte Carlo a l'optimització energètica dels edificis.” II Congrés Català d'Energies Solar i Renovables. Girona.

[ROS2006a] Roset J., 2006, “Física aplicada a l'ensenyament de l'arquitectura”, PhD Thesis, Universitat Politecnica de Catalunya.

[ROS2006b] Roset J., 2006, “Física aplicada a l'ensenyament de l'arquitectura”, Architecture, City and Environment / Arquitectura, Ciudad y Entorno, ACE, vol.1, núm.2. Pàgines 132 a 156.

[SAK2013] Saka M. P. , Geem Z. W., 2013, “Mathematical and metaheuristic applications in design optimization of steel frame structures: An extensive review”, Mathematical problems in engineering, Vol. 2013, Art ID 271031, Hindawi Publishing Corporation.

[SEX2011] Sextos A. G. , Balafas G. K., 2011, “Using the new SAP2000 Open Application Programming Interface to develop an interactive front end for the modal pushover analysis of bridges”, COMPDYN 2011 3rd ECCOMAS Thematic Conference on Computational Methods in Structural Dynamics and Earthquake Engineering, M. Papadrakakis, M. Fragiadakis, V. Plevris (eds.), Corfu, Greece, 25–28 May

2011

- [SHA1997]** Shabana A. A., 1997, “Flexible Multibody Dynamics: Review of Past and Recent Developments”, *Multibody System Dynamics* 1: 189–222.
- [SHA2008]** Shabana A.A., 2008, “Computational Continuum Mechanics”, Cambridge University Press
- [SMI1978]** Smit G.D., 1978, “Numerical Solution of Partial Differential Equations by Finite Difference Methods”, 2nd ed. Oxford Applied Mathematics and Computing Science Series, UK.
- [SUK2003]** Sukumar N., Dolbow J., Devan A., Yvonnet J., Chinesta F., 2003, “Meshless Methods and Partition of Unity Finite Elements”, 6th International ESAFORM Conference on Material Forming
- [TSE2002]** Tseng T. Y., Caticha A., 2002, “Yet another resolution of the Gibbs paradox: an information theory approach”, *AIP Conference Proceedings*, Vol. 617, Issue 1
- [UDW1992]** Udawadia F.E., Kalaba R.E, 1992, “A new perspective on constrained motion”, *Proceedings of the Royal Society of London*, A439, 407-410
- [VEN1968]** V. B. Venkayya, N. S. Khot, V. S. Reddy, 1968, “Optimization of structures based on the study of energy distribution”, Air Force Flight Dynamics Lab.
- [VID2004]** Vidal Y., 2004, “Mesh-free methods for dynamic problems: incompressibility and large strains”, PhD Thesis, Universitat Politècnica de Catalunya
- [WAN2012]** Wang Q.A. , Wang R., 2012 “Is it possible to formulate least action principle for dissipative systems?”, Cornell University Library, web version in <http://arXiv.org/abs/1201.6309>
- [WAS2003]** Wasfy T.M., Noor A.K., 2003, “Computational strategies for flexible multibody systems”, *Applied Mechanics Reviews*, vol 56, no 6
- [WES2004]** West M., 2004, “Variational Integrators”, PhD Thesis, Presented at California Institute of Technology, USA
- [WIL1996]** Wilson E.L., 1996-2001, “Three dimensional static and dynamics analysis of structures”, Computers and Structures Inc., USA
- [WIL2004]** Wilson E.L., 2004, “Static and dynamic analysis of structures”, Computers and Structures Inc., USA
- [WUN2002]** Wunderlich W., Pilkey W., 2002. “Mechanics of structures. Variational and computational methods”, CRC Press, pp.: 852-877